UNIVERSITY OF TROMSØ UIT

FACULTY OF SCIENCE AND TECHNOLOGY
DEPARTMENT OF PHYSICS AND TECHNOLOGY

Drift wave turbulence and zonal flows

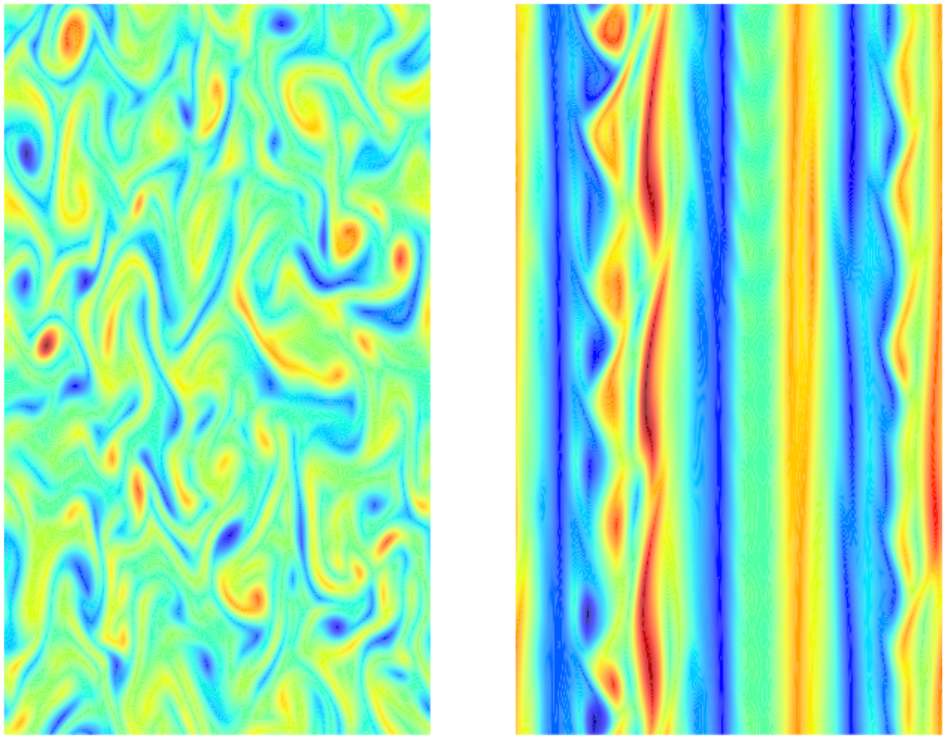

Ole Meyer

FYS-3900 Master's Thesis in Physics

November 2012

Drift wave turbulence and zonal flows

Ole Meyer
Department of Physics and Technology,
University of Tromsø,
Tromsø,
Norway N-9037

February - November 2012

Abstract

Anomalously large radial transport levels in fusion devices is commonly believed to be the cause of small-scale edge localized electrostatic drift wave turbulence. We review the basic drift wave instability mechanism and show how poloidally elongated structures can self-consistently emerge from the small-scale turbulent motions through envelope modulation governed by the cubic nonlinear Schrödinger equation. There has been extensive study of the zonal flow - drift wave system recently, showing that zonal structures effectively reduce radial transport levels. We study the drift wave turbulence model due to Hasegawa and Wakatani (OHW), which upon subtle modification (MHW) also allows for zonal flow formation which is characteristic for the edge region of fusion devices. There is experimental evidence of long-range correlations; we investigate whether zonal flows give rise to such behavior in the hydrodynamic and quasi-adiabatic state of the OHW and MHW models. Rescaled range analysis gives no indication of long-range correlation. Structure function analysis confirm this finding for the zonal flow free simulations where fluctuations are essentially Gaussian. Heavy tails in probability distributions of turbulent quantities due to the emergence of zonal flows in the quasi-adiabatic state of MHW complicate the analysis and increase in self-similarity parameters computed from structure functions cannot be used as proof for long-range correlation. The finding of this work is that significantly longer time-series are needed to clarify whether long-range correlations are an artefact of zonal structures or not.

Acknowledgements

On a personal note, I would like to thank my friends and family who always supported me throughout my studies. Their continuous motivation to continue with this work is greatly appreciated.

Concerning academics, a big thanks to Ralph Kube is appropriate. Ralph modified the code to include the MHW equations and selflessly helped me improve my programming skills a great deal. This work would not have been possible without his guidance through the jungle of numerical pitfalls.
I am grateful to my advisor Odd Erik Garcia whose superb supervision and physical intuition made me appreciate the true beauty of physics. Of course, inviting me to visit him at the MIT for a month was the highlight of the last year - once again, thank you!

Contents

Chapter 1

Introduction

Turbulent transport of particles and heat towards the confining walls in fusion plasmas is a major design challenge for next generation Tokamak devices. It is generally recognized that electrostatic drift wave turbulence is the cause for turbulent transport in the plasma edge, where free energy is provided by density gradients which are necessary to keep the plasma confined ([24]). Fusion plasmas are typically highly magnetized such that turbulent dynamics in the edge region are approximately described by a two-dimensional geometry. A specific two-dimensional drift wave model is the Hasegawa - Wakatani (HW) set of coupled partial differential equations for vorticity and density fluctuations ([4]), which has been extensively studied before ([17],[27]). The benefits of employing this model is its simplicity, which makes it a popular candidate for long-time numerical simulations. Experimental evidence of electrostatic turbulence allows for a static magnetic field, magnetic shear can be neglected when considering slab-geometry such as shown in Figure 1.1 inside the last closed magnetic flux surface. The figure shows a poloidal cross section of the Alcator C - Mod Tokamak device at the Massachusetts Institute of Technology (MIT), imagine the box being located slightly to the left such as to lie entirely inside the magenta shaded ares, indicating magnetic flux surfaces. Slab geometry is then the local approximation of radial vs. poloidal direction mapped into a rectangular coordinate system, which we shall employ. The HW system of equations adequately describes radial fluxes since the phase relation between density and potential fluctuations is accurately modeled. To incorporate for shear velocities resulting from zonal structures in turbulent quantities, one has to modify the HW and arrives at the modified Hasegawa Wakatani equations (MHW). Zonal structures in the turbulent potential improve the confining properties of the plasma by extracting energy from turbulent fluctuations which in turn reduces radial transport. Recently, there has been carried out extensive research seeking to describe the role of self - consistent zonal flows in the drift wave turbulence, see f.ex. Diamond [5] for an excellent review on this topic, but not whether zonal flows give rise to long range correlation. It should be noted that focus has been on more sophisticated models than the one we shall employ. There is experimental evidence of long-range correlations in fusion devices. Long-range correlation is commonly believed to be indirect evidence of self-organized criticality (SOC) which is associated with local density profile relaxation due to turbulent motions which looses its drive when the profile is relaxed, making it possible to rise to a certain threshold before fueling the turbulence again. Long-range correlation is the collective memory of such local effects that eventually lead to experimentally observed avalanche effects in radial flux [26]. We seek to investigate whether the simple HW and MHW models describe this artefact of plasma micro-turbulence.

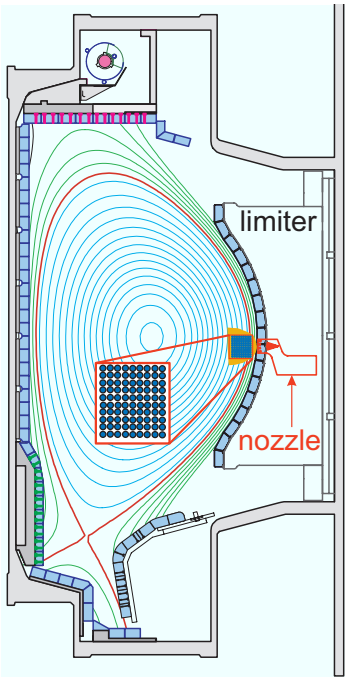

Figure 1.1: Poloidal cross section of the Alcator C - Mod at MIT. Slab geometry is essentially indicated by the box.

The structure of this work is as follows. In chapter 2 we derive the necessary model equations and consider specific analytic limits of it to predict results for the numerical simulations. We give important physical arguments on how zonal flows can self-consistently arise due to modulation of small-scale drift wave turbulence in chapter 3. Statistical concepts and the numerics of the employed code are presented in chapter 5. Numerical results obtained from the hydrodynamic and quasi - adiabatic limit of ordinary and modified Hasegawa - Wakatani equations respectively are presented in chapter 6.

Chapter 2

Resistive drift wave dynamics

2.1 Physical mechanism

In the following we present the basic setting for drift wave dynamics to occur. This section is merely of illustrative value since the equations are oversimplified which yields stable branches in the dispersion relation. Nonetheless the simple arguments presented here shall help to give a deeper understanding of the more realistic case for resistive drift wave dynamics which is described in the next section.
The following derivation follows Pésceli [1] closely.
Consider the ion continuity equation in three dimensional slab-geometry, where we take the magnetic field to be constant and along the positive z-direction, $\mathbf{B} = B\,\widehat{\mathbf{z}}$,

$$\frac{\partial n_\mathrm{i}}{\partial t} + n_\mathrm{i}\nabla\cdot\mathbf{v}_\mathrm{i} + \mathbf{v}_\mathrm{i}\cdot\nabla n_\mathrm{i} = 0, \tag{2.1}$$

as well as the cold ion, i.e., $T_\mathrm{i} = 0$, momentum equation where resistive dissipation is neglected

$$M\left(\frac{\partial}{\partial t} + \mathbf{v}_\mathrm{i}\cdot\nabla\right)\mathbf{v}_\mathrm{i} = -e\nabla\phi + e\mathbf{v}_\mathrm{i}\times\mathbf{B}, \tag{2.2}$$

where we have introduced the electrostatic potential $\mathbf{E} = -\nabla\phi$ and M denotes the ion mass. Crossing the momentum equation with $\mathbf{B}$ yields the ion perpendicular velocity

$$\mathbf{v}_{\perp\mathrm{i}} = -\frac{1}{B^2}\nabla\phi\times\mathbf{B} - \frac{M}{eB^2}\left[\frac{\partial}{\partial t}(\mathbf{v}_\mathrm{i}\times\mathbf{B}) + \mathbf{v}_\mathrm{i}\cdot\nabla\mathbf{v}_\mathrm{i}\times\mathbf{B}\right], \tag{2.3}$$

which we note to be compressible, $\nabla\cdot\mathbf{v}_{\perp\mathrm{i}} \neq 0$. We assume that the wavelengths are long enough to allow for quasi-neutrality, i.e., $k\lambda_D \ll 1$, where the Debye length for electrons is given by $\lambda_D^2 = \epsilon_0 T_\mathrm{e}/e^2 n_0$. Furthermore, we are considering low frequency, electrostatic waves that satisfy

$$v_\mathrm{thi} \ll \omega/k_z \ll v_\mathrm{the}, \tag{2.4}$$

which means that electrons are free to flow along the magnetic field from wave crest to trough in order to preserve quasi-neutrality. For all practical purposes we assume quasi-neutrality to hold and use Poisson's Equation to compute the density deviation from the electrostatic potential,

$$\epsilon_0\nabla^2\phi = e(n_e - n_i). \tag{2.5}$$

Due to the above, it is reasonable to assume that electrons follow a Boltzmann distribution,

$$n_\mathrm{e} = n_0(x)\exp\left(\frac{e\phi}{T_\mathrm{e}}\right), \tag{2.6}$$

where the temperature is measured in terms of energy units (i.e., eV)such that the conventional Boltzmann factor does not appear. One easily converts to the Kelvin scale upon division of $T_{\rm e}$ by the Boltzmann factor, k.

Conventional drift ordering dictates the velocity to lowest order in $\omega/\omega_{\rm ci}$ is given by the electric drift. Iteration of the RHS in Eq. (2.3) by using the electric drift we obtain the familiar second order correction, namely the ion polarization drift,

$$\mathbf{v}_{\perp \rm i} = -\frac{1}{B^2}\nabla\phi\times\mathbf{B} - \frac{M}{eB^2}\left(\frac{\partial}{\partial t} - \frac{1}{B^2}\nabla\phi\times\mathbf{B}\cdot\nabla\right)\nabla_\perp\phi. \tag{2.7}$$

The ieration is valid if the electric field varies only on slow time and long spatial scales respectively. Note that due to the second order correction the ion perpendicular velocity is no longer incompressible. Invoking quasi-neutrality such that all subscripts "e" and "i" on the densities are redundant and inserting the Boltzmann distributed density, Eq. (2.6) in Eq. (2.1) gives then

$$\frac{\partial\phi}{\partial t} + \frac{T_{\rm e}}{e}\nabla\cdot(\mathbf{v}_{\perp \rm i} + v_{\shortparallel i}\mathbf{b}) + (\mathbf{v}_{\perp \rm i} + v_{\shortparallel i}\mathbf{b})\cdot\nabla\phi + \frac{T_{\rm e}}{en_0(x)}\frac{dn_0}{dx}\mathbf{v}\cdot\widehat{\mathbf{x}}, \tag{2.8}$$

where obviously $\mathbf{v} = \mathbf{v}_\perp + v_{\shortparallel}\mathbf{b}$ and we have defined a unit vector in the direction of the magnetic field, $\mathbf{b} = \mathbf{B}/B$. The equation above is readily seen to allow for a trivial equilibrium, i.e., $\phi = 0$ and $\mathbf{v}_{\rm i} = \mathbf{0}$. Linearizing about this equilibrium denoted by $\phi_0, \mathbf{v}_{\rm i0}$, with perturbation $\phi_1, \mathbf{v}_{\rm i1}$, where the perturbation by definition of the linearizing concept is assumed to be small, we obtain

$$\frac{\partial\phi_1}{\partial t} + \frac{T_{\rm e}}{e}\left(\nabla\cdot\mathbf{v}_{\perp \rm i1} + \frac{\partial}{\partial z}v_{\shortparallel i1}\right) + \frac{T_{\rm e}}{en_0(x)}\frac{dn_0}{dx}\mathbf{v}_{\perp \rm i1}\cdot\widehat{\mathbf{x}}, \tag{2.9}$$

and

$$\mathbf{v}_{\perp \rm i1} = -\frac{1}{B^2}\nabla\phi_1\times\mathbf{B} - \frac{M}{eB^2}\frac{\partial}{\partial t}\nabla_\perp\phi_1. \tag{2.10}$$

The parallel component of Eq. (2.2) is

$$M\left(\frac{\partial}{\partial t} + \mathbf{v}_{\rm i}\cdot\nabla\right)v_{\shortparallel \rm i} = -e\frac{\partial}{\partial z}\phi, \tag{2.11}$$

which admits the equilibrium with $\phi_0 = 0$, $\mathbf{v}_{0\rm i} = \mathbf{0}$. We may linearize the parallel component equation to close the linearized system of eqs.

$$M\frac{\partial}{\partial t}v_{\shortparallel \rm i1} = -e\frac{\partial}{\partial z}\phi_1. \tag{2.12}$$

Taking the time derivative of Eq. (2.9) and substituting Eq. (2.10) and Eq. (2.12) leads to

$$\frac{\partial^2\phi_1}{\partial t^2} + \frac{T_{\rm e}}{e}\left(-\frac{M}{eB^2}\frac{\partial^2}{\partial t^2}\nabla_\perp^2\widetilde{\phi}_1 - \frac{e}{M}\frac{\partial}{\partial t}\frac{\partial^2\phi_1}{\partial z^2}\right) + \frac{T_{\rm e}}{e}\frac{n_0'}{n_0}\left(-\frac{1}{B}\frac{\partial}{\partial t}\frac{\partial\phi_1}{\partial y} - \frac{M}{eB^2}\frac{\partial^2}{\partial t^2}\frac{\partial\phi_1}{\partial y}\right) = 0, \tag{2.13}$$

where now $n_0' = dn_0/dx$. Upon introducing the ion cyclotron frequency, $\Omega_{\rm ci} = eB/M$, the hybrid quantities ion sound speed at electron temperature, $C_{\rm s}^2 = T_{\rm e}/M$, and the ion Larmor radius at electron temperature, $\rho_{\rm s}^2 = C_{\rm s}^2/\Omega_{\rm ci}^2 = MT_{\rm e}/e^2B^2$ we have

$$\frac{\partial^2}{\partial t^2}\left(\phi_1 - \rho_{\rm s}^2\nabla_\perp^2\phi_1\right) - C_{\rm s}\frac{\partial^2}{\partial z^2}\phi_1 - \frac{C_{\rm s}^2}{\Omega_{\rm ci}}\frac{n_0'}{n_0}\frac{\partial}{\partial t}\frac{\partial}{\partial y}\phi_1 - \rho_{\rm s}^2\frac{n_0'}{n_0}\frac{\partial^2}{\partial t^2}\frac{\partial}{\partial x}\phi_1 = 0. \tag{2.14}$$

We study the edge of confined plasmas where density gradients naturally occur, we therefore initialize an exponential background profile,

$$n_0(x) = n_{00}\exp(-x/L_n),$$

where L_n is the characteristic scale-length of the density gradient. The density gradient is in the radial direction and the plasma is assumed to be homogeneous in y- and z - direction, such that we are considering fluctuations on the form

$$\phi_1(x,y,z,t) = \widehat{\phi}(x)\exp(ik_y y + ik_z z - i\omega t),$$

which gives

$$\omega^2\rho_{\rm s}^2\left(\frac{\partial^2\phi_1}{\partial x^2} + \frac{n_0'}{n_0}\frac{\partial\phi_1}{\partial x}\right) - \left(\omega^2 + \omega^2\rho_{\rm s}^2k_y^2 - C_{\rm s}^2k_z^2 + \omega\frac{C_{\rm s}^2}{\Omega_{\rm ci}^2}\frac{n_0'}{n_0}k_y\right)\phi_1 = 0. \quad (2.15)$$

We may assume that the amplitude varies only weakly with x such that the derivatives acting on it vanish and also considering long wavelengths along the magnetic field (we still have $v_{\rm thi} \ll \omega/k_z \ll v_{\rm the}$) then yields the more simple second order equation

$$\omega^2(1+\rho_{\rm s}^2k_y^2) - \omega k_y u_{\rm De} \approx 0, \quad (2.16)$$

where the diamagnetic drift velocity for electrons is given by

$$u_{\rm De} = \frac{T_{\rm e}}{eB}\left|\frac{n_0'}{n_0}\right| = \kappa C_{\rm s}, \quad (2.17)$$

and we have also introduced the normalized density scaling $\kappa \equiv \rho_{\rm s}/L_n$. It follows that

$$\omega = \frac{u_{\rm De}k_y}{1+\rho_{\rm s}^2k_y^2}. \quad (2.18)$$

The factor $\rho_{\rm s}^2k_y^2$ arises due to the non-zero divergence of the ion polarization drift. In even more simplified models, where the ion polarization is not considered, the dispersion relation is simply $\omega = u_{\rm De}k_y$, which is commonly denoted as the *drift wave frequency*, $\omega = \omega^* \equiv u_{\rm De}k_y$. Note that if the fluctuations also were allowed to vary in the x-direction (still the amplitude should only vary weakly with x) we would get

$$\omega = \frac{u_{\rm De}k_y}{1+\rho_{\rm s}^2k_\perp^2}, \quad (2.19)$$

where $k_\perp^2 = k_x^2 + k_y^2$.

Physical Interpretation

As shown above, the obtained frequency is real, thus there is no instability of the drift wave. This result follows from the assumption of Boltzmann distributed electrons, which upon linearization gives that density fluctuations are *in phase* with potential fluctuations.

Cf. Figure 2.1. The figure describes a density perturbation. At point A the fluctuating density is greater than its equilibrium value, the linearized Boltzmann distribution then gives an in-phase potential at point A, $n_1/n_0 = e\phi_1/T_{\rm e}$. At point B the corresponding fluctuations are less than its equilibrium value, thus there is a potential drop between A and B and consequently an electric field directed from to A to B arises due to the density perturbation. Recall that there is no equilibrium field present, so the electric field is really a perturbed quantity, and together with the (constant) magnetic field this gives rise to a *perturbed* electric drift, $\mathbf{v}_1 = \mathbf{E}_1 \times \mathbf{B}_0/B_0^2$, which between A and B is directed in the $-x$ direction and further down the y-axis the drift is in the positive x direction. Now, recall that there is a gradient in the equilibrium density profile which also is directed in the negative x direction. The drift is maximum when the perturbed density equals its

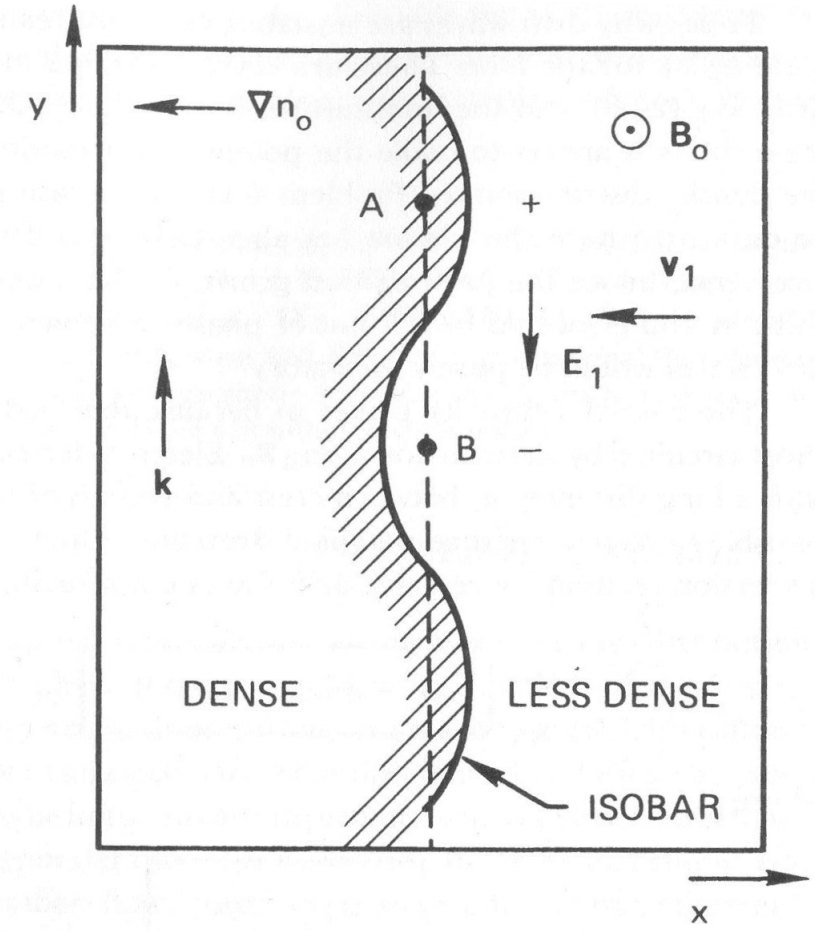

Figure 2.1: Figure taken from Chen [2], chapter 6, figure 14. Density fluctuations about its equilibrium (broken line) causes in-phase potential fluctuation in the adiabatic limit, which results in an oscillating $\mathbf{E} \times \mathbf{B}$ drift that is $\pi/2$ out of phase with respect to the density perturbation, cf. Figure refelectricdrift. Less dense plasma is transported to the left in the upper part of the figure, whereas denser plasma is transported to the right in the lower part. A stationary observer on the broken line will see plasma slushing back and forth as the perturbation propagates along the positive y-axis since the electric drift is such that it pushes the density perturbation at a fixed y-position to values it takes a little lower hence causing propagation of the density profile.

equilibrium value (cf. Figure 2.2), thus at point 2, located the distance between A and B below point B, the local plasma density will increase, whereas the local plasma density decreases at point 1 between A and B since less dense plasma flows in there. The effect is that the density is modified by the oscillating electric drift in such a way that it takes values it had a little earlier at smaller y coordinate. Thus the whole perturbation propagates in the positive y direction while the local plasma density at positions A and B is observed to slosh back and forth, as does the electric drift. Since fluctuations are perfectly in phase, there is no instability mechanism present.
We realize that any mechanism that makes the potential fluctuations lag *behind* the density fluctuations will cause the electric drift to assume its maximum value in the positive x direction at positions where the fluctuating density is greater than its equilibrium value thus enhancing the perturbation by transporting excessive plasma density away from such points and similarly, the electric drift assumes its maximum value in the negative x direction at positions where the perturbed plasma density is less than its equilibrium value, and the depletion is enhanced by plasma transport of less dense plasma into such areas. If the perturbed potential *leads* the density perturbations, there will be no instability, since the situation is reversed, and the drift maxima will occur where the density fluctuations are minimum, thus the perturbation is flattened out. Clearly the violation of Boltzmann distributed species corresponds to electrons not being able to flow along the magnetic field instantaneously in order to preserve quasi-neutrality. Thus any kind of resistivity along the magnetic field may intuitively yield instability. Mechanisms making the potential fluctuations lag the density perturbations are for instance ([1]) electron - neutral collisions, electron - ion collisions, Landau damping and inductance.
Electron - neutral collisions are present in weakly ionized gases which may occur in ionospheric plasmas.
Electron - ion collisions give rise to resistivity in fully ionized plasmas which is considered in the next section.
Wave - particle interaction yielding Landau damping is important in collision-less plasmas when the electron distribution function is disturbed by electrons with thermal velocities comparable to the drift wave phase velocity along the magnetic field, which is not the case for drift waves, since $v_{\mathrm{thi}} \ll \omega/k_z \ll v_{\mathrm{the}}$.
For high β plasmas, i.e., when the parallel phase velocity is of the order of the Alfvén speed, the representation of the electric field by an electrostatic potential is no longer valid since the magnetic field created by the electron flow back-reacts with the background magnetic field. Thus the magnetic field is no longer static and the the electric field no longer curl-free.

Resistive Drift Waves

The next step of generalization is to allow for electron-resistivity along $\mathbf{B}$, hence the name *resistive* drift waves. Then, proceeding according to Bellan [3] we derive the dispersion relation for resistive drift waves. Consider the parallel electron momentum equation with resistivity,

$$0 = e\frac{\partial \phi}{\partial z} - T_{\mathrm{e}}\frac{\partial}{\partial z}\ln(n_{\mathrm{e}}) - \nu_{\mathrm{ei}} m_{\mathrm{e}} u_{\mathrm{ez}}, \tag{2.20}$$

where the ion parallel velocity is negligible compared to the electron parallel velocity and we have again made use of $v_{\mathrm{thi}} \ll \omega/k_z \ll v_{\mathrm{the}}$. We may linearize about an equilibrium with $n_0 = n_0(x), \phi_0 = 0, u_{ez} = 0$ and take a spatial Fourier transform of the fluctuating quantities in y and z direction (the plasma is inhomogeneous in the x - direction, as before the Fourier amplitudes may depend on x, yet it is

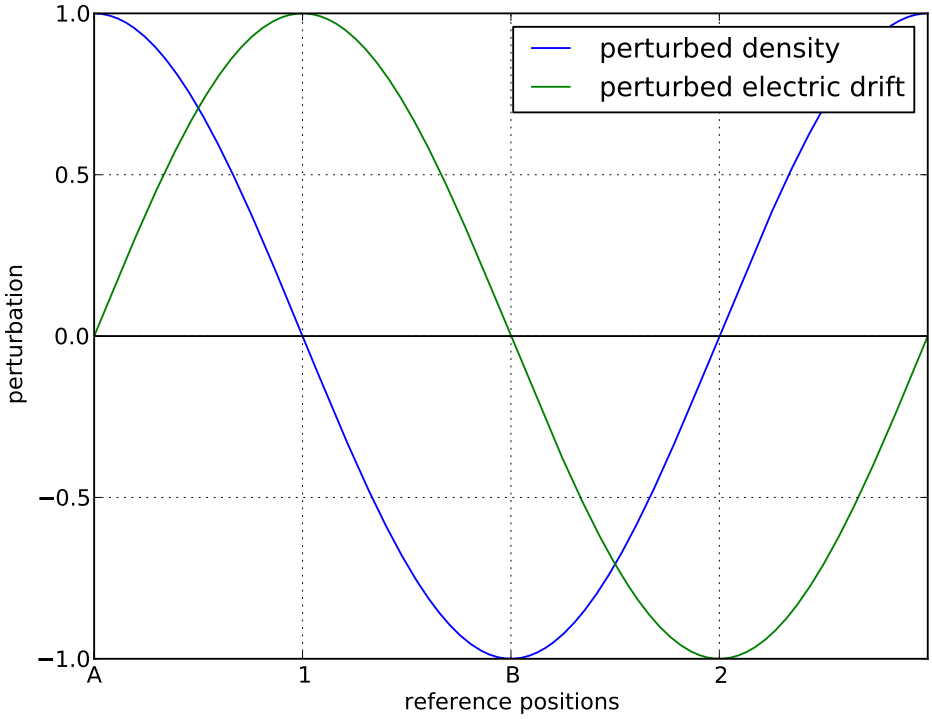

Figure 2.2: Electric drift extrema relative to perturbed density

more fruitful to assume only weak variation of amplitude in order to obtain simpler equations without considerable loss of generality). We write

$$f = f_0 + f_1 = f_0 + \widehat{f}\exp(ik_y + ik_z - i\omega t), \tag{2.21}$$

where f stands for electron density, potential or components of involved velocity respectively. The subscript "0" denotes equilibrium quantities and of course $|f_1/f_0| \ll 1$. The logarithm is treated according to

$$\ln n = \ln\left[n_0\left(1 + \frac{n_1}{n_0}\right)\right] \approx \ln n_0 + \frac{n_1}{n_0}. \tag{2.22}$$

Invoking the equilibrium given above, linearization gives the parallel electron velocity (Fourier) component

$$\widehat{u}_{\mathrm{e}z} = -\frac{ik_z T_\mathrm{e}}{\nu_{\mathrm{ei}} m_\mathrm{e}}\left(\frac{\widehat{n}_\mathrm{e}}{n_{\mathrm{e}0}} - \frac{e\widehat{\phi}}{T_\mathrm{e}}\right). \tag{2.23}$$

Assuming $|\omega_{\mathrm{ce}}/\nu_{\mathrm{ei}}| \gg 1$, we may drop the collision term for the perpendicular motion

$$0 = e\nabla_\perp\phi - e\mathbf{u}_\mathrm{e}\times\mathbf{B} - T_\mathrm{e}\nabla_\perp \ln n_\mathrm{e}, \tag{2.24}$$

and the inertia term is negligible compared to the pressure term in virtue of $\omega/k_z \ll v_{\mathrm{the}}$. The perpendicular electron flux is now given by

$$\mathbf{\Gamma}_{\mathrm{e}\perp} = n_\mathrm{e}\mathbf{u}_{\mathrm{e}\perp} = -\frac{n_\mathrm{e}}{B^2}\nabla_\perp\phi\times\mathbf{B} + \frac{T_\mathrm{e}}{eB^2}\nabla_\perp n_\mathrm{e}\times\mathbf{B}. \tag{2.25}$$

Substituting the perpendicular electron flux in the electron continuity equation on the form

$$\frac{\partial n_\mathrm{e}}{\partial t} + \nabla\cdot\mathbf{\Gamma}_{\mathrm{e}\perp} + \frac{\partial}{\partial z}(n_\mathrm{e}u_{\mathrm{e}z}) = 0, \tag{2.26}$$

yields

$$\frac{\partial n_\mathrm{e}}{\partial t} + \frac{\partial}{\partial z}(n_\mathrm{e}u_{\mathrm{e}z}) - \frac{1}{B^2}\nabla n_\mathrm{e}\cdot\nabla\phi\times\mathbf{B} = 0, \tag{2.27}$$

where we have used that the electric and diamagnetic drifts are incompressible in the magnetic field configuration we are using here. Linearizing about the equilibrium stated above we find

$$\frac{\partial n_{\mathrm{e}1}}{\partial t} + n_{\mathrm{e}0}\frac{\partial}{\partial z}u_{\mathrm{e}z1} - \frac{n'_{\mathrm{e}0}}{B^2}\widehat{\mathbf{x}}\cdot\nabla\phi_1\times\mathbf{B} = 0. \tag{2.28}$$

Ivoking Eq. (2.21) for the fluctuating density and potential and also using Eq. (2.23) for the Fourier amplitude of the fluctuating parallel velocity component we arrive at

$$-i\omega\frac{\widehat{n}_\mathrm{e}}{n_{\mathrm{e}0}} + n_{\mathrm{e}0}ik_z\left[-\frac{ik_z T_\mathrm{e}}{\nu_{\mathrm{ei}} m_\mathrm{e}}\left(\frac{\widehat{n}}{n_{\mathrm{e}0}} - \frac{e\widehat{\phi}}{T_\mathrm{e}}\right)\right] + \frac{ik_y\widehat{\phi}}{BL_n} = 0, \tag{2.29}$$

which may be rearranged to obtain

$$\frac{\widehat{n}}{n_{\mathrm{e}0}} = \frac{e\widehat{\phi}}{T_\mathrm{e}}\frac{\left(-i\omega_* + \frac{1}{\tau_\shortparallel}\right)}{\left(-i\omega + \frac{1}{\tau_\shortparallel}\right)}, \tag{2.30}$$

where we have introduced the nominal time required for electrons to diffuse a distance of the order of a parallel wavelength, $\tau_\shortparallel = \nu_{\mathrm{ei}} m_\mathrm{e}/k_z^2 T_\mathrm{e}$. This is readily seen by considering the parallel diffusion coefficient $D_\shortparallel = (\Delta z)^2/\nu_{\mathrm{ei}} \sim v_{\mathrm{the}}^2/\nu_{\mathrm{ei}} = T_\mathrm{e}\nu_{\mathrm{ei}}/m_\mathrm{e}$

, where Δz denotes a random step length in the parallel direction. It is then clear that $\tau_{\shortparallel} \to 0$ corresponds to Boltzmann distribution, whereas $\tau_{\shortparallel} \neq 0$ introduces a phase lag between density and potential fluctuations which ultimately is the cause for drift wave instability as we shall see shortly.
The idea is to find an expression for the ion density perturbation as a function of the perturbed potential, invoking quasi-neutrality should then lead to the dispersion relation we set out to determine. The ion equation of motion for cold and singly charged ions, i.e., $q_{\mathrm{i}} = e$,

$$M\frac{d}{dt}\mathbf{u}_{\mathrm{i}} = e(-\nabla\phi + \mathbf{u}_{\mathrm{i}} \times \mathbf{B}) - \nu_{\mathrm{ie}}M(\mathbf{u}_{\mathrm{i}} - \mathbf{u}_{\mathrm{e}}), \tag{2.31}$$

may be linearized in the parallel direction under the assumption that the inertial term is much larger than the collisional term. Note that we have introduced the lowest order convective derivative

$$\frac{d}{dt} = \frac{\partial}{\partial t} + \mathbf{v}_{\mathrm{E}} \cdot \nabla = \frac{\partial}{\partial t} - \frac{1}{B^2}\nabla\phi \times \mathbf{B} \cdot \nabla.$$

The linearized parallel component of the ion equation of motion is readily found to be

$$M\frac{\partial}{\partial t}\mathbf{u}_{\mathrm{i}1} = -e\nabla\phi_1 + \mathbf{u}_{\mathrm{i}1} \times \mathbf{B}, \tag{2.32}$$

where we have linearized about the equilibrium $\phi_0 = 0$, $\mathbf{u}_{\mathrm{i}0} = 0$. Using Eq. (2.21) we find

$$\widehat{u}_{\mathrm{i}z} = \frac{ek_z\widehat{\phi}}{\omega M} = \frac{k_z C_{\mathrm{s}}^2}{\omega}\frac{e\widehat{\phi}}{T_{\mathrm{e}}}. \tag{2.33}$$

Similarly we find the linearized ion perpendicular equation of motion

$$M\frac{\partial}{\partial t}\mathbf{u}_{\mathrm{i}1\perp} = -e\nabla_\perp\phi_1 + e\mathbf{u}_{\mathrm{i}\perp 1} \times \mathbf{B}, \tag{2.34}$$

which upon iteration of the RHS by the linearized electric drift yields

$$\mathbf{u}_{\mathrm{i}\perp 1} = -e\nabla_\perp\phi_1 \times \mathbf{B} - \frac{M}{eB^2}\frac{\partial}{\partial t}\nabla_\perp\phi_1. \tag{2.35}$$

The linearized ion perpendicular flux is

$$\mathbf{\Gamma}_{\mathrm{i}\perp 1} = n_{\mathrm{i}0}\mathbf{u}_{\mathrm{i}\perp 1},$$

with divergence

$$\nabla \cdot \mathbf{\Gamma}_{\mathrm{i}\perp 1} = -\frac{1}{B^2}\nabla n_{\mathrm{i}0}\nabla\phi_1 \times \mathbf{B} - \frac{n_{\mathrm{i}0}M}{eB^2}\frac{\partial}{\partial t}\nabla_\perp^2\phi_1. \tag{2.36}$$

The linearized ion continuity equation,

$$\frac{\partial n_{\mathrm{i}1}}{\partial t} + n_{\mathrm{i}0}\frac{\partial}{\partial z}u_{\mathrm{i}z1} + \nabla \cdot \mathbf{\Gamma}_{\mathrm{i}\perp 1} = 0, \tag{2.37}$$

then becomes

$$\frac{\partial n_{\mathrm{i}1}}{\partial t} + n_{\mathrm{i}0}\frac{\partial}{\partial z}u_{\mathrm{i}z1} - \frac{1}{B^2}\nabla n_{\mathrm{i}0}\nabla\phi_1 \times \mathbf{B} - \frac{n_{\mathrm{i}0}M}{eB^2}\frac{\partial}{\partial t}\nabla_\perp^2\phi_1 = 0. \tag{2.38}$$

Making use of Eq. (2.21) and rearranging gives

$$\frac{\widehat{n}_{\mathrm{i}}}{n_{\mathrm{i}0}} = \frac{e\widehat{\phi}}{T_{\mathrm{e}}}\left(\frac{k_z^2 C_{\mathrm{s}}^2}{\omega^2} + \frac{\omega_*}{\omega} - k_y^2\rho_{\mathrm{s}}^2\right). \tag{2.39}$$

Equating Eq. (2.30) with Eq. (2.39) by means of quasi-neutrality finally results in

$$\frac{\left(-i\omega_* + \frac{1}{\tau_{\shortparallel}}\right)}{\left(-i\omega + \frac{1}{\tau_{\shortparallel}}\right)} = \frac{k_z^2 C_{\mathrm{s}}^2}{\omega^2} + \frac{\omega_*}{\omega} - k_y^2\rho_{\mathrm{s}}^2. \tag{2.40}$$

When making the various simplifications, we have implicitly assumed that $\omega\tau_{\shortparallel} = \omega\nu_{\mathrm{ei}} m_{\mathrm{e}}/k_z^2 T_{\mathrm{e}} \ll 1$ which states that parallel diffusion is not dominant on the time scale of the wave period and $\omega \sim \omega_*$ which is necessary in order for Eq. (2.21) to be valid. The LHS may be expanded in the small parameter $\omega\tau_{\shortparallel}$ such that

$$\begin{aligned}\frac{\left(-i\omega_* + \frac{1}{\tau_{\shortparallel}}\right)}{\left(-i\omega + \frac{1}{\tau_{\shortparallel}}\right)} &\approx 1 + i(\omega - \omega_*)\tau_{\shortparallel} + \omega_*\omega\tau_{\shortparallel}^2 \\ &\approx 1 + i(\omega - \omega_*)\tau_{\shortparallel}.\end{aligned}$$

The dispersion relation may thus be cast in the form

$$D(\omega, k_y, k_z) = 1 - \frac{\omega_*}{\omega} - \frac{k_z^2 C_{\mathrm{s}}^2}{\omega^2} + k_y^2\rho_{\mathrm{s}}^2 + i(\omega - \omega_*)\tau_{\shortparallel} = 0. \tag{2.41}$$

For clarity, we split up the dispersion relation into its real and imaginary part according to

$$D = D_r + iD_i,$$

where

$$D_r = 1 - \frac{\omega_*}{\omega} + k_y^2\rho_{\mathrm{s}}^2 - \frac{k_z^2 C_{\mathrm{s}}^2}{\omega^2},$$

and

$$D_i = (\omega - \omega_*)\tau_{\shortparallel}.$$

The drift mode distincts itself from the ion acoustic wave by a much greater phase velocity, $\omega/k_z \gg C_{\mathrm{s}}$, thus we may neglect the last term for the real part of the dispersion relation above. We may assume that the drift wave is weakly damped/growing and check for consistency later, then $\omega_i \ll \omega_r$ and we expand Eq. (2.41) in the small parameter $i\omega_i$ to second order:

$$\begin{aligned}D(\omega_r + i\omega_i) &\approx D_r(\omega)|^{\omega=\omega_r} + iD_i(\omega)|^{\omega=\omega_r} + (i\omega_i)\left(\frac{\partial D_r}{\partial\omega}\right)\Bigg|^{\omega=\omega_r} + i(i\omega_i)\left(\frac{\partial D_i}{\partial\omega}\right)\Bigg|^{\omega=\omega_r} \\ &= \left[D_r(\omega_r) - \omega_i\left(\frac{\partial D_i}{\partial\omega}\right)\Bigg|^{\omega=\omega_r}\right] + i\left[D_i(\omega_r) + \omega_i\left(\frac{\partial D_r}{\partial\omega}\right)\Bigg|^{\omega=\omega_r}\right] \\ &\approx D_r(\omega_r) + i\left[(\omega_r - \omega_*)\tau_{\shortparallel} - \omega_i\frac{\omega_*}{\omega_r^2}\right]\end{aligned}$$

Insisting that the dispersion relation vanishes identically, i.e., for both real and imaginary part we find

$$\omega_r = \frac{\omega_*}{1 + k_y^2\rho_{\mathrm{s}}^2}, \tag{2.42}$$

and

$$\begin{aligned}\omega_i &= -\omega_*\frac{(\omega_r - \omega_*)\tau_{\shortparallel}}{(1 + k_y^2)^2\rho_{\mathrm{s}}^2} \\ &= \omega_*\tau_{\shortparallel}\frac{(1 + k_y^2\rho_{\mathrm{s}}^2)\omega_* - \omega_*}{(1 + k_y^2\rho_{\mathrm{s}}^2)^3} \\ &= \omega_*\tau_{\shortparallel}\frac{\omega_* k_y^2\rho_{\mathrm{s}}^2}{(1 + k_y^2\rho_{\mathrm{s}}^2)^3}.\end{aligned} \tag{2.43}$$

Checking for consistency,

$$\omega_i/\omega_r = \omega_* \tau_{\shortparallel} \frac{k_y^2 \rho_{\rm s}^2}{(1+k_y^2\rho_{\rm s}^2)^2} \ll 1,$$

since $\omega_* \sim \omega$ and $\omega\tau_{\shortparallel} \ll 1$. As indicated before, we have found that collisional drift waves are always unstable since the growth rate is positive definite. Furthermore it is the phase lag between potential and density fluctuations that causes the instability, as can be seen by $\tau_{\shortparallel}$ and thus $\nu_{\rm ei}$ appearing explicitly in the above expression. The longer the parallel wavelength, the stronger is the growth rate (recall $\tau_{\shortparallel} \sim k_z^{-2}$), thus we may expect drift waves to have the longest possible parallel wavelength subject to the boundary conditions. Note that the presence of ${\omega_*}^2$, which is proportional to L^{-2}, indicates that drift waves are occurring whenever there is a considerable density gradient, which typically is the case near the edge of confined plasmas. The growth rate has a maximum for $k_y\rho_{\rm s} \sim 1$.

2.2 Turbulence driven transport

Collisional transport

In the preceding section we have neglected diffusion and viscosity to highlight the underlying physics. To be consistent, but mainly for numerical purposes, it is of significant importance to include diffusional and viscous effects. Let us first consider diffusion and to this end, consider the two-fluid momentum equation for particle species α co-existing with particle species β,

$$m_\alpha n_\alpha \left(\frac{\partial}{\partial t} + \mathbf{u}_\alpha \cdot \nabla\right) \mathbf{u}_\alpha = -\nabla p_\alpha + q_\alpha n_\alpha \left(\mathbf{E} + \mathbf{u}_\alpha \times \mathbf{B}\right) - m_\alpha n_\alpha \nu_{\alpha\beta} (\mathbf{u}_\alpha - \mathbf{u}_\beta),$$

where $\nu_{\alpha\beta}$ is the momentum relaxation rate of particle species α due to collisions with species β. Now, the perpendicular drift in increasing order of $\delta = \rho_{\rm s}/L$, where L is the characteristic length scale of field quantities, is readily found to be

$$\mathbf{u}_{\perp\alpha} = \mathbf{u}_{\rm E} + \mathbf{u}_{d\alpha} + \mathbf{u}_{p\alpha} + \mathbf{u}_{\nu\alpha} + \mathcal{O}(\delta^3),$$

where the electric drift, diamagnetic drift, polarization drift and resistive drift are given by

$$\begin{aligned}
\mathbf{u}_{\rm E} &= \frac{1}{B^2}\mathbf{E}_\perp \times \mathbf{B}, \\
\mathbf{u}_{d\alpha} &= -\frac{1}{q_\alpha n_\alpha B}\nabla_\perp p_\alpha \times \mathbf{b}, \\
\mathbf{u}_{p\alpha} &= \frac{1}{\omega_{{\rm c}\alpha} B}\left[\frac{\partial}{\partial t}\mathbf{E}_\perp + (\mathbf{u}_{{\rm E}_\perp} \cdot \nabla_\perp)\mathbf{E}\right], \\
\mathbf{u}_{\nu\alpha} &= \frac{\nu_{\alpha\beta}}{\omega_{{\rm c}\alpha}}\mathbf{b} \times (\mathbf{u}_\alpha - \mathbf{u}_\beta).
\end{aligned}$$

To obtain an expression for the resistive drift, we iterate the RHS of the last expression above to first order in δ. Assuming cold ions and isothermal electrons for simplicity this results in

$$\begin{aligned}
\mathbf{u}_{\nu{\rm e}} &= -\frac{\nu_{\rm ei}}{\omega_{\rm ce}}\left(\frac{T_{\rm e}}{e n_{\rm e} B}\nabla_\perp n_{\rm e}\right), \\
\mathbf{u}_{\nu{\rm i}} &= -\frac{\nu_{\rm ie}}{\omega_{\rm ci}}\left(\frac{T_{\rm e}}{e n_{\rm e} B}\nabla_\perp n_{\rm e}\right).
\end{aligned}$$

Momentum conservation requires the momentum transfer from species α to species β to be equal, hence we have the constraint

$$m_\alpha n_\alpha \nu_{\alpha\beta} = m_\beta n_\beta \nu_{\beta\alpha},$$

which gives upon invoking quasi neutrality

$$\nu_{\mathrm{ie}} = \frac{m_\mathrm{e}}{m_\mathrm{i}} \nu_{\mathrm{ei}}.$$

Using the above we find that both ions and electrons have the same resistive drift

$$\mathbf{u}_r = -\frac{m_\mathrm{e}\nu_{\mathrm{ei}} T_\mathrm{e}}{e^2 n_\mathrm{e} B^2} \nabla_\perp n_\mathrm{e}.$$

Inserting this drift into the continuity equation for either electron or ions, we obtain a diffusion equation,

$$\frac{\partial n}{\partial t} - \frac{m_\mathrm{e}\nu_{\mathrm{ei}} T_\mathrm{e}}{e^2 B^2} \nabla_\perp^2 n = 0,$$

thus we may define the two-fluid diffusion coefficient

$$D_{\mathrm{classical}} = \frac{m_\mathrm{e}\nu_{\mathrm{ei}} T_\mathrm{e}}{e^2 n_\mathrm{e} B^2}. \tag{2.44}$$

We find that collisions causes perpendicular drift through the proportionality with respect to ν_{ei}, whereas a strong **B**-field reduces the cross field transport by confining particles to magnetic field lines.

Viscosity

Following standard fluid dynamics, we approximate the divergence of the stress tensor that enters the momentum equations similarly to what is customary for the two-dimensional Navier-Stokes equation by $\mu\nabla^2\mathbf{v}$, where μ is the dynamic viscosity due to shearing of neighboring fluid elements on each other.

Quasi-linear effective diffusion

The time averaged radial drift wave induced particle flux is given by

$$\begin{aligned}
\Gamma_x &= \langle \Re(n_1)\ \Re(u_{1x}) \rangle \\
&= \left\langle \frac{1}{2}\left(\widehat{n} e^{i\theta} + \widehat{n}^* e^{-i\theta} \right) \frac{1}{2} (\widehat{u}_{1x} e^{i\theta} + \widehat{u}_{1x}^* e^{-i\theta} \right) \Bigg\rangle \\
&= \left\langle \frac{1}{4}\left(\widehat{n}\widehat{u}_{1x} e^{2i\theta} + \widehat{n}^*\widehat{u}_{1x} + \widehat{u}_{1x}^*\widehat{n} + \widehat{n}^*\widehat{u}_{1x}^* e^{-2i\theta} \right) \right\rangle \\
&= \frac{1}{4}\left(\widehat{n}^*\widehat{u}_{1x} + \widehat{u}_{1x}^*\widehat{n} \right) \\
&= \frac{1}{4}\left(\widehat{n}\widehat{u}_{1x}^* + (\widehat{n}\widehat{u}_{1x}^*)^* \right) \\
&= \frac{1}{2}\Re\left(n_1\ u_{1x}^* \right).
\end{aligned}$$

To lowest order the radial velocity for both ions and electrons is given by the x component of the electric drift,

$$u_{1x} = -\widehat{\mathbf{x}} \cdot \frac{1}{B^2} \nabla\phi_1 \times \mathbf{B} = -\frac{ik_y \widehat{\phi}}{B}. \tag{2.45}$$

The electron density perturbation from Eq. (2.30) with the RHS expanded as before is (recall that ω^* is in fact real and the drift wave frequency)

$$\widehat{n} = \frac{n_0 e\widehat{\phi}}{T_\mathrm{e}} \left(1 - i(\omega^* - \omega)\tau_{\shortparallel}\right). \tag{2.46}$$

Inserting both expressions in the time averaged particle flux yields

$$\begin{aligned}
\Gamma_x &= \frac{1}{2}\Re\left[\frac{n_0 e\widehat{\phi}}{T_\mathrm{e}}\left(1 - i(\omega^* - \omega)\tau_{\shortparallel}\right)\frac{ik_y\widehat{\phi}^*}{B}\right] \\
&= \frac{1}{2}\Re\left[\frac{n_0 e}{T_\mathrm{e}}(\omega^* - \omega)\tau_{\shortparallel}\frac{k_y\left|\widehat{\phi}\right|^2}{B}\right] \\
&= \left(\frac{k_y^2\rho_\mathrm{s}^2}{1 + k_y^2\rho_\mathrm{s}^2}\right)\frac{k_y^2\left|\phi_1\right|^2}{2L_n B^2}\frac{\nu_\mathrm{ei} n_0 m_\mathrm{e}}{k_z^2 T_\mathrm{e}} \\
&= -D_\mathrm{dw}\frac{dn_0}{dx},
\end{aligned}$$

where we have introduced the drift wave induced diffusion coefficient

$$D_\mathrm{dw} = \left(\frac{k_y^2\rho_\mathrm{s}^2}{1 + k_y^2\rho_\mathrm{s}^2}\right)\frac{k_y^2\left|\phi_1\right|^2}{2B^2}\frac{\nu_\mathrm{ei} m_\mathrm{e}}{k_z^2 T_\mathrm{e}}. \tag{2.47}$$

It is indeed the equilibrium density profile gradient that drives the outward particle flux, which we may interpret as some kind of wave induced diffusion, which is why we have introduced the diffusion coefficient. Hence, the density gradient provides the free energy necessary for the drift wave instability to occur. Note that the diffusive property of the particle flux implies that the equilibrium density gradient eventually will be flattened out if there are no external agencies sustaining it.
Recall the classical two-fluid (and MHD) diffusion coefficient from the previous section

$$D_\mathrm{classical} = \frac{m_\mathrm{e}\nu_\mathrm{ei} T_\mathrm{e}}{e^2 B^2}, \tag{2.48}$$

such that the ratio between drift wave induced and classical diffusion is given by

$$\frac{D_\mathrm{dw}}{D_\mathrm{classical}} = \left(\frac{k_y^2\rho_\mathrm{s}^2}{1 + k_y^2\rho_\mathrm{s}^2}\right)\frac{e^2 k_y^2\left|\phi_1\right|^2}{2k_z^2 T_\mathrm{e}^2}, \tag{2.49}$$

we may consider the typical case $k_y\rho_\mathrm{s} \sim 1$, then

$$\frac{D_\mathrm{dw}}{D_\mathrm{classical}} \sim \left(\frac{e\left|\phi_1\right|}{T_\mathrm{e}}\right)^2\frac{1}{k_z^2\rho_\mathrm{s}^2}, \tag{2.50}$$

which for long wavelengths in the parallel direction reveals that drift wave induced diffusion down the density profile gradient is (far) more dominant than classical diffusion provided that $e\left|\phi_1\right|/T_\mathrm{e} > k_z\rho_\mathrm{s}$.

2.3 The Ordinary Hasegawa - Wakatani model (OHW)

We start out with the familiar **B** perpendicular velocities for electrons, retaining the electric- and diamagnetic drift, and ions, retaining the electric-, inertial- and viscous drift respectively. This is equivalent to assuming cold ions and neglecting

electron inertia due to their high mobility. We shall use rectilinear coordinates with the magnetic field being constant along the positive z-direction, $\mathbf{B} = B\hat{\mathbf{z}}$.

$$\mathbf{u}_{\perp \mathrm{e}} = -\frac{1}{B^2}\nabla_\perp \phi \times \boldsymbol{B} + \frac{T_\mathrm{e}}{eB^2}\nabla_\perp \ln n_\mathrm{e} \times \boldsymbol{B} \tag{2.51a}$$

$$\mathbf{u}_{\perp \mathrm{i}} = -\frac{1}{B^2}\nabla_\perp \phi \times \boldsymbol{B} - \frac{M}{eB^2}\left(\frac{\partial}{\partial t} - \frac{1}{B^2}\nabla_\perp \phi \times \boldsymbol{B} \cdot \nabla_\perp\right)\nabla_\perp \phi + \frac{\mu}{\omega_{\mathrm{ci}} B}\nabla^2 \nabla \phi \tag{2.51b}$$

Here M denotes the ion mass, μ is the $\mathbf{B}$ perpendicular ion viscosity and $\omega_{\mathrm{ci}} = eB/M$ is the ion cyclotron frequency (for singly charged ions). Note that $\nabla_\perp \cdot \mathbf{u}_{\perp \mathrm{e}} = 0$. From $\boldsymbol{j} = -en_\mathrm{e}\boldsymbol{u}_\mathrm{e}$ we deduce the linearized current density $\mathbf{j}_1 = -en_0\mathbf{u}_{\mathrm{e}1}$ and it follows $\nabla_\parallel u_{\parallel 1} = -\frac{1}{en_0}\frac{\partial}{\partial z} j_{z1}$. Using the above and (2.51a) in the electron continuity equation we obtain

$$\frac{\partial}{\partial t}\ln n_\mathrm{e} + \frac{1}{B}\widehat{\mathbf{z}} \times \nabla_\perp \phi \cdot \nabla_\perp \ln n_\mathrm{e} = \frac{1}{en_0}\frac{\partial}{\partial z} j_{z1} \tag{2.52}$$

In the $\mathbf{B}$ parallel direction we include resistivity in the electron momentum equation, whose z-component when neglecting electron inertia
(provided $\omega \ll \nu_{\mathrm{ei}}$, the electron - ion momentum relaxation rate) is given by

$$en_\mathrm{e}\frac{\partial \phi}{\partial z} - T_\mathrm{e}\frac{\partial n_\mathrm{e}}{\partial z} + \zeta e n_0 j_{z1} = 0, \tag{2.53}$$

where $\zeta = m\nu_{\mathrm{ei}}/n_0 e^2$ is the (electron) resistivity.
This may be rearranged to express the parallel current as

$$j_{z1} = \frac{T_\mathrm{e}}{e\zeta}\frac{\partial}{\partial z}\left(\ln n_\mathrm{e} - \frac{e\phi}{T_\mathrm{e}}\right) \tag{2.54}$$

Inserting (2.54) into the electron continuity equation (2.52), we obtain a relation between density and potential fluctuations due to electron dynamics

$$\frac{\partial}{\partial t}\ln n_\mathrm{e} + \frac{1}{B}\widehat{\mathbf{z}} \times \nabla_\perp \phi \cdot \nabla_\perp \ln n_\mathrm{e} = \frac{1}{en_\mathrm{e}}\frac{T_\mathrm{e}}{e\zeta}\frac{\partial^2}{\partial z^2}\left(\ln n_\mathrm{e} - \frac{e\phi}{T_\mathrm{e}}\right) \tag{2.55}$$

Considering the ions, we firstly approximate the ion continuity equation according to

$$\frac{\partial \ln n_\mathrm{i}}{\partial t} + \nabla \cdot \boldsymbol{u}_{\perp \mathrm{i}} + \boldsymbol{u}_E \cdot \nabla \ln n_\mathrm{i} = 0 \tag{2.56}$$

where we have assumed that the advection is dominated by the electric drift.

When calculating the divergence of the viscous drift we realize that $\nabla \cdot \nabla^2 \nabla \phi$ using index notation is just

$$\frac{\partial}{\partial x_i}\frac{\partial}{\partial x_j}\frac{\partial}{\partial x_j}\frac{\partial \phi}{\partial x_i} \tag{2.57}$$

and we readily see that the "i"s and "j"s commute to give

$$\frac{\partial}{\partial x_j}\frac{\partial}{\partial x_j}\frac{\partial}{\partial x_i}\frac{\partial \phi}{\partial x_i} \tag{2.58}$$

which in turn results in $\nabla^2 \nabla^2 \phi = \nabla^4 \phi$. We also apply $\nabla_\perp \phi \times \boldsymbol{B} \cdot \nabla_\perp \phi = 0$ and $\nabla_\perp \cdot (\nabla_\perp \phi \times \boldsymbol{B} \cdot \nabla_\perp)\nabla_\perp \phi = (\nabla_\perp \phi \times \boldsymbol{B} \cdot \nabla_\perp)\nabla_\perp^2 \phi$.

Calculating (2.56) using the above and inserting from (2.51b) the ion continuity equation becomes

$$\frac{\partial}{\partial t}\left(\ln n_{\mathrm{i}}-\frac{1}{B\omega_{\mathrm{ci}}}\nabla_{\perp}^{2}\phi\right)+\frac{1}{B}\widehat{\mathbf{z}}\times\nabla_{\perp}\phi\cdot\nabla_{\perp}\left(\ln n_{\mathrm{i}}-\frac{1}{B\omega_{\mathrm{ci}}}\nabla_{\perp}^{2}\phi\right)=-\frac{\mu}{\omega_{\mathrm{ci}}B}\nabla_{\perp}^{4}\phi \tag{2.59}$$

Let us now assume *quasi-neutrality*, i.e. $n_{\mathrm{e}}\approx n_{\mathrm{i}}$, and discard the indices labeling the densities. It is customary to simplify (2.59) and (2.55) by perturbing the density as previously according to $n=n_0+n_1=n_0(1+n_1/n_0)$ where $n_1\ll n_0$ and the subscript zero denotes an equilibrium quantity. The logarithm is linearized as before, cf. Eq. (2.22),

$$\ln n=\ln\left[n_0\left(1+\frac{n_1}{n_0}\right)\right]=\ln n_0+\ln\left(1+\frac{n_1}{n_0}\right)\approx\ln n_0+\frac{n_1}{n_0} \tag{2.60}$$

where the smallness of the fluctuating part is exploited by means of a Taylor expansion.

The equations we have arrived at by now are

$$\frac{\partial}{\partial t}\left(\frac{n_1}{n_0}\right)+\frac{1}{B}\widehat{\mathbf{z}}\times\nabla_{\perp}\phi\cdot\nabla_{\perp}\left(\frac{n_1}{n_0}\right)-\frac{1}{B}\frac{n_0'}{n_0}\frac{\partial\phi}{\partial y}=\frac{1}{en_0}\frac{T_{\mathrm{e}}}{e\zeta}\frac{\partial^2}{\partial z^2}\left(\frac{n_1}{n_0}-\frac{e\phi}{T_{\mathrm{e}}}\right) \tag{2.61}$$

$$\begin{aligned}\frac{\partial}{\partial t}\left(\frac{n_1}{n_0}\right)+\frac{1}{B}\widehat{\mathbf{z}}\times\nabla_{\perp}\phi\cdot\nabla_{\perp}\left(\frac{n_1}{n_0}\right)-\frac{1}{B}\frac{n_0'}{n_0}\frac{\partial\phi}{\partial y}=\\ \frac{\partial}{\partial t}\frac{1}{B\omega_{\mathrm{ci}}}\nabla_{\perp}^{2}\phi+\frac{1}{B}\widehat{\mathbf{z}}\times\nabla_{\perp}\phi\cdot\nabla_{\perp}\frac{1}{B\omega_{\mathrm{ci}}}\nabla_{\perp}^{2}\phi-\frac{\mu}{\omega_{\mathrm{ci}}B}\nabla_{\perp}^{4}\phi\end{aligned} \tag{2.62}$$

Substituting (2.61) in (2.62) gives

$$\frac{\partial}{\partial t}\frac{1}{B\omega_{ci}}\nabla_{\perp}^{2}\phi+\frac{1}{B}\widehat{z}\times\nabla_{\perp}\phi\cdot\nabla_{\perp}\frac{1}{B\omega_{ci}}\nabla_{\perp}^{2}\phi-\frac{\mu}{\omega_{ci}B}\nabla_{\perp}^{4}\phi=\frac{1}{en_0}\frac{T_e}{e\zeta}\frac{\partial^2}{\partial z^2}\left(\frac{n_1}{n_0}-\frac{e\phi}{T_e}\right) \tag{2.63}$$

At this point it is convenient to normalize (2.61) and (2.63) according to

$$\begin{aligned}(x,y)\rightarrow&\rho_{\mathrm{s}}(x',y'),z\rightarrow\lambda_c z',\omega_{ci}t\rightarrow t',\\ &\frac{n_1}{n_0}\rightarrow\eta,\frac{e\phi}{T_e}\rightarrow\Phi\end{aligned} \tag{2.64}$$

where $\rho_s^2=\frac{T_e}{M}/\omega_{ci}^2$ is the ion gyration radius at electron temperature and λ_c the collisional mean-free path of the electrons (along the magnetic field lines).

We use the chain rule for the various differential operators and recall the definition of the normalized density scaling length, $\kappa=\rho_{\mathrm{s}}n_0'/n_0$ (assumed to be constant

and the density gradient must, of course, not be too violent). Furthermore, we introduce the parameter describing the coupling of the equations,

$$\mathcal{C} = T_e/e^2 n_0 \zeta \omega_{ci} \lambda_c. \tag{2.65}$$

Now, realizing that the equilibrium density profile is only a function of x, we obtain the normalized *Hasegawa-Wakatani* equations (Hasegawa & Wakatani [4])

$$\left(\frac{\partial}{\partial t} + \widehat{\mathbf{z}} \times \nabla_\perp \Phi \cdot \nabla_\perp\right) \nabla_\perp^2 \Phi = \mathcal{C} \frac{\partial^2}{\partial z^2}(\eta - \Phi) + \varpi \nabla_\perp^4 \Phi \tag{2.66a}$$

$$\left(\frac{\partial}{\partial t} + \widehat{\boldsymbol{z}} \times \nabla_\perp \Phi \cdot \nabla_\perp\right) \eta + \kappa \frac{\partial}{\partial y} \Phi = \mathcal{C} \frac{\partial^2}{\partial z^2}(\eta - \Phi), \tag{2.66b}$$

where we have re-labeled the primes to the more convenient unprimed form insisting that all coordinates are normalized and we have also normalized the diffusion coefficient according to

$$\varpi = \frac{\mu T_\mathrm{e}}{e \omega_\mathrm{ci}^2 B \rho_\mathrm{s}^4}.$$

Note from section Collisional transport that we really should include the diffusive drift when evaluating the continuity equation. This merely introduces a diffusion term for the density as was shown there and we shall make use of this now. Furthermore, numerical studies in three dimensions demand a great deal of computational power, hence the above model is customary taken to be two-dimensional by assuming that fluctuations along the magnetic field can be described by a *constant* wavenumber ([17],[26]), $\partial_z \to ik_z$ and $\partial_{zz}^2 \to -k_z^2$. Defining the *adiabacity* parameter

$$\alpha = T_e k_z^2 / e^2 n_0 \zeta \omega_{ci} \lambda_c,$$

and introducing the vorticity as $\Omega = \nabla^2 \phi$, we obtain the two-dimensional Hasegawa Wakatani system

$$\frac{\partial \Omega}{\partial t} + \{\phi, \Omega\} = \alpha\,(\phi - n) + D^\Omega \nabla_\perp^2 \Omega \tag{2.67a}$$

$$\frac{\partial n}{\partial t} + \{\phi, n\} = \alpha\,(\phi - n) - \kappa \frac{\partial \phi}{\partial y} + D_\mathrm{classical} \nabla^2 n. \tag{2.67b}$$

Eq. (2.67a) is indeed the evolution equation for the vorticity. Let us interpret the electrostatic potential as the stream function for our flow field, $\mathbf{v} = \widehat{\mathbf{z}} \times \nabla \phi$. Then, from fluid dynamics, we define the vorticity according to $\boldsymbol{\Omega} = \nabla \times \mathbf{v}$. Calculating the curl of the electric drift yields

$$\begin{aligned}
\boldsymbol{\Omega} &= \nabla \times (\widehat{\mathbf{z}} \times \nabla \phi) \\
&= \widehat{\mathbf{z}}(\nabla \cdot \nabla \phi) - \nabla \phi (\nabla \cdot \widehat{\mathbf{z}}) + (\nabla \phi \cdot \nabla)\widehat{\mathbf{z}} - (\widehat{\mathbf{z}} \cdot \nabla)\nabla \phi \\
&= \widehat{\mathbf{z}} \nabla^2 \phi \\
&\equiv \Omega \widehat{\mathbf{z}},
\end{aligned}$$

where we have used that the fluctuations in the potential are two-dimensional. Considering the highly adiabatic regime of the Hasegawa Wakatani system,i.e., $n \to \phi$, we find after subtracting the vorticity equation from the density equation

$$\left(1 - \nabla_\perp^2\right) \frac{\partial}{\partial t} \phi + \kappa \frac{\partial}{\partial y} \phi - \mathbf{v}_E \cdot \nabla \nabla_\perp^2 \phi = 0\ , \tag{2.68}$$

which is the conventional form of the Hasegawa Mima equation commented on in the next section.

2.4 The Modified Hasegawa - Wakatani model (MHW)

Fluctuating vs. Zonal components

The purpose of this project is to investigate the role of zonal flows in the self-consistent drift wave - zonal flow system. To proceed analytically from the Hasegawa-Wakatani model is rather difficult, therefore we shall restrict our analytical considerations to the *adiabatic* limit, i.e., $\mathcal{C} \to \infty$. To this end we shall reduce the Hasegawa - Wakatani model to a modified version, which in turn can be analyzed in the adiabatic limit by means of the modified Hasegawa - Mima equation, which we shall derive in the next section. Let us first shed light on what we mean by zonal- and fluctuating components. We separate the fields into a small - scale fluctuating part and a y-averaged part which we may interpret as a zonal flow, i.e. an elongated structure in the azimuthal direction; in the approximated rectilinear coordinate system we are using this may be expressed as $k_y = 0$. We have,

$$\begin{aligned} n &= \bar{n}(x,t) + \widetilde{n}(x,y,z,t), \\ \phi &= \bar{\phi}(x,t) + \widetilde{\phi}(x,y,z,t) \end{aligned} \tag{2.69}$$

where the zonal part of a scalar field $f = f(x,y,z,t)$ is defined as

$$\bar{f}(x,t) = \frac{1}{L_y}\int_0^{L_y} f(x,y,z,t)dy \tag{2.70}$$

and L_y is the domain length in the y-direction. There are two trivial consequences from the definitions, applying (2.70) we find

$$\bar{\bar{f}} = \frac{1}{L_y}\int_0^{L_y} \bar{f}(x)dy = \bar{f}, \tag{2.71}$$

and

$$\bar{\widetilde{f}} = \frac{1}{L_y}\int_0^{L_y} (f - \bar{f})dy = \frac{1}{L_y}\int_0^{L_y} f dy - \bar{f} = 0\ . \tag{2.72}$$

One can easily appreciate the existence of zonal flows, and therefore justify the decomposition of field quantities in zonal averages and fluctuating components (Diamond *et al.* [5]). Zonal flows are not capable of driving radial plasma transport. This may easily be seen upon calculating the flux associated with a zonal structure in the electrostatic potential, $\overline{\phi}$. The associated particle flux is given by

$$\mathbf{\Gamma}^{\mathrm{ZF}} = n\overline{\mathbf{v}}_E = n\widehat{\mathbf{z}} \times \nabla\overline{\phi} = n\widehat{\mathbf{z}} \times \frac{\partial\overline{\phi}}{\partial x}\widehat{\mathbf{x}} = n\frac{\partial\overline{\phi}}{\partial x}\widehat{\mathbf{y}}, \tag{2.73}$$

thus there is no net *radial* transport associated with zonal flows. A direct consequence is that zonal flows cannot "tap" expansion free energy sources stored in for instance density gradients that are radially directed and therefore must be driven by non-linear mechanisms. They form a *benign repository* for free energy. As we shall see later, zonal flows play a major roll in the shearing process of drift waves. In the process energy is transferred from the turbulent drift waves to the quasi-stationary zonal flow, thus contributing to better confinement properties of a plasma where zonal flows are present since the drift waves are associated with radial particle flux. Zonal flows may be thought of as a transport barrier. Zonal flows act as to flatten the initial density profile which is the driving force for the radial turbulent flux,

consequently the ZF effectively removes the driving mechanism for radially induced particle flux. Equivalently one could say that for the same radial transport level a steeper background density gradient is allowed in the vicinity of a zonal flow compared to a setting with no zonal flow. Either way the zonal flow improves the confinement of the plasma substantially. An additional feature of zonal flows is that the small wavenumber allows for minimal Landau damping, which becomes important for $k\lambda_D \sim 1$.

The ordinary Hasegawa - Wakatani equations do not incorporate for the fact that the zonal components have $k_y = 0$ by definition which necessarily also implies $k_z = 0$ since fluctuations on a magnetic flux surface are effectively short-circuited by electrons flowing along the magnetic field to preserve quasi-neutrality ([7], [21]). Thus the coupling operator, $\mathcal{C}\ \partial_{zz}^2 = k_z^2$, does not act on these components and we need to write the Hasegawa - Wakatani equations in a slightly modified form.

The Hasegawa - Wakatani equations are modified to incorporate for short-circuiting on a magnetic flux surface by means of

$$\frac{\partial \Omega}{\partial t} + \{\phi, \Omega\} = \alpha \left(\widetilde{\phi} - \widetilde{n}\right) + D^{\Omega} \nabla_{\perp}^2 \Omega \tag{2.74a}$$

$$\frac{\partial n}{\partial t} + \{\phi, n\} = \alpha \left(\widetilde{\phi} - \widetilde{n}\right) - \kappa \frac{\partial \phi}{\partial y} + D^{n} \nabla_{\perp}^2 n, \tag{2.74b}$$

where now for numerical convenience also a diffusion operator for the density is introduced. The equations above are the *modified Hasegawa - Wakatani Equations* which are suited to describe zonal flows arising in drift wave turbulence. From the modified equations we see that the parameter α describes the systems ability to react adiabatically for $\alpha \to \infty$ implying $\widetilde{n} \to \widetilde{\phi}$ which reduces to the Boltzmann relation for the fluctuating components and corresponds to collisonless plasmas described by the previously derived Hasegawa - Mima equation. For $\alpha \to 0$ the system effectively decouples and merely reduces to the 2 D Navier - Stokes equation for the vorticity and an advection equation for the (passive) scalar density driven by the the flow obtained from the vorticity equation. We proceed by invoking the adiabatic limit on the fluctuating components to derive the *Modified Hasegawa - Mima Equation* (OHM), which in the litterature is also frequently referred to as the *generalized* Hasegawa - Mima Equation. Clearly, the main set - back of those simple models is, that it disregards drift wave instability, since we have explicitly assumed the field quantities to follow a Boltzmann distribution. According to our earlier derivations, see end of the section Resistive Drift Waves , we know that it is indeed the *deviation* from the Boltzmann distribution that allows drift waves to grow unstable. However, it turns out that both models may help to gain some insight into the generation mechanism of zonal flows, especially the MHM which is the appropriate equation to use in plasma physics due the consideration of the short-circuiting effect indicated earlier. We note that the HM equation does not respect this fact, however, it also describes zonal flow generation, but is more suited for atmospherical sciences, where the short-circuiting is not present. In atmospherics, this equation is commonly referred to as the *Hasegawa - Mima - Charney Equation*, where the analogy to plasma physics is incorporated by the two first names, and Charney is credited for having derived quite a similar equation as early as 1948. The analogy between zonal flows in plasmas and geostrophic fluids as well as the close relation between the different models involved is neatly described in [5]

2.5 The Modified Hasegawa - Mima model (MHM)

Consider again the modified Hasegawa - Wakatani equations without diffusion for simplicity,

$$\frac{\partial n}{\partial t} + \boldsymbol{v}_E \cdot \nabla n + \kappa \frac{\partial \phi}{\partial y} = \alpha(\widetilde{\phi} - \widetilde{n}) \tag{2.75}$$

$$\frac{\partial \nabla_\perp^2 \phi}{\partial t} + \boldsymbol{v}_E \cdot \nabla \nabla_\perp^2 \phi = \alpha(\widetilde{\phi} - \widetilde{n}) \ . \tag{2.76}$$

Writing all fields in (2.76) as fluctuating and zonal part and averaging over y we obtain,

$$\frac{\partial}{\partial t} \nabla_\perp^2 \bar{\phi} + \overline{\widetilde{\boldsymbol{v}}_E \cdot \nabla \nabla_\perp^2 \widetilde{\phi}} = 0, \tag{2.77}$$

where we have used the periodic boundary conditions

$$\phi(L_y) = \phi(0),\ \partial_y \phi(L_y) = \partial_y \phi(0),\ \partial_y^2 \phi(L_y) = \partial_y^2 \phi(0) \ ,$$

when explicitly calculating the averaged terms. Subtracting (2.77) from the expanded form of (2.76) we arrive at

$$\frac{\partial}{\partial t} \nabla_\perp^2 \widetilde{\phi} + \bar{\boldsymbol{v}_E} \cdot \nabla \nabla_\perp^2 \widetilde{\phi} + \widetilde{\boldsymbol{v}}_E \cdot \nabla \nabla_\perp^2 \bar{\phi} + \widetilde{\boldsymbol{v}}_E \cdot \nabla \nabla_\perp^2 \widetilde{\phi} - \overline{\widetilde{\boldsymbol{v}}_E \cdot \nabla \nabla_\perp^2 \widetilde{\phi}} = \alpha(\widetilde{\phi} - \widetilde{n}) \tag{2.78}$$

Averaging the density equation, (2.75), yields

$$\frac{\partial \bar{n}}{\partial t} + \overline{\widetilde{\boldsymbol{v}}_E \cdot \nabla \widetilde{n}} = 0 \tag{2.79}$$

and subtracting (2.79) from (2.75)

$$\frac{\partial \widetilde{n}}{\partial t} + \widetilde{\boldsymbol{v}}_E \cdot \nabla \bar{n} + \bar{\boldsymbol{v}}_E \cdot \nabla \widetilde{n} + \widetilde{\boldsymbol{v}}_E \cdot \nabla \widetilde{n} + \kappa \frac{\partial \widetilde{\phi}}{\partial y} - \overline{\widetilde{\boldsymbol{v}}_E \cdot \nabla \widetilde{n}} = \alpha(\widetilde{\phi} - \widetilde{n}) \tag{2.80}$$

Letting $\widetilde{n} \to \widetilde{\phi}$ we have

$$\frac{\partial \widetilde{\phi}}{\partial t} + \widetilde{\boldsymbol{v}}_E \cdot \nabla \bar{n} + \bar{\boldsymbol{v}}_E \cdot \nabla \widetilde{\phi} + \kappa \frac{\partial \widetilde{\phi}}{\partial y} = 0 \tag{2.81}$$

where now $\widetilde{\boldsymbol{v}}_E \cdot \nabla \widetilde{\phi} = 0$.
From (2.81) we subtract (2.78) (applying $\widetilde{n} \to \widetilde{\phi}$) which leaves us with

$$\begin{aligned} \frac{\partial \widetilde{\phi}}{\partial t} - \frac{\partial}{\partial t} \nabla_\perp^2 \widetilde{\phi} - \frac{\partial}{\partial t} \nabla_\perp^2 \bar{\phi} + \widetilde{\boldsymbol{v}}_{\boldsymbol{E}} \cdot \nabla \bar{n} + \bar{\boldsymbol{v}}_{\boldsymbol{E}} \cdot \nabla \widetilde{\phi} + \kappa \frac{\partial \widetilde{\phi}}{\partial y} \\ - \widetilde{\boldsymbol{v}}_{\boldsymbol{E}} \cdot \nabla \nabla_\perp^2 \bar{\phi} - \widetilde{\boldsymbol{v}}_{\boldsymbol{E}} \cdot \nabla \nabla_\perp^2 \widetilde{\phi} - \bar{\boldsymbol{v}}_{\boldsymbol{E}} \cdot \nabla \nabla_\perp^2 \widetilde{\phi} = 0 \end{aligned} \tag{2.82}$$

where we have made use of (2.77) to eliminate the over-lined term.

Eq (2.82) can be written in a more compact form if we add $\widetilde{\boldsymbol{v}}_{\boldsymbol{E}} \cdot \nabla \widetilde{\phi} = 0$ and subtract $\bar{\boldsymbol{v}}_{\boldsymbol{E}} \cdot \nabla \bar{\phi} = 0$.
Collecting terms we get the *Modified Hasegawa - Mima* equation

$$\left(\frac{\partial}{\partial t} + \mathbf{v}_E \cdot \nabla + \kappa \frac{\partial}{\partial y} \right) \widetilde{\phi} - \left(\frac{\partial}{\partial t} + \mathbf{v}_E \cdot \nabla \right) \nabla_\perp^2 \phi + \widetilde{\mathbf{v}}_E \cdot \nabla \overline{n} = 0. \tag{2.83}$$

Note that Eq. (2.79) reduces to $\overline{n} = constant$ when $\widetilde{n} \to \widetilde{\phi}$. Recalling that the normalized *deviation* from the equilibrium value of the density enters in the Hasegawa - Wakatani equations it follows that for initially zero deviation from equilibrium and zero perturbation due to fluctuating motions the zonal average of n vanishes. However, we have just shown that $\overline{n} = constant$ and consequently the zonal part vanishes for all times. Thus the last term on the LHS of Eq. (2.83) vanishes and we are left with

$$\left(\frac{\partial}{\partial t} + \mathbf{v}_E \cdot \nabla + \kappa \frac{\partial}{\partial y}\right) \widetilde{\phi} - \left(\frac{\partial}{\partial t} + \mathbf{v}_E \cdot \nabla\right) \nabla_\perp^2 \phi. \tag{2.84}$$

We now give simple arguments to show how zonal flows may be excited.

Chapter 3

Zonal flow dynamics

Energy transfer

The first Hasegawa - Wakatani eq, the ordinary- and modified Hasegawa - Mima, as well as the 2 D Navier - Stokes equation (using the stream function formalism) may be cast into the form

$$\frac{\partial}{\partial t}\nabla_\perp^2\phi + \mathbf{v}\cdot\nabla\nabla_\perp^2\phi + \mathcal{L}_\phi(n,\phi,...) = 0, \tag{3.1}$$

where $\mathcal{L}_\phi(n,\phi,...)$ is some operator acting on ϕ and possibly several of the state variables, such as density or pressure. $\mathbf{v} = \widehat{\mathbf{z}}\times\nabla\phi$ in fluid mechanics with the interpretation of ϕ as the stream function. In plasma physics $\mathbf{v} = \mathbf{v}_E = \widehat{\mathbf{z}}\times\nabla\phi$ is the electric drift and ϕ is interpreted as the electrostatic potential.
To simplify notation, we introduce the Poisson - brackets according to

$$\{\phi, f\} = \widehat{\mathbf{z}}\times\nabla\phi\cdot\nabla f = \partial_y(f\partial_x\phi) - \partial_x(f\partial_y\phi). \tag{3.2}$$

We then have

$$\frac{\partial}{\partial t}\nabla_\perp^2\phi + \left\{\phi, \nabla_\perp^2\phi\right\} + \mathcal{L}_\phi(n,\phi,...) = 0. \tag{3.3}$$

We shall demonstrate some interesting properties of the energy transfer between fluctuating and zonal components in the following. Let us firstly consider the simplest possible operator $\mathcal{L}_\phi(n,\phi,...) = 0$. The following property of the Poisson brackets shall aid us in the following calculations,

$$\begin{aligned}\phi\partial_y(f\partial_x\phi) - \phi\partial_x(f\partial_y\phi) &= \partial_y(\phi f\partial_x\phi) - (\partial_y\phi)f(\partial_x\phi) - \partial_x(\phi f\partial_y\phi) + (\partial_x\phi)f(\partial_y\phi) \\ &= \partial_y(\phi f\partial_x\phi) - \partial_x(\phi f\partial_y\phi).\end{aligned} \tag{3.4}$$

Let $\Omega = \nabla_\perp^2\phi$, multiply Eq. (3.3) (where now $\mathcal{L}_\phi(n,\phi,...) = 0$) by ϕ and use Eq. (3.4) to obtain

$$\phi\partial_t\Omega + \partial_y(\phi\Omega\phi\partial_x\phi) - \partial_x(\phi\Omega\partial_y\phi) = 0. \tag{3.5}$$

The first term on the LHS can be written as

$$\begin{aligned}\phi\frac{\partial}{\partial t}\nabla_\perp^2\phi &= \nabla\cdot\left(\phi\frac{\partial}{\partial t}\nabla_\perp\phi\right) - \nabla\phi\cdot\frac{\partial}{\partial t}\nabla_\perp\phi \\ &= \nabla\cdot\left(\phi\frac{\partial}{\partial t}\nabla_\perp\phi\right) - \frac{\partial}{\partial t}\left[\frac{1}{2}\left(\nabla_\perp\phi\right)^2\right].\end{aligned} \tag{3.6}$$

Integrating the above over coordinate space which we assume to be bound by a surface S with outward pointing normal vector $d\mathbf{A}$ and using Gauss' Theorem for the first term on the RHS in Eq. (3.6) we get

$$\int d\mathbf{A}\cdot\left(\phi\frac{\partial}{\partial t}\nabla_\perp\phi\right)-\frac{\partial}{\partial t}\int d\mathbf{x}\frac{1}{2}\left(\nabla_\perp\phi\right)^2+\int d\mathbf{x}\left[\partial_y(\phi\Omega\phi\partial_x\phi)-\partial_x(\phi\Omega\partial_y\phi)\right]=0. \tag{3.7}$$

Invoking the boundary conditions

$$\phi(L_y)=\phi(0),\ \partial_y\phi(L_y)=\partial_y\phi(0),\ \partial_y^2\phi(L_y)=\partial_y^2\phi(0)\ ,$$

we see that

$$\begin{aligned}\int d\mathbf{A}\cdot\left(\phi\frac{\partial}{\partial t}\nabla_\perp\phi\right)&=0\\ \int dx(\phi\Omega\phi\partial_x\phi)|^{\mathrm{bdy}}&=0\\ \int dy(\phi\Omega\partial_y\phi)|^{\mathrm{bdx}}&=0\end{aligned}$$

Defining the total energy

$$E=\int d\mathbf{x}\frac{1}{2}\left(\nabla_\perp\phi\right)^2, \tag{3.8}$$

we have deduced that

$$\frac{d}{dt}\int d\mathbf{x}\frac{1}{2}\left(\nabla_\perp\phi\right)^2=0\quad\Rightarrow \mathrm{E}^{\mathrm{tot}}=\mathrm{cst}.. \tag{3.9}$$

To compute the zonal energy we first average Eq. (3.5) over y,

$$\begin{aligned}&\frac{1}{L_y}\int_0^{L_y}dy\frac{\partial}{\partial t}\Omega+\frac{1}{L_y}\int_0^{L_y}dy\left[\partial_y(\Omega\partial_x\phi)-\partial_x(\Omega\partial_y\phi)\right]\\ &=\frac{1}{L_y}\int_0^{L_y}dy\frac{\partial}{\partial t}\Omega+\frac{1}{L_y}\left(\Omega\partial_x\phi\right)|_0^{L_y}-\frac{1}{L_y}\frac{\partial}{\partial x}\int_0^{L_y}dy\Omega\partial_y\phi\\ &=\frac{1}{L_y}\int_0^{L_y}dy\frac{\partial}{\partial t}\Omega-\frac{1}{L_y}\frac{\partial}{\partial x}\int_0^{L_y}dy\Omega\partial_y\phi=0.\end{aligned}$$

Define the averages

$$\Omega_0=\frac{1}{L_y}\int dy\Omega, \tag{3.10}$$

and

$$\left(\Omega\partial_y\phi\right)_0=\frac{1}{L_y}\int_0^{L_y}dy\Omega\partial_y\phi. \tag{3.11}$$

and rewrite the preliminary result

$$\frac{\partial}{\partial t}\Omega_0=\frac{\partial}{\partial x}\left(\Omega\partial_y\phi\right)_0. \tag{3.12}$$

Note that due to the periodic boundary conditions as stated in the previous section we have

$$\Omega_0=\frac{\partial^2}{\partial x^2}\overline{\phi}.$$

Integrating Eq. (3.12) over x,

$$\frac{\partial}{\partial t}\frac{\partial\overline{\phi}}{\partial x}=\left(\Omega\partial_y\phi\right)_0, \tag{3.13}$$

multiplying by $\overline{\phi}$ and integrating once more over x leaves

$$\frac{\partial}{\partial t}\int dx\ \frac{1}{2}\left(\partial_x\overline{\phi}\right)^2 = \int d\mathbf{x}\ \overline{\phi}\left(\Omega\partial_y\phi\right), \tag{3.14}$$

which upon defining the zonal flow energy (note again that $\overline{\phi}$ is independent of y)

$$U = \int dx\frac{1}{2}\left(\partial_x\overline{\phi}\right)^2 = \int d\mathbf{x}\frac{1}{2}\left(\nabla\overline{\phi}\right)^2, \tag{3.15}$$

is written as

$$\frac{d}{dt}U = \int d\mathbf{x}\overline{\phi}\frac{\partial}{\partial x}\left(\Omega\partial_y\phi\right). \tag{3.16}$$

In Appendix A we show that

$$\int d\mathbf{x}\ \overline{\phi}\left(\Omega\partial_y\phi\right) = \int d\mathbf{x}\ \overline{\phi}\left(\widetilde{\Omega}\partial_y\widetilde{\phi}\right) = -\int d\mathbf{x}\ v_0\frac{\partial}{\partial x}\left(\widetilde{v}_x\widetilde{v}_y\right), \tag{3.17}$$

with $v_0 = \partial\overline{\phi}/\partial x$ the mean (shear) flow velocity and the fluctuating velocity components given by $\widetilde{v}_x = -\partial_y\widetilde{\phi}$ and $\widetilde{v}_y = \partial_x\widetilde{\phi}$ respectively. Subtracting Eq. (3.16) from Eq. (3.9) we get an expression for the energy contained in the fluctuating motions,

$$\frac{d}{dt}\mathrm{K} = \int d\mathbf{x}\frac{1}{2}\left(\nabla_\perp\widetilde{\phi}\right)^2 = \int d\mathbf{x}\ v_0\frac{\partial}{\partial x}\left(\widetilde{v}_x\widetilde{v}_y\right). \tag{3.18}$$

The terms driving the zonal flow and fluctuating energy respectively have opposite sign, thus they act as transfer terms, transferring energy from either the fluctuating motions into the zonal flow or vice versa, leaving the total energy conserved. The transfer term is governed by shear flow velocity and the divergence of the Reynolds-stress. Integrating the transfer term by parts leaves

$$\begin{aligned}-\int d\mathbf{x}\ v_0\frac{\partial}{\partial x}\left(\widetilde{v}_x\widetilde{v}_y\right) &= -\int dy\ \left(v_0\widetilde{v}_x\widetilde{v}_y\right)\big|^{\mathrm{bdx}} + \int d\mathbf{x}\frac{\partial v_o}{\partial x}\left(\widetilde{v}_x\widetilde{v}_y\right)\\ &= \int d\mathbf{x}\frac{\partial v_o}{\partial x}\left(\widetilde{v}_x\widetilde{v}_y\right).\end{aligned}$$

This tells us that fluctuating structures (in our description this may equally well be convective cells) oriented such as to transport positive y-directed momentum in the direction of the shear flow gradient may effectively transfer energy from the fluctuating motions to the zonal flow. Cf. Figure 3.1 taken from Garcia *et al.* [15].

HM energetics

It is now straightforward to apply the same analysis to a different operator in Eq. (3.3). Take for instance $\mathcal{L}_\phi = -\partial_t - \kappa\partial_y$, i.e., Eq. (3.3) is now the conventional form of the Hasegawa - Mima equation. We then get upon introducing the generalized energy,

$$E^{\mathrm{HM}} = \frac{1}{2}\int d\mathbf{x}\left[\left(\nabla_\perp\phi\right)^2 + \phi^2\right], \tag{3.19}$$

analogous to Eq. (3.9) another conservation equation

$$\frac{d}{dt}E^{HM} = 0. \tag{3.20}$$

Furthermore, the generalized zonal flow energy

$$U^{\mathrm{HM}} = \frac{1}{2}\int d\mathbf{x}\left[\left(\nabla\overline{\phi}\right)^2 + \overline{\phi}^2\right], \tag{3.21}$$

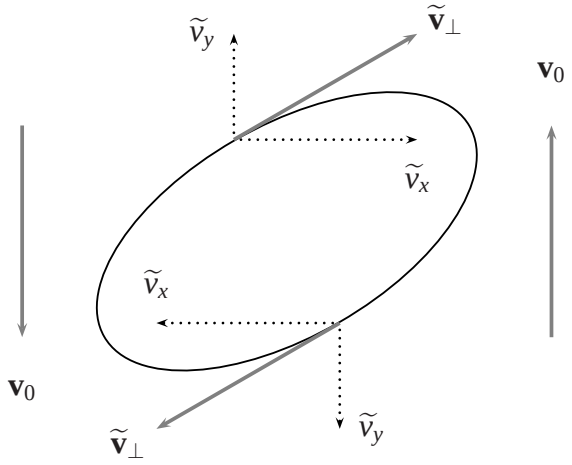

Figure 3.1: Momentum transfer to zonal flow

is found to be driven by the small scale fluctuations as before,

$$\frac{d}{dt}U^{\mathrm{HM}} = -\int d\mathbf{x}\; v_0 \frac{\partial}{\partial x}\left(\widetilde{v}_x\widetilde{v}_y\right). \tag{3.22}$$

Subtracting Eq. (3.22) from Eq. (3.20) we get

$$\frac{d}{dt}K^{\mathrm{HM}} = \int d\mathbf{x}\; v_0 \frac{\partial}{\partial x}\left(\widetilde{v}_x\widetilde{v}_y\right), \tag{3.23}$$

where the generalized energy of the fluctuating motions is given by

$$K^{\mathrm{HM}} = \frac{1}{2}\int d\mathbf{x}\left[\left(\nabla\widetilde{\phi}\right)^2 + \widetilde{\phi}^2\right]. \tag{3.24}$$

Again we see that the energy transfer is conservative between the zonal flow and the fluctuating motions and fully determined by the shearing properties of the small scale fluctuations.
Note that we have used the following identities when subtracting Eq. (3.22) from Eq. (3.20):

$$\begin{aligned}\int d\mathbf{x}\phi^2 &= \int d\mathbf{x}\left(\widetilde{\phi}^2 + \overline{\phi}^2 + 2\widetilde{\phi}\overline{\phi}\right)\\ &= \int d\mathbf{x}\widetilde{\phi}^2 + \int d\mathbf{x}\overline{\phi}^2 + 2\int dx\overline{\phi}\int dy\widetilde{\phi}\\ &= \int d\mathbf{x}\widetilde{\phi}^2 + \int d\mathbf{x}\overline{\phi}^2\end{aligned}$$

and

$$\begin{aligned}\int d\mathbf{x}\left(\nabla_\perp\phi\right)^2 &= \int d\mathbf{x}\left(\nabla_\perp\widetilde{\phi}\right)^2 + \int d\mathbf{x}\left(\nabla_\perp\overline{\phi}\right)^2 + 2\int d\mathbf{x}\nabla\widetilde{\phi}\cdot\nabla\overline{\phi}\\ &= \int d\mathbf{x}\left(\nabla_\perp\widetilde{\phi}\right)^2 + \int d\mathbf{x}\left(\nabla_\perp\overline{\phi}\right)^2 + 2\int dx\frac{\partial\overline{\phi}}{\partial x}\frac{\partial}{\partial x}\int dy\widetilde{\phi}\\ &= \int d\mathbf{x}\left(\nabla_\perp\widetilde{\phi}\right)^2 + \int d\mathbf{x}\left(\nabla_\perp\overline{\phi}\right)^2,\end{aligned} \tag{3.25}$$

since $\overline{\phi}$ and $\partial\overline{\phi}/\partial x$ are independent of y.

MHM energetics

The MHM-equation is obtained when using the operator

$$\mathcal{L}_\phi \phi = -\partial_t \phi - \kappa \partial_y \phi - \{\phi, \widetilde{\phi}\}.$$

We then get the evolution equation for the total energy,

$$\frac{d}{dt} E^{\mathrm{MHM}} \equiv \frac{1}{2}\frac{d}{dt}\int \, dV \left[(\nabla_\perp \phi)^2 + \widetilde{\phi}^2 \right] = 0. \tag{3.26}$$

The energy contained in the zonal structures is governed by

$$\frac{d}{dt} U^{\mathrm{MHM}} \equiv \frac{1}{2}\frac{d}{dt}\int \, dV \left(\nabla_\perp \overline{\phi} \right)^2 = -\int d\mathbf{x} \; v_0 \frac{\partial}{\partial x} \left(\widetilde{v}_x \widetilde{v}_y \right), \tag{3.27}$$

and the kinetic energy contained in the fluctuating motions evolves according to

$$\frac{d}{dt} K^{\mathrm{MHM}} \equiv \frac{1}{2}\frac{d}{dt}\int \, dV \left[\left(\nabla_\perp \widetilde{\phi} \right)^2 + \widetilde{\phi}^2 \right] = \int d\mathbf{x} \; v_0 \frac{\partial}{\partial x} \left(\widetilde{v}_x \widetilde{v}_y \right). \tag{3.28}$$

We may compare the energy transfer rate to the zonal flow for the models described above. To this end, assume that the driving Reynolds-stress (RS) is the same for both the HM and MHM model. Furthermore, consider the single Fourier modes of the fluctuating and zonal part of the potential

$$\widetilde{\phi} \sim \widehat{\phi_k} \exp(i\mathbf{k}\cdot\mathbf{x}) + cc. \; , \overline{\phi} \sim \widehat{\phi_q} \exp(i\mathbf{q}\cdot\mathbf{x}) + cc.. \tag{3.29}$$

We then find that the kinetic energy in the fluctuating motions in both the HM and the MHM model scales as

$$\begin{aligned} \frac{d}{dt} K^{\mathrm{HM}} &= \frac{d}{dt}\frac{1}{2}\int \, dV (1+k^2) \left| \widehat{\phi_k} \right|^2 = \mathrm{RS} \\ \frac{d}{dt} t K^{\mathrm{MHM}} &= \frac{d}{dt}\frac{1}{2}\int \, dV (1+k^2) \left| \widehat{\phi_k} \right|^2 = \mathrm{RS}, \end{aligned}$$

whereas the zonal flows have energy transfer rates

$$\begin{aligned} \frac{d}{dt} U^{\mathrm{HM}} &= \frac{d}{dt}\frac{1}{2}\int \, dV (1+q^2) \left| \widehat{\phi_q} \right|^2 = -\mathrm{RS} \\ \frac{d}{dt} U^{\mathrm{MHM}} &= \frac{d}{dt}\frac{1}{2}\int \, dV q^2 \left| \widehat{\phi_q} \right|^2 = -\mathrm{RS}. \end{aligned}$$

The energy contained in the fluctuating Fourier modes is consequently

$$\frac{d}{dt}\int \, dV \left| \widehat{\phi_k} \right|^2 \sim \frac{1}{1+k^2}\mathrm{RS}$$

for the kinetic energy in both the HM and MHM model. For the zonal modes in the HM we find

$$\frac{d}{dt}\int \, dV \left| \widehat{\phi_q} \right|^2 \sim \frac{1}{1+q^2}\mathrm{RS}, \tag{3.30}$$

while for the MHM model

$$\frac{d}{dt}\int \, dV \left| \widehat{\phi_q} \right|^2 \sim \frac{1}{q^2}\mathrm{RS}. \tag{3.31}$$

This shows that energy-extraction from the fluctuating motions happens at the same rate in both the HM and the MHM model, but the input of energy into the

zonal flows is faster for the MHM model by a factor $(1+q^2)/q^2$ compared to the HM model. Thus the MHM is the preferred model to use when seeking to describe zonal flow dynamics. We shall quantify the growth rates for the zonal flows in both models in a later section, explicitly showing that zonal flows arise sooner in the MHM model than in the HM model. The reasoning presented is of course only valid instantaneously and only for a certain point in time when the integrated Reynold-stress is indeed equal for both models; as the zonal flows obtain more energy, the Reynolds-stress changes (RS $\sim q\left|\widehat{\phi_q}\right|$) and the reasoning above is no longer valid.

Convection Model

To visualize the findings from the previous section, we consider the case of the simple hydrodynamic convection model, Eq. (3.3) with $\mathcal{L} \equiv 0$. Following [15] we define a stream function,

$$\begin{aligned}\psi(\mathbf{x},t) =& \Psi_{1,1}\sin(k_x x)\sin(k_y y) + \Psi_{1,0}\sin(k_x x) \\ &+ \Psi_{2,1}\sin(2k_x x)\cos(k_y y).\end{aligned}$$

Here, $\Psi_{1,1}$ is assumed to represent a constant amplitude pump-wave, $\Psi_{1,0}$ is the zonal flow which has no y-variation and $\Psi_{2,1}$ is a sideband of the pump-wave. Inserting the above in the convection model, Eq. (3.3), with $\mathcal{L} \equiv 0$ and equating terms with identical sine and cosine dependence, we get the set of equations governing the evolution of the amplitudes in this simple model,

$$\begin{aligned}\frac{d\Psi_{1,0}}{d\ t} &= -\frac{3}{4}k_x k_y \Psi_{2,1}\Psi_{1,1}, \\ \frac{d\Psi_{2,1}}{d\ t} &= \frac{k_x k_y^3}{8k_x^2 + 2k_y^2}\Psi_{1,0}\Psi_{1,1}.\end{aligned}$$

Taking the time-derivative of the first equation above and substituting the second then yields the equation for the zonal - flow amplitude,

$$\frac{d^2\Psi_{1,0}}{d\ t^2} = -\frac{3}{8}\frac{k_x^2 k_y^4}{4k_x^2 + k_y^2}\Psi_{1,1}^2\Psi_{1,0}, \tag{3.32}$$

which admits exponentially growing solutions with growth rate

$$\gamma^2 = \frac{3}{8}\frac{k_x^2 k_y^4}{4k_x^2 + k_y^2}\Psi_{1,1}^2. \tag{3.33}$$

This may be compared with the growth rate obtained in [15] which is identical when making the replacement $k_x \to \pi$ and $k_y \to k_c$. Figure 3.2 below illustrates how the arising sheared zonal flow acts to tilt the pump-cell and further enhances the positive momentum transfer to itself. Compare with Figure 3.1.
We further note, that the growth rate is crucially dependent on the aspect-ratio, as is characteristic for zonal-flows in plasmas. In Figure 3.2 we have used $k_x/k_y = 1/3$, we again refer to Figure 3.1 where the physics behind this dependence lies. The smaller the aspect ratio, the more effective is the momentum transfer to the zonal flow. Eq. (3.33),may be written in normalized form

$$\frac{1}{k_y^2}\frac{\gamma^2}{v_x^2} = \frac{3}{8}\frac{k_x^2/k_y^2}{4k_x^2/k_y^2 + 1}, \tag{3.34}$$

where we have introduced the pump-wave induced radial velocity, $v_x^2 = k_y^2\Psi_{1,1}^2$. Cf.

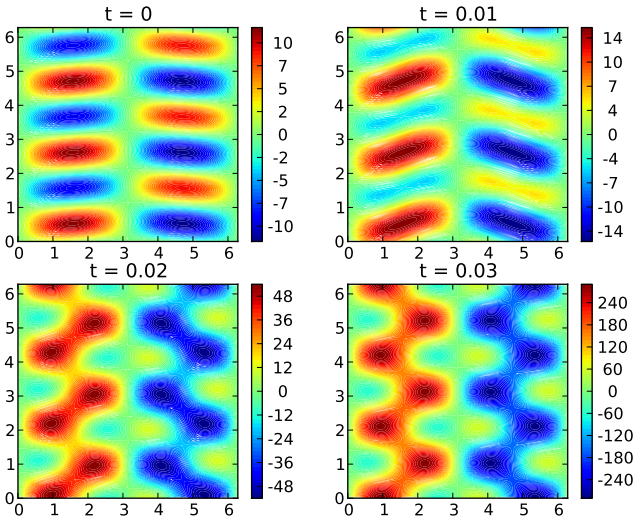

Figure 3.2: Zonal flow generation

Parametric Instability

From our previous deduction of the MHM and OHM equations, we get the intuition the the modified version more adequately describes zonal flow generation compared to the ordinary cast, since we expect the naiivity involved to disregard important information. That this is indeed the case will be shown explicitely later. For now we shall consider the MHM equation bearing in mind that this is the one to use when seeking a simple zonal flow description. Note, however, that Boltzmann distribution disregards any kind of drift wave instability as indicated earlier. Thus the MHM model is far from complete, yet it effectively describes zonal flow growth mechanisms as we shall see now.

In this section we show how zonal flow generation is incorporated in the modified Hasegawa - Mima model, inspired by Kaladze *et al.* [6]. Consider again the evolution equation for the zonal part of the potential, (2.77), and (2.83) describing its interaction with the fluctuating part:

$$\frac{\partial}{\partial t}\nabla_\perp^2\bar{\phi} + \overline{\widetilde{\boldsymbol{v}}_E \cdot \nabla\nabla_\perp^2\widetilde{\phi}} = 0 \tag{3.35}$$

$$\left(\frac{\partial}{\partial t} + \boldsymbol{v}_E\cdot\nabla + \kappa\frac{\partial}{\partial y}\right)\widetilde{\phi} - \left(\frac{\partial}{\partial t} + \boldsymbol{v}_E\cdot\nabla\right)\nabla_\perp^2\phi = 0 \tag{3.36}$$

Assume that the drift wave (denoted by $\widetilde{\phi}$) we are considering is superposed of a pump wave, ϕ_0, and two sidebands, ϕ_+ and ϕ_- such that $\widetilde{\phi} = \phi_0 + \phi_+ + \phi_-$. The drift wave drives a zonal flow given by

$$\bar{\phi} = \phi_q \exp(i\boldsymbol{q}\cdot\boldsymbol{x} - i\Omega t) + \phi_q^* \exp(-i\boldsymbol{q}\cdot\boldsymbol{x} + i\Omega t)$$

Note that the zonal flow has by definition no y dependence, thus $\boldsymbol{q} = q\widehat{\boldsymbol{x}}$.
The drift wave and its sidebands are expressed as

$$\phi_0 = \phi_k \exp(i\boldsymbol{k}\cdot\boldsymbol{x} - i\omega t) + \phi_k^* \exp(-i\boldsymbol{k}\cdot\boldsymbol{x} + i\omega t)$$
$$\phi_+ = \phi_+ \exp(i\boldsymbol{k}_+\cdot\boldsymbol{x} - i\omega_+ t) + \phi_+^* \exp(-i\boldsymbol{k}_+\cdot\boldsymbol{x} + i\omega_+ t)$$
$$\phi_- = \phi_- \exp(i\boldsymbol{k}_-\cdot\boldsymbol{x} - i\omega_- t) + \phi_-^* \exp(-i\boldsymbol{k}_-\cdot\boldsymbol{x} + i\omega_- t)$$

with $\boldsymbol{k}_\pm = \boldsymbol{k} \pm \boldsymbol{q}$ and $\omega_\pm = \omega \pm \Omega$.

Inserting $\widetilde{\phi}$ and $\bar{\phi}$ into (3.35) gives after a lengthy but straightforward calculation

$$\Omega\phi_q = -\frac{ik_y}{q}\left[(k_-^2 - k^2)\phi_k\phi_-^* - (k_+^2 - k^2)\phi_+\phi_k^*\right] \tag{3.37}$$

where $k_\pm^2 = k^2 + q^2 \pm 2k_x q$.

To arrive at (3.37) we have equated terms with $\exp(i\boldsymbol{q}\cdot\boldsymbol{x} - i\Omega t)$ dependence and also made use of the fact that the zonal average does not act on these terms since $\boldsymbol{q}$ has no y component.

Inserting for $\widetilde{\phi}$ and $\phi = \widetilde{\phi} + \bar{\phi}$ in (3.36) and equating terms proportional to $\exp(i\boldsymbol{k}_+ \cdot \boldsymbol{x} - i\omega_+ t) = \exp(i\boldsymbol{k}\cdot\boldsymbol{x} + i\boldsymbol{q}\cdot\boldsymbol{x} - i\omega t - i\Omega t)$ and $\exp(-i\boldsymbol{k}_-\cdot\boldsymbol{x} + i\omega_- t) = \exp(-i\boldsymbol{k}\cdot\boldsymbol{x} + i\boldsymbol{q}\cdot\boldsymbol{x} + i\omega t - i\Omega t)$ respectively yields after a *very* lengthy but still straightforward computation

$$\phi_+ = \frac{ik_y q(1 + k^2 - q^2)}{(\Omega + \delta\omega_+)(1 + k_+^2)}\phi_q\phi_k \tag{3.38}$$

and

$$\phi_-^* = -\frac{ik_y q(1 + k^2 - q^2)}{(\Omega - \delta\omega_-)(1 + k_-^2)}\phi_q\phi_k^* \tag{3.39}$$

where we have introduced

$$\delta\omega_\pm = \omega - \frac{\kappa k_y}{1 + k_\pm^2} \tag{3.40}$$

Combining (3.38), (3.39) and (3.37) yields

$$\Omega = -k_y^2(1 + k^2 - q^2)|\phi_0|^2\left[\frac{(k_+^2 - k^2)}{(\Omega + \delta\omega_+)(1 + k_+^2)} + \frac{(k_-^2 - k^2)}{(\Omega - \delta\omega_-)(1 + k_-^2)}\right] \tag{3.41}$$

with $\phi_k\phi_k^* = |\phi_0|^2$.

In order to deduce any physics from (3.41) we may simplify by considering the case where the zonal flow varies on a much larger scale as the drift wave turbulence, i.e. $q \ll k$. In this case we have the approximations

$$\delta\omega_\pm \approx \mp q v_{gx} - \frac{q^2 v'_{gx}}{2} \tag{3.42}$$

and

$$\left[\frac{(k_+^2-k^2)}{(\Omega+\delta\omega_+)(1+k_+^2)}+\frac{(k_-^2-k^2)}{(\Omega-\delta\omega_-)(1+k_-^2)}\right]\approx-\frac{q^2\Omega v'_{gx}}{\omega}\frac{1}{(\Omega-qv_{gx})^2-(q^2v'_{gx}/2)^2} \tag{3.43}$$

where the x-component of the group velocity is given by

$$v_{gx}\equiv\frac{\partial\omega}{\partial k_x}=-\frac{2k_x\omega}{1+k^2} \tag{3.44}$$

and

$$v'_{gx}\equiv\frac{\partial^2\omega}{\partial k_x^2}=-2\omega\frac{1+k_y^2-3k_x^2}{(1+k^2)^2} \tag{3.45}$$

(3.42) is deduced by expanding (3.40) in the small parameter q/k in the denominator of the second term in Eq. (3.40). Inserting into the square-bracket term in (3.41) and cracking through the algebra then yields (3.43).

Using the approximations in (3.41) and solving the simple second order equation leaves the more useful

$$\begin{aligned}\Omega_\pm&\approx qv_{gx}\pm\sqrt{\frac{q^2k_y^2(1+k^2-q^2)v'_{gx}}{\omega}|\phi_0|^2+\left(\frac{q^2v'_{gx}}{2}\right)^2}\\&=qv_{gx}\pm\sqrt{-\frac{2q^2k_y^2(1+k^2-q^2)(1+k_y^2-3k_x^2)}{(1+k^2)^2}|\phi_0|^2+\left(\frac{q^2v'_{gx}}{2}\right)^2}\end{aligned} \tag{3.46}$$

For Ω to be complex and thus leading to instability it is necessary that

$$1+k_y^2-3k_x^2>0. \tag{3.47}$$

Again making use of $q\ll k$ allows us to neglect the second term in the square root,

$$\begin{aligned}\frac{\left(\frac{q^2v'_{gx}}{2}\right)^2}{\frac{2q^2k_y^2(1+k^2-q^2)(1+k_y^2-3k_x^2)}{(1+k^2)^2}|\phi_0|^2}&=\frac{q^2\omega^2(1+k_y^2-3k_x^2)(1+k^2)^2}{2k_y^2(1+k^2-q^2)\left|\phi_0\right|^2}\\&=\frac{q^2\kappa^2(1+k_y^2-3k_x^2)}{2(1+k^2-q^2)\left|\phi_0\right|^2}\\&\approx\frac{q^2\kappa^2(1+k_y^2-3k_x^2)}{2(1+k^2)\left|\phi_0\right|^2}\ll1,\end{aligned}$$

since Eq. (3.47) is of the order unity.
Furtheremore, considering the small wavelength limit, i.e. $k\gg1$ then gives

$$\Omega_\pm\approx qv_{gx}\pm\sqrt{-\frac{2q^2k_y^2(k_y^2-3k_x^2)}{k_x^2+k_y^2}|\phi_0|^2}. \tag{3.48}$$

It is fruitful to consider the case of largest growth which occurs when $k_x=0$, cf. Figure 3.3. Realizing that the x projection of the group velocity in this limit is small ($v_{gx}\sim k_xk_y/k^4\ll1$) The maximum growth rate is then given by

$$\begin{aligned}\gamma_{max}&=-i\Omega_+=\sqrt{2q^2k_y^2|\phi_0|^2}\\&=\sqrt{2}qk_y|\phi_0|,\end{aligned} \tag{3.49}$$

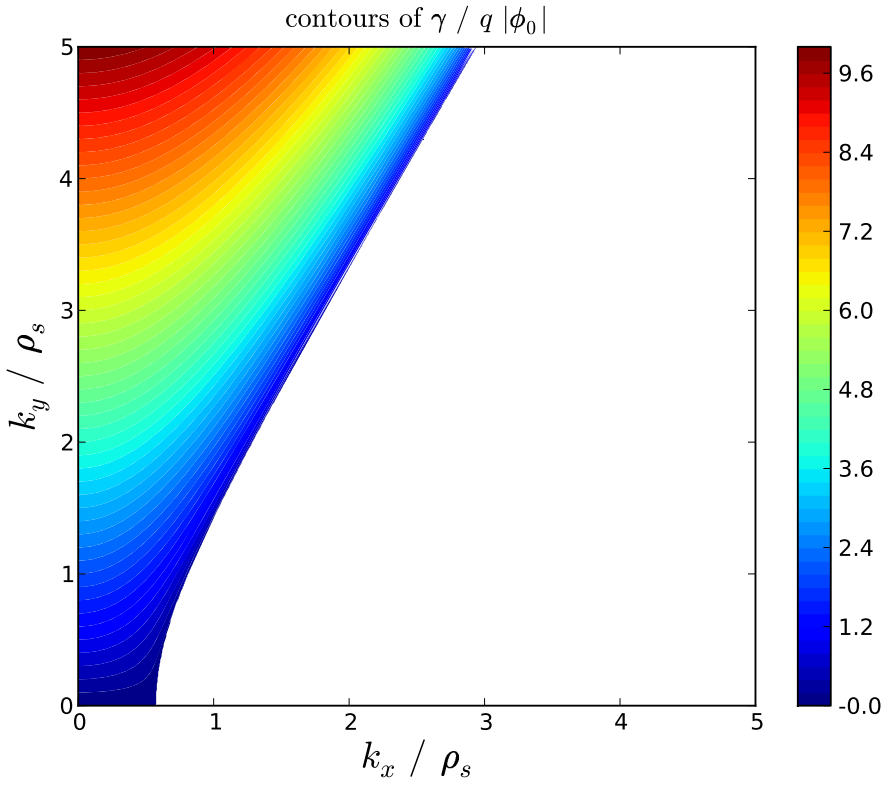

Figure 3.3: Contourplot of zonal flow growth rate for the MHM model-

which may be compared to the result for zonal flow growth found by Manfredi *et al.* [7]. The authors of this paper use the x direction for all zonal flow related variables, which is contrary to the more commonly used y direction used in this presentation. Identifying the zonal flow, $k_1 = q$, the pump wave with k_{2x} (note that $k_y = 0$ here instead of $k_x = 0$ as in our presentation), and the pump wave amplitude given by $|\phi_2|^2$ instead of our $|\phi_0|^2$ and normalizing as we have done, one finds the exact same growth rate, checking our result at least to some degree for consistency with [7] From Figure 3.4 we see that drift waves with a small aspect ratio are the cause for zonal growth (the red line gives the growth domain; growth corresponds to $\gamma^2 > 0$). Physically, the explanation lies in Figure 3.1 showing that the tilting of the convection cell is important for energy transfer to the zonal flow.

It is interesting to apply the same analysis to the conventional Hasegawa - Mima equation. The growth rate for the zonal flow one obtains is then slightly different,

$$\begin{aligned}\Omega_{\pm}^{\mathrm{HM}} &\approx q v_{gx} \pm \sqrt{\frac{q^4 k_y^2 (k^2 - q^2)}{1 + q^2} \frac{v'_{gx}}{\omega} |\phi_0|^2 + \left(\frac{q^2 v'_{gx}}{2}\right)^2} \\ &= q v_{gx} \pm \sqrt{-\frac{2q^4 k_y^2 (k^2 - q^2)(1 + k_y^2 - 3k_x^2)}{(1 + q^2)(1 + k^2)^2} |\phi_0|^2 + \left(\frac{q^2 v'_{gx}}{2}\right)^2}. \end{aligned} \tag{3.50}$$

Let us neglect the last term under the square root in Eq. (3.46) and Eq. (3.50) as well as the first term on the RHS above (scales as $\sim q k_x k_y / k^4 \ll 1$ for $q \ll k$) for

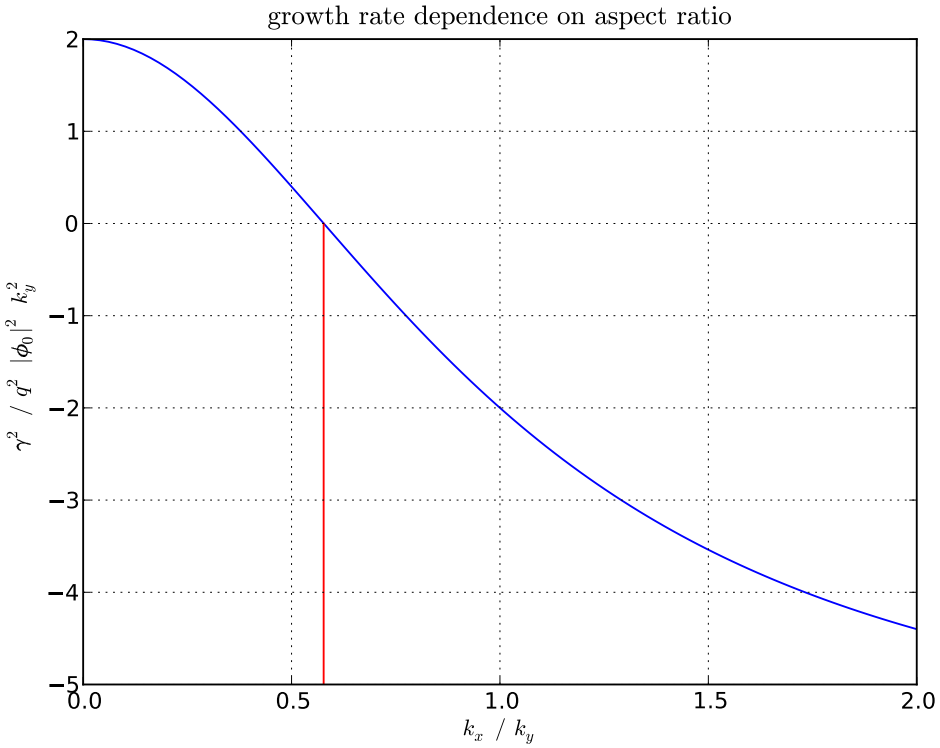

Figure 3.4: Aspect ratio for MHM growth rate

the moment. We then get

$$\gamma^2_{\mathrm{MHM}}/\gamma^2_{\mathrm{HM}} = \frac{(1+k^2-q^2)(1+q^2)}{q^2(k^2-q^2)} \approx \left(1+\frac{1}{k^2}\right)\left(1+\frac{1}{q^2}\right)$$
$$= 1 + \frac{1}{q^2} + \frac{1}{k^2} + \frac{1}{k^2 q^2} \gg 1,$$

where we have assumed that $q \ll 1$.
We may interpret this analogous to Holland *et al.* [8] as prescribing different 'effective inertias' to the zonal flows in the two models considered here. We may state that zonal flows described by the Hasegawa - Mima equation are 'heavy' and thus more difficult to initialize compared to 'light' zonal flows described by the modified Hasegawa - Mima equation. From a numerical point of view it is thus preferable to use the modified equation when seeking to describe zonal flow dynamics since the zonal flows are more explicit in this model.

Modulational Instability

In this section we perform a derivative perturbation method on the modified Hasegawa - Mima equation quite similar to Abdullatif *et al.* [9] and deduce a form of the Nonlinear Schrödinger equation for the drift wave amplitude. We then analyze stability and deduce the instability criterion for modulations of the amplitude. It turns out, that this method reproduces Eq. (3.47). Similar work has been done by Champeux and Diamond [10] on the HW model using the reductive perturbation method.

Deriving the Nonlinear Schrödinger Equation

Following [9] we perform a multiple-scale derivative perturbation of Eq. (2.84) which in coordinate form reads

$$(\partial_t + \kappa\partial_y)\widetilde{\phi} + \partial_x\overline{\phi}\partial_y\widetilde{\phi} - (\partial_t + \partial_x\phi\partial_y - \partial_y\phi\partial_x)(\partial_x^2 + \partial_y^2)\phi = 0. \tag{3.51}$$

We expand the derivatives as sets of independent variables at different scales,

$$\{x_0, x_1, x_2, ..., x_N; y_0, y_1, ...y_N, t_0, t_1, ..., t_N\}, \tag{3.52}$$

where $x_n = \epsilon^n x$, $y_n = \epsilon^n y$ and $t_n = \epsilon^n t$ and ϵ is assumed to be a small parameter. Consequently we have

$$\phi(x, y, t) = \phi(x_0, ..., x_N; y_0, ..., y_N; t_0, ..., t_N),$$

applying the chain rule then gives the expanded differential operators

$$\begin{aligned}
\frac{\partial}{\partial x} &= \frac{\partial}{\partial x_0} + \epsilon\frac{\partial}{\partial x_1} + \epsilon^2\frac{\partial}{\partial x_2} + ... + \epsilon^N\frac{\partial}{\partial x_N}, \\
\frac{\partial}{\partial y} &= \frac{\partial}{\partial y_0} + \epsilon\frac{\partial}{\partial y_1} + \epsilon^2\frac{\partial}{\partial y_2} + ... + \epsilon^N\frac{\partial}{\partial y_N}, \\
\frac{\partial}{\partial t} &= \frac{\partial}{\partial t_0} + \epsilon\frac{\partial}{\partial t_1} + \epsilon^2\frac{\partial}{\partial t_2} + ... + \epsilon^N\frac{\partial}{\partial t_N}.
\end{aligned}$$

The crucial assumption underlying a multiple-scale expansion is that the perturbation can be represented as a superposition of perturbations at different scales, which is conveniently written as a power series expansion in the small parameter ϵ.

$$\begin{aligned}
\phi(x, y, t) &= \phi(x_0, ..., x_N; y_0, ..., y_N; t_0, ..., t_N) \\
&= \sum_{n=0}^{N} \epsilon^n \phi_n(x_0, ..., x_N; y_0, ..., y_N; t_0, ..., t_N).
\end{aligned}$$

We shall also use the composition into fluctuating part,

$$\begin{aligned}
\widetilde{\phi}(x, y, t) &= \widetilde{\phi}(x_0, ..., x_N; y_0, ..., y_N; t_0, ..., t_N) \\
&= \sum_{n=0}^{N} \epsilon^n \widetilde{\phi}_n(x_0, ..., x_N; y_0, ..., y_N; t_0, ..., t_N),
\end{aligned}$$

and y averaged, i.e., zonal, part,

$$\begin{aligned}
\overline{\phi}(x, t) &= \overline{\phi}(x_0, ..., x_N; t_0, ..., t_N) \\
&= \sum_{n=0}^{N} \epsilon^n \overline{\phi}_n(x_0, ..., x_N; t_0, ..., t_N),
\end{aligned}$$

where the zonal part is independent of y. It is now straightforward to substitute the expressions above into the modified Hasegawa - Mima equation. The calculations leading to the amplitude relations at different orders in ϵ are, however, lengthy and thus given in Appendix B. We explicitly state necessary assumptions in order to simplify as much as possible, yet retaining a great deal of generality. For notational convenience we discard the zero-order contributions to the potential, this introduces merely a Doppler shift in the frequency in addition to reproducing the same equations as we shall find, only at order $n-1$, i.e., the order ϵ equation arises at order ϵ^0 and so on, see also Appendix B. The zonal flow should depend on variables at least one scale-order larger than the (small scale) fluctuations, thus the zonal components

should *not* depend on $\{x_0; t_0\}$ compared to the fluctuating motions. Furthermore the zonal components vary on a time scale much longer than the fluctuating components. Inserting into Eq. (3.51) and truncating the expansion at $N = 4$ yields to first order in ϵ

$$\left[1 - \left(\frac{\partial^2}{\partial x_0^2} + \frac{\partial^2}{\partial y_0^2}\right)\right] \frac{\partial \widetilde{\phi}_1}{\partial t_0} + \kappa \frac{\partial \widetilde{\phi}_1}{\partial y_0} = 0. \tag{3.53}$$

The above may be solved upon assuming a plane wave for the fluctuation at lowest order,

$$\widetilde{\phi}_1 = A \exp(ik_x x_0 + ik_y y_0 - \omega t_0) + A^* \exp(-ik_x x_0 - ik_y y_0 + \omega t_0), \tag{3.54}$$

where we furthermore restrict the amplitude to vary on scales longer and slower than the phase, i.e.,

$$A = A(x_1, x_2, x_3, x_4; y_1, y_2, y_3, y_4; t_1, t_2, t_3, t_4).$$

Periodicity in x and y requires that the box size, $[0, L_x] \times [0, L_y]$ satisfies $\lambda_x = L_x/n$ and $\lambda_y = L_y/m$ with $\{n, m\} \in \mathbb{N}$ and λ_x, λ_y are the wavelengths in the x and y directions respectively. Inserting into Eq. (3.53) yields the previously found dispersion relation for (resistive) drift waves

$$\omega = \frac{\kappa k_y}{1 + k_\perp^2}. \tag{3.55}$$

To second order in ϵ we get

$$\begin{aligned}
&\left[1 - \left(\frac{\partial^2}{\partial x_0^2} + \frac{\partial^2}{\partial y_0^2}\right)\right] \frac{\partial \widetilde{\phi}_2}{\partial t_0} + \kappa \frac{\partial \widetilde{\phi}_2}{\partial y_0} \\
&+ e^{i\theta} \left(\frac{\partial A}{\partial t_1} + k^2 \frac{\partial A}{\partial t_1} + \kappa \frac{\partial A}{\partial y_1} - 2\omega k_x \frac{\partial A}{\partial x_1} - 2\omega k_y \frac{\partial A}{\partial y_1}\right) \\
&+ e^{-i\theta} \left(\frac{\partial A^*}{\partial t_1} + k^2 \frac{\partial A^*}{\partial t_1} + \kappa \frac{\partial A^*}{\partial y_1} - 2\omega k_x \frac{\partial A^*}{\partial x_1} - 2\omega k_y \frac{\partial A^*}{\partial y_1}\right) = 0,
\end{aligned} \tag{3.56}$$

where we have introduced $\theta = ik_x x_0 + ik_y y_0 - i\omega t_0$ and $k^2 = k_x^2 + k_y^2$. Now, Eq. (3.56) is such that the exponentials are eigenfunctions of the kernel of the operator acting on $\widetilde{\phi}_2$, thus they give rise to resonance phenomenon and secular growth, which we shall discard as unphysical. Thus we have to remove the terms proportional to the exponentials via insisting that

$$\begin{aligned}
\frac{\partial A}{\partial t_1} + k^2 \frac{\partial A}{\partial t_1} + \kappa \frac{\partial A}{\partial y_1} - 2\omega k_x \frac{\partial A}{\partial x_1} - 2\omega k_y \frac{\partial A}{\partial y_1} = 0 \\
\frac{\partial A^*}{\partial t_1} + k^2 \frac{\partial A^*}{\partial t_1} + \kappa \frac{\partial A^*}{\partial y_1} - 2\omega k_x \frac{\partial A^*}{\partial x_1} - 2\omega k_y \frac{\partial A^*}{\partial y_1} = 0.
\end{aligned} \tag{3.57}$$

Computing the group velocity

$$\mathbf{v}_\mathrm{g} \equiv \frac{\partial \omega}{\partial \mathbf{k}} = \frac{\kappa}{1 + k^2} \widehat{\mathbf{y}} - \frac{2\omega}{1 + k^2} \mathbf{k}, \tag{3.58}$$

we may write the above as

$$(1 + k^2) \left(\frac{\partial A}{\partial t_1} + \mathbf{v}_\mathrm{g} \cdot \nabla_1 A\right) = 0, \tag{3.59}$$

where $\nabla_1 = \partial_{x_1} \widehat{\mathbf{x}} + \partial_{y_1} \widehat{\mathbf{y}}$. Eq. (3.59) describes advection of the amplitude at the velocity of the drift wave. It also tells us that the amplitude is constant on

scales $\mathcal{O}(\epsilon^{-1})$ measured in a frame of reference moving at the group velocity in the direction of drift wave propagation. What is left of Eq. (3.56) is

$$\left[1-\left(\frac{\partial^2}{\partial x_0^2}+\frac{\partial^2}{\partial y_0^2}\right)\right]\frac{\partial\widetilde{\phi}_2}{\partial t_0}+\kappa\frac{\partial\widetilde{\phi}_2}{\partial y_0}=0, \tag{3.60}$$

which has the exact same structure as Eq. (3.53). It is therefore reasonable to adopt the solution for $\widetilde{\phi}_2$ into $\widetilde{\phi}_1$ and set $\widetilde{\phi}_2=0$ in the further calculation, always bearing in mind that $\widetilde{\phi}_2$ really is present as a correction term for $\widetilde{\phi}_1$. To order ϵ^3 we then get

$$\begin{aligned}&\left[1-\left(\frac{\partial^2}{\partial x_0^2}+\frac{\partial^2}{\partial y_0^2}\right)\right]\frac{\partial\widetilde{\phi}_3}{\partial t_0}+\kappa\frac{\partial\widetilde{\phi}_3}{\partial y_0}\\&+e^{i\theta}\left(ik_yA\frac{\partial\overline{\phi}_1}{\partial x_1}+ik_x^2k_yA\frac{\partial\overline{\phi}_1}{\partial x_1}+ik_y^3A\frac{\partial\overline{\phi}_1}{\partial x_1}+\frac{\partial A}{\partial t_2}+k_x^2\frac{\partial A}{\partial t_2}+k_y^2\frac{\partial A}{\partial t_2}-2\omega k_y\frac{\partial A}{\partial y_2}\right.\\&\left.+\kappa\frac{\partial A}{\partial y_2}-2ik_y\frac{\partial^2A}{\partial y_1\partial t_1}+i\omega\frac{\partial^2A}{\partial y_1^2}-2\omega k_x\frac{\partial A}{\partial x_2}-2ik_x\frac{\partial^2A}{\partial x_1\partial t_1}+i\omega\frac{\partial^2A}{\partial x_1^2}\right)+cc.=0,\end{aligned}$$

where cc. stands for complex conjugate and denotes all the terms containing the complex amplitude and are proportional to $e^{-\theta}$. Again invoking the solvability condition upon insisting that

$$\begin{aligned}&ik_yA\frac{\partial\overline{\phi}_1}{\partial x_1}+ik_x^2k_yA\frac{\partial\overline{\phi}_1}{\partial x_1}+ik_y^3A\frac{\partial\overline{\phi}_1}{\partial x_1}+\frac{\partial A}{\partial t_2}+k_x^2\frac{\partial A}{\partial t_2}+k_y^2\frac{\partial A}{\partial t_2}-2\omega k_y\frac{\partial A}{\partial y_2}\\&+\kappa\frac{\partial A}{\partial y_2}-2ik_y\frac{\partial^2A}{\partial y_1\partial t_1}+i\omega\frac{\partial^2A}{\partial y_1^2}-2\omega k_x\frac{\partial A}{\partial x_2}-2ik_x\frac{\partial^2A}{\partial x_1\partial t_1}+i\omega\frac{\partial^2A}{\partial x_1^2}=0,\end{aligned}$$

which may be reformulated as

$$\begin{aligned}\left[\frac{\partial A}{\partial t_2}+\mathbf{v}_{\mathrm{g}}\cdot\nabla_2A\right]+i\frac{1}{1+k^2}\Big[&(\omega+2k_xv_{\mathrm{g}x})\frac{\partial^2A}{\partial x_1^2}+(\omega+2k_yv_{\mathrm{g}y})\frac{\partial^2A}{\partial y_1^2}\\&+2(k_xv_{\mathrm{g}y}+k_yv_{\mathrm{g}x})\frac{\partial^2A}{\partial x_1\partial y_1}\Big]+ik_yA\frac{\partial\overline{\phi}_1}{\partial x_1}=0.\end{aligned} \tag{3.61}$$

We have made use of Eq. (3.59) to arrive at the above. Again, we are left with

$$\left[1-\left(\frac{\partial^2}{\partial x_0^2}+\frac{\partial^2}{\partial y_0^2}\right)\right]\frac{\partial\widetilde{\phi}_3}{\partial t_0}+\kappa\frac{\partial\widetilde{\phi}_3}{\partial y_0}=0,$$

suggesting that also $\widetilde{\phi}_3$ may be absorbed into $\widetilde{\phi}_1$ and consequently set to zero in the further calculations. We then proceed to order ϵ^4,

$$
\begin{aligned}
&\left[1-\left(\frac{\partial^2}{\partial x_0^2}+\frac{\partial^2}{\partial y_0^2}\right)\right]\frac{\partial\widetilde{\phi}_4}{\partial t_0}+\kappa\frac{\partial\widetilde{\phi}_4}{\partial y_0}\\
&-\frac{\partial^3\overline{\phi}_1}{\partial x_1^2\partial t_1}-4k_xk_y\frac{\partial A}{\partial y_1}\frac{\partial A^*}{\partial y_1}-2k_xk_yA^*\frac{\partial^2A}{\partial y_1^2}-2k_xk_yA\frac{\partial^2A^*}{\partial y_1^2}-2k_x^2\frac{\partial A^*}{\partial y_1}\frac{\partial A}{\partial x_1}\\
&+2k_y^2\frac{\partial A^*}{\partial y_1}\frac{\partial A}{\partial x_1}-2k_x^2\frac{\partial A}{\partial y_1}\frac{\partial A^*}{\partial x_1}+2k_y^2\frac{\partial A}{\partial y_1}\frac{\partial A^*}{\partial x_1}+4k_xk_y\frac{\partial A}{\partial x_1}\frac{\partial A^*}{\partial x_1}-2k_x^2A^*\frac{\partial^2A}{\partial x_1\partial y_1}\\
&+2k_y^2A^*\frac{\partial^2A}{\partial x_1\partial y_1}-2k_x^2A\frac{\partial^2A^*}{\partial x_1\partial y_1}+2k_y^2A\frac{\partial^2A^*}{\partial x_1\partial y_1}+2k_xk_yA^*\frac{\partial^2A}{\partial x_1^2}+2k_xk_yA\frac{\partial^2A}{\partial y_1^2}\\
&+e^{i\theta}\Bigg(ik_yA\frac{\partial\overline{\phi}_1}{\partial x_2}+ik_x^2k_yA\frac{\partial\overline{\phi}_1}{\partial x_2}+ik_y^3A\frac{\partial\overline{\phi}_1}{\partial x_2}+ik_yA\frac{\partial\overline{\phi}_2}{\partial x_1}+ik_x^2k_yA\frac{\partial\overline{\phi}_2}{\partial x_1}\\
&+ik_y^3A\frac{\partial\overline{\phi}_2}{\partial x_1}+\frac{\partial\overline{\phi}_1}{\partial x_1}\frac{\partial A}{\partial y_1}+k_x^2\frac{\partial\overline{\phi}_1}{\partial x_1}\frac{\partial A}{\partial y_1}+3k_y^2\frac{\partial\overline{\phi}_1}{\partial x_1}\frac{\partial A}{\partial y_1}-i2k_y\frac{\partial^2A}{\partial y_2\partial t_1}\\
&-i2k_y\frac{\partial^2A}{\partial y_1\partial t_2}+i2\omega\frac{\partial^2A}{\partial y_1\partial y_2}-\frac{\partial^3A}{\partial y_1^2\partial t_1}-i2k_x\frac{\partial^2A}{\partial x_2\partial t_1}+2k_xk_y\frac{\partial\overline{\phi}_1}{\partial x_1}\frac{\partial A}{\partial x_1}\\
&-i2k_x\frac{\partial^2A}{\partial x_1\partial t_2}+i2\omega\frac{\partial^2A}{\partial x_1\partial x_2}-\frac{\partial^3A}{\partial x_1^2\partial t_1}\Bigg)\\
&+e^{2i\theta}\Bigg[2k_x^2A\frac{\partial^2A}{\partial x_1\partial y_1}+2k_xk_yA\frac{\partial^2A}{\partial y_1^2}-2k_xk_yA\frac{\partial^2A}{\partial x_1^2}-2k_y^2A\frac{\partial^2A}{\partial x_1\partial y_1}\\
&+2k_xk_y\left(\frac{\partial A}{\partial x_1}\right)^2+2k_y^2\frac{\partial A}{\partial x_1}\frac{\partial A}{\partial y_1}-2k_x^2\frac{\partial A}{\partial x_1}\frac{\partial A}{\partial y_1}-2k_xk_y\left(\frac{\partial A}{\partial y_1}\right)^2\Bigg]+cc.=0.
\end{aligned}
$$

In this case cc. represents the complex conjugate of all the terms proportional to either $e^{i\theta}$ or $e^{2i\theta}$. We proceed by averaging over the y_0 coordinate and use our previous assumption of periodic boundary conditions. The required box length in the y_0 direction is as stated above $\lambda_y = L_y/m$. Note that the terms proportional to the exponentials are all independent of y_0. Furthermore the exponentials vanish upon averaging,

$$
\begin{aligned}
&\frac{1}{L_y}\int_0^{L_y}\exp(ik_xx_0+ik_yy_0-i\omega t_0)dy_0=\frac{1}{L_y}\exp(ik_xx_0-i\omega t_0)\left(\frac{1}{ik_y}e^{ik_yy_0}\right)\Bigg|_0^{L_y}\\
&=\frac{1}{L_y}\exp(ik_xx_0-i\omega t_0)\frac{1}{ik_y}\left[\exp\left(i\frac{2\pi mL_y}{L_y}\right)-1\right]=0,
\end{aligned}
$$

and

$$
\begin{aligned}
&\frac{1}{L_y}\int_0^{L_y}\exp(2ik_xx_0+2ik_yy_0-2i\omega t_0)dy_0\\
&=\frac{1}{L_y}\exp(2ik_xx_0-2i\omega t_0)\frac{1}{2ik_y}\left[\exp\left(2i\frac{2\pi mL_y}{L_y}\right)-1\right]=0.
\end{aligned}
$$

The first term also vanishes since

$$
\frac{1}{L_y}\int_0^{L_y}\widetilde{\phi}_4\equiv 0,
$$

and periodicity also applies to $\partial_{y_1}\widetilde{\phi}_4$. We then have only the first order terms left, which can be rewritten as

$$
\frac{\partial^2}{\partial x_1^2}\left(\frac{\partial\overline{\phi}_1}{\partial t_1}\right)=\left[2k_xk_y\left(\frac{\partial^2}{\partial x_1^2}-\frac{\partial^2}{\partial y_1^2}\right)+2\left(k_x^2-k_y^2\right)\frac{\partial^2}{\partial x_1\partial y_1}\right]|A|^2. \tag{3.62}
$$

Clearly the LHS is independent of y_1 which implies that the RHS must not depend on y_1 either. Consequently, averaging over y_1 gives

$$\frac{\partial^2}{\partial x_1^2}\left(\frac{\partial\overline{\phi}_1}{\partial t_1}\right) = 2k_xk_y\frac{\partial^2}{\partial x_1^2}\overline{|A|^2}, \tag{3.63}$$

and it follows

$$\frac{\partial\overline{\phi}_1}{\partial t_1} = 2k_xk_y\overline{|A|^2}, \tag{3.64}$$

upon integration with respect to x_1. The zonal flow is driven by the drift wave amplitude, which to lowest order is a function of $\zeta = x_1 - v_{\mathrm{g}x}t_1$ and $A \approx A(\zeta)$. Applying the chain rule then allows us to rewrite Eq. (3.64) as

$$\frac{\partial\overline{\phi}_1}{\partial x_1} = -\frac{2k_xk_y}{v_{\mathrm{g}x}}\overline{|A|^2}, \tag{3.65}$$

which we may insert for the last term in Eq. (3.61) to obtain

$$\begin{aligned} i\left[\frac{\partial A}{\partial t_2} + \mathbf{v}_{\mathrm{g}}\cdot\nabla_2 A\right] - \frac{1}{1+k^2}\Bigg[&(\omega + 2k_xv_{\mathrm{g}x})\frac{\partial^2 A}{\partial x_1^2} + (\omega + 2k_yv_{\mathrm{g}y})\frac{\partial^2 A}{\partial y_1^2} \\ &+ 2(k_xv_{\mathrm{g}y} + k_yv_{\mathrm{g}x})\frac{\partial^2 A}{\partial x_1\partial y_1}\Bigg] + \frac{1}{v_{\mathrm{g}x}}2k_xk_y^2\overline{|A|^2}A = 0. \end{aligned} \tag{3.66}$$

Eq. (3.66) can be further simplified upon transforming to a reference frame moving at the group velocity in the direction of drift wave propagation and also noting that the plasma we are considering is inhomogeneous only in the x direction, thus we may restrict the amplitude to be weakly varying with respect to y. What drops out is the one dimensional, nonlinear, cubic Schrödinger equation:

$$i\frac{\partial A}{\partial t_2} - \frac{1}{1+k^2}(\omega + 2k_xv_{\mathrm{g}x})\frac{\partial^2 A}{\partial x_1^2} + \frac{1}{v_{\mathrm{g}x}}2k_xk_y^2\overline{|A|^2}A = 0. \tag{3.67}$$

From Eq. (3.64) we find that a growth in drift wave amplitude causes also a growth in zonal flow amplitude. Below we derive the instability region for the equation above.

Instability criterion

A detailed derivation of the dispersion relation is given in Appendix B. Consider

$$i\frac{\partial A}{\partial t} + P\frac{\partial^2 A}{\partial x^2} + Q\,|A|\,A = 0, \tag{3.68}$$

and perturb a solution, A_0, that is supposed to satisfy the above. The dispersion relation is then given by (Swanson [11])

$$\Omega^2 = P^2k^4 - 2PQk^2\,|A_0|^2\,. \tag{3.69}$$

The instability criterion is clearly

$$PQ > 0,$$

such that the wavenumber satisfies

$$0 < k^2 < 2Q\,|A_0|^2\,/P,$$

and the maximum growth occurs for

$$k = \sqrt{Q \left|A_0\right|^2 / P},$$

with maximum growth rate

$$\gamma_{\max} = Q \left|A_0\right|^2.$$

Comparing with Eq. (3.67) and recognizing

$$P = -\frac{1}{1+k^2}(\omega + 2k_x v_{\mathrm{g}x}),$$

as well as

$$Q = \frac{1}{v_{\mathrm{g}x}} 2k_x k_y^2,$$

we have the instability criterion for modulational instability of drift waves satisfying the modified Hasegawa - Mima equation:

$$-\frac{1}{1+k^2}(\omega + 2k_x v_{\mathrm{g}x}) \frac{1}{v_{\mathrm{g}x}} 2k_x k_y^2 > 0, \tag{3.70}$$

which is satisfied when

$$1 + k_y^2 - 3k_x^2 > 0. \tag{3.71}$$

Note that this is just what we would expect from section (6.2) where we deduced Eq. (3.47) in order for drift waves to generate a growing zonal flow. This can be understood by means of Eq. (3.64), where we stated that zonal flow amplitude growth is caused by growth in drift wave amplitude. Thus we see that drift waves are modulational unstable and zonal flows generated by beating of drift waves are growing in the same wave number regime. This is a good indicator for drift waves being the main driving mechanism for zonal flow generation.

Nonlinear frequency shift

We may identify the middle term, P, of the LHS of Eq. (3.67) as the group dispersion and the last term of the LHS in Eq. (3.67), Q, as the nonlinear frequency shift. Recall the relations,

$$\omega = \frac{\kappa k_y}{1+k^2},\ v_{gx} = -\frac{2k_x\omega}{1+k^2},\ \frac{\partial v_{gx}}{\partial k_x} = -2\omega\frac{1+k_y^2-3k_x^2}{1+k^2}. \tag{3.72}$$

Using the above we rewrite the middle term,

$$\begin{aligned} P &= -\frac{\omega + 2k_x v_{gx}}{1+k^2} \\ &= -\frac{1}{1+k^2}(\omega - 4k_x^2 \frac{\omega}{1+k^2}) \\ &= -\frac{\omega}{1+k^2}(1+k^2-4k_x^2) \\ &= -\frac{\omega}{1+k^2}(1+k_y^2-3k_x^2) \\ &= \frac{1}{2}\frac{\partial v_{gx}}{\partial k_x}, \end{aligned}$$

to find the group dispersion. Furthermore,

$$\begin{aligned} Q &= \frac{1}{v_{gx}} 2k_x k_y^2 \\ &= -(1+k^2)^2 \frac{k_y}{\kappa}, \end{aligned}$$

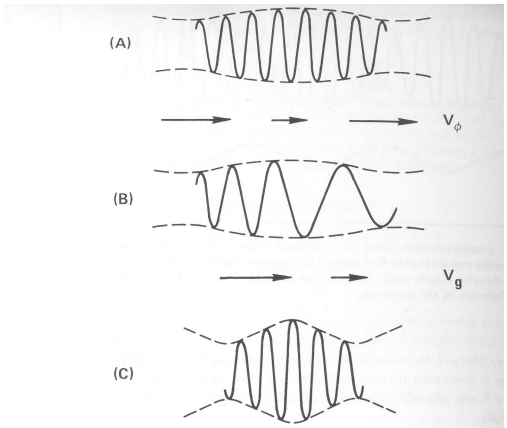

FIGURE 8-27 Modulational instability occurs when the nonlinear frequency shift and the group velocity dispersion have opposite signs.

Figure 3.5: Modulation mechanism.

takes the place of the nonlinear frequency shift, $\delta\omega \propto \partial\omega/\partial\left|A\right|^2$. Recall that we started out with $Q = \partial\overline{\phi}/\partial x_1 \propto \left|A\right|^2$, cf. Eq. (3.65), and since a nonlinear frequency shift in general is a functional of the amplitude, Q takes indeed the place of the frequency shift. Instead of the more mathematical arguments giving the constraints for instability, we also want to show the more physical arguing of Chen (ch. 8.8.82, pp.337 in [2]). Consider Figure 8-27 in [2]. The ripple in the envelope modulation can only grow if there is an energy pile up where the intensity of the modulation already is high. This happens precisely when the the nonlinear frequency shift and the group dispersion have opposite sign. In this case, the nonlinear frequency shift, which is proportional to ω induces an opposite variation of the phase-velocity, $v_p = \omega/k$, with respect to the group dispersion. Take for instance $P > 0$ and $Q > 0$, then $\delta\omega \propto \frac{\partial\omega}{\partial|A|^2} < 0$, thus in regions of increasing wave-intensity, the frequency is shifted downwards. Therefore the phase-velocity is lower in those regions, than in regions where the wave-intensity decreases. This then leads to a pile up of wave crests to the left of intensity maxima, which in turn leads to a local increase in k there. Then, since $P > 0$ the group velocity in regions of increasing intensity is also higher than in regions of decreasing intensity ($P \propto \partial v_{gx}/\partial k_x > 0$). We are in the situation of 8-27 (C) and the modulation is unstable due to the pile up of wave energy at intensity maxima. If $PQ < 0$, the situation is reversed, and the modulation is flattened out. We have thus, also physically deduced, that for drift-waves to go unstable we need $PQ > 0$ which according to our identifications in the previously derived NLS corresponds to

$$-\frac{1}{2}\frac{\partial v_{gx}}{\partial k_x}(1+k^2)^2\frac{k_y}{\kappa} > 0 \;\Leftrightarrow\; k_y^2(1+k_y^2-3k_x^2) > 0,$$

and consequently we have the constraint

$$1 + k_y^2 - 3k_x^2 > 0. \tag{3.73}$$

Wave Kinetic Equation

There exists an overwhelming amount of literature on the derivation of different kinds of wave kinetic equations. We use a somewhat different approach based on the assumption that in a saturated state, the wave action density is approximately unchanged. Introduce the phase-space spanned by Cartesian coordinates,

$\mathbf{x} = (x, y)$, and wavenumbers, $\mathbf{k} = (k_x, k_y)$, which both are parametrized by the time-variable, t, such that $\mathbf{x} = \mathbf{x}(t)$ and $\mathbf{k} = \mathbf{k}(t)$. We then define the *wave action density* according to

$$N(\mathbf{x}, \mathbf{k}, t) \equiv \frac{\mathcal{E}_k}{\omega_k}, \tag{3.74}$$

where $\mathcal{E}_k$ is the energy density corresponding to a wave with wave-vector k and ω_k is the wave-frequency measured in a reference frame moving with the wave under consideration. In the saturated state, the action density is conserved in phase-space (McDonald [16]), which is also intuitively deduced from wave action density being conserved in a frame of reference moving with the group velocity (Whitham [12], Smolyakov [13], Hayes [14]).

$$\frac{\partial}{\partial t} N + \frac{\partial}{\partial x_i} \left(\frac{dx_i}{dt} N \right) \approx 0, \tag{3.75}$$

where x_i stands for either of the phase-space coordinates and summation over repeated indices is implied. Following Bellan [3] we arrive at expressions relating the phase-space velocities to the local dispersion relation. Suppose that the solution of the local dispersion relation is given as a functional relation on the form $\omega = \omega(\mathbf{x}, \mathbf{k}) = 0$. Close by, i.e., at $(\mathbf{x} + \delta\mathbf{x}, \mathbf{k} + \delta\mathbf{k})$, the solution can be found upon Taylor-expanding the above, given that the medium changes smoothly, thus

$$\omega(\mathbf{x} + \delta\mathbf{x}, \mathbf{k} + \delta\mathbf{k}) \approx \omega(\mathbf{x}, \mathbf{k}) + \delta\mathbf{x} \frac{\partial \omega}{\partial \mathbf{x}} + \delta\mathbf{k} \frac{\partial \omega}{\partial \mathbf{k}} = \delta\mathbf{x} \frac{\partial \omega}{\partial \mathbf{x}} + \delta\mathbf{k} \frac{\partial \omega}{\partial \mathbf{k}} = 0,$$

since $\omega(\mathbf{x}, \mathbf{k}) = 0$ is satisfied, and $\omega(\mathbf{x} + \delta\mathbf{x}, \mathbf{k} + \delta\mathbf{k}) = 0$ by definition of being a solution of the local dispersion relation. Now, suppose that the phase space coordinates are parametrized by a time variable, $(\mathbf{x}, \mathbf{k}) = (\mathbf{x}(t), \mathbf{k}(t))$. Then we have the relations $\delta\mathbf{x} = d\mathbf{x}/dt \ \delta t$ and $\delta\mathbf{k} = d\mathbf{k}/dt \ \delta t$. The equation above thus reads

$$0 \approx \frac{d\mathbf{x}}{dt} \frac{\partial \omega}{\partial \mathbf{x}} \delta t + \frac{d\mathbf{k}}{dt} \frac{\partial \omega}{\partial \mathbf{k}} \delta t,$$

which is solved by

$$\frac{d\mathbf{x}}{dt} = \frac{\partial \omega}{\partial \mathbf{k}} \tag{3.76a}$$

$$\frac{d\mathbf{k}}{dt} = -\frac{\partial \omega}{\partial \mathbf{x}}. \tag{3.76b}$$

These relations, familiar from *geometric optics* are inserted into Eq. (3.75) yielding the wave kinetic equation for a quasi-stationary state (i.e., no dissipation or generation of wave action)

$$\frac{\partial N}{\partial t} + \frac{\partial \omega}{\partial \mathbf{k}} \cdot \frac{\partial N}{\partial \mathbf{x}} - \frac{\partial \omega}{\partial \mathbf{x}} \cdot \frac{\partial N}{\partial \mathbf{k}} = 0, \tag{3.77}$$

where we have used that the divergence of the flow-velocity in phase-space vanishes due to the Hamiltonian structure dependence on the dispersion relation described above,

$$\begin{aligned} \frac{\partial}{\partial x_i} \frac{dx_i}{dt} &= \frac{\partial}{\partial x} \frac{dx}{dt} + \frac{\partial}{\partial y} \frac{dy}{dt} + \frac{\partial}{\partial k_x} \frac{dk_x}{dt} + \frac{\partial}{\partial k_y} \frac{dk_y}{dt} \\ &= \frac{\partial}{\partial x} \frac{\partial \omega}{\partial k_x} + \frac{\partial}{\partial y} \frac{\partial \omega}{\partial k_y} - \frac{\partial}{\partial k_x} \frac{\partial \omega}{\partial x} - \frac{\partial}{\partial k_y} \frac{\partial \omega}{\partial y} \\ &= 0. \end{aligned}$$

Note that Eq. (3.77) may be written by means of Poisson brackets

$$\frac{\partial N}{\partial t} + \{N, \omega\} = 0 \ , \tag{3.78}$$

which clearly resembles the close analogy to a non-dissipative one-particle system with canonical coordinate vector $\mathbf{q}$, conjugate momentum $\mathbf{p}$ and distribution function $f = f(\mathbf{q}, \mathbf{p})$ where the evolution of the distribution function is governed by

$$\frac{\partial f}{\partial t} + \{f, H\} = 0 \ , \tag{3.79}$$

and H is the systems Hamiltonian. By analogy, the solution of the dispersion relation (more precisely, the dispersion relation itself) then represents the Hamiltonian and the wave action density resembles the distribution function.

Consider now the coupling of a spectrum of drift waves to the zonal flow mode. To this end we average the evolution equation for the zonal flow, Eq. (3.13) over an ensemble of small - scale drift wave realizations to obtain

$$\frac{\partial}{\partial t}\frac{\partial^2}{\partial x^2}\overline{\phi} = \frac{\partial}{\partial x}\left\langle \frac{\partial \widetilde{\phi}}{\partial y}\widetilde{\Omega} \right\rangle , \tag{3.80}$$

where the angle brackets denote the average in k -space. From Appendix A we have the relation

$$\frac{\partial \widetilde{\phi}}{\partial y}\widetilde{\Omega} = \frac{\partial}{\partial x}\left(\frac{\partial \widetilde{\phi}}{\partial x}\frac{\partial \widetilde{\phi}}{\partial y} \right),$$

which casts Eq. (3.80) as

$$\frac{\partial}{\partial t}\frac{\partial^2}{\partial x^2}\overline{\phi} = \frac{\partial^2}{\partial x^2}\int d^2\ k k_x k_y \left|\phi_k\right|^2 . \tag{3.81}$$

Along a given wave ray trajectory, the density of waves is constant. According to [5] the population density identifies with the wave action for drift waves here, which for the MHM equation is given by ([5], [13])

$$N_k = (1 + k_\perp^2)^2 \left|\phi_k\right|^2 . \tag{3.82}$$

In the presence of a zonal flow, this equilibrium wave action density is modulated according to ([5], [13])

$$N_k \to N_0 + \widetilde{N}. \tag{3.83}$$

Consequently the zonal flow evolution expressed in terms of the modulated wave action is then from Eq. (3.81)

$$\frac{\partial}{\partial t} v'_{ZF} = \frac{\partial^2}{\partial x^2}\int d^2\ k \frac{k_x k_y}{(1 + k_\perp^2)^2}\widetilde{N}, \tag{3.84}$$

where we have followed [5] by introducing the zonal flow velocity, $v_{ZF} = \partial_x \overline{\phi}$ and $'$ means differentiation with respect to x. Note that the part including N_0 vanishes, since the equilibrium value is assumed to describe an isotropic spectrum (i.e., $\partial_x^2 N_0 = 0$). We proceed by calculating the modulation of the wave action density. Let us assume that the perturbation of the equilibirum wave action density due to the zonal flow can be written as $\widetilde{N} \sim e^{iqx - i\Omega t}$. Inserting into the wave kinetic

equation, Eq. (3.77), and using the drift wave frequency $\omega = k_y v_{ZF} + \kappa k_y/(1+k_\perp^2)$ gives

$$\frac{\partial N_0}{\partial t} - i\Omega\widetilde{N} + \frac{\partial\omega}{\partial k_x} iq\widetilde{N} + \frac{\partial\omega}{\partial k_x}\frac{\partial N_0}{\partial x} + \frac{\partial\omega}{\partial k_y}\frac{\partial N_0}{\partial y} - \frac{\partial\omega}{\partial x}\frac{\partial N_0}{\partial k_x} - \frac{\partial\omega}{\partial y}\frac{\partial N_0}{\partial k_y} - \frac{\partial\omega}{\partial y}\frac{\partial\widetilde{N}}{\partial k_y} = 0.$$

The equilibrium wave action is assumed to be a function of wave numbers only (isotropic in coordinate space), such that solving for the modulation gives

$$\widetilde{N} = -q^2\overline{\phi}k_y\frac{\partial N_0}{\partial k_x}\frac{i}{\Omega - qv_g}, \tag{3.85}$$

where of course $v_g = \partial_{k_x}\omega$. Note that we have used the *intrinsic* drift wave frequency, i.e., the frequency observed in a frame of reference moving with the drift waves. Clearly the presence of the zonal flow induces a Doppler shift in this frame of reference, contributing by $k_y v_{ZF}$ to the measured frequency. Note that the equations describing the evolution of the phase-space coordinates, Eqs. (3.76), are derived in such a moving frame of reference (following the particle/wave in phase-space). Now, inserting the expression above into Eq. (3.84) yields

$$\Omega = q^2\int d^2k\ \frac{k_x k_y}{(1+k_\perp^2)^2}k_y\frac{\partial N_0}{\partial k_x}\frac{i}{\Omega - qv_g}. \tag{3.86}$$

Assuming that the wave-packet is localized at some wave number, $\mathbf{k}_0$ such that $N_0 = N^0\delta(\mathbf{k}-\mathbf{k}_0)$, we may integrate by parts to arrive at

$$\Omega = -q^2\int d^2k\ k_y^2 N_0\frac{\partial}{\partial k_x}\left[\frac{k_x}{(1+k_\perp^2)^2}\frac{1}{\Omega - qv_g}\right], \tag{3.87}$$

where we have used that $N_0(\text{bdy } k_x) = 0$, since the wave - packet is assumed to be localized. From Eq. (3.44) we read off

$$\frac{v_g}{2\kappa k_y} = -\frac{k_x}{(1+k^2)^2},$$

which allows us to rewrite the derivative under the integral above,

$$\begin{aligned}\frac{\partial}{\partial k_x}\left[\frac{k_x}{(1+k^2)^2}\frac{1}{\Omega - qv_g}\right] &= \frac{\partial}{\partial k_x}\left(-\frac{v_g}{2\kappa k_y}\frac{1}{\Omega - qv_g}\right)\\ &= -\frac{1}{\Omega - qv_g}\frac{1}{2\kappa k_y}\frac{\partial v_g}{\partial k_x} - \frac{1}{2\kappa k_y}\frac{qv_g}{(\Omega - qv_g)^2}\frac{\partial v_g}{\partial k_x}\\ &= -\frac{\Omega}{(\Omega - qv_g)^2}\frac{1}{2\kappa k_y}\frac{\partial v_g}{\partial k_x}.\end{aligned}$$

Eq. (3.87) becomes

$$1 = q^2\int d^2k\ k_y^2\frac{N_0}{2\kappa k_y}\frac{\partial v_g}{\partial k_x}\frac{1}{(\Omega - qv_g)^2}, \tag{3.88}$$

or equivalently

$$(\Omega - qv_g)^2 = q^2k_y^2\frac{N^0}{2\kappa k_y}\frac{\partial v_g}{\partial k_x}, \tag{3.89}$$

and the integral over the delta-distribution vanishes for all $\mathbf{k}$ except for $\mathbf{k}_0 \equiv (k_x, k_y)$. Clearly, for instability to occur we have the criterion

$$\frac{N^0}{2\kappa k_y}\frac{\partial v_g}{\partial k_x} < 0, \tag{3.90}$$

which upon calculation of the group velocity reduces to (see Eq. (3.45))

$$\frac{N^0}{(1+k^2)^3}(1+k_y^2-3k_x^2)>0, \tag{3.91}$$

which is precisely what we have discovered before when considering four mode coupling, cf. Eq. (3.47), and also by the multiple - scale expansion technique, cf. Eq. (3.73) . The growth rate is hence given by

$$\Omega = qv_g - i\sqrt{\frac{q^2N^0k_y^2}{(1+k^2)^3}(1+k_y^2-3k_x^2)}, \tag{3.92}$$

which is comparable to Eq. (3.46) for $N^0 = 2(1+k^2)\left|\phi_0\right|^2$ and $q \ll 1$.
What we have deduced by now is the following. Decomposition into turbulent and zonal averaged components show that there is energy transfer from fluctuating motions into zonal structures by means of turbulent velocity shearing, quantified by the Reynolds-stress. Parametric instability due to beating of a pump drift wave with its sidebands may result in zonal structures if the aspect ratio of the drift waves satisfies $1+k_y^2-3k_x^2>0$. The same instability domain is found by considering modulational instability of drift wave amplitudes, which is accompanied by zonal flow amplitude growth, cf. Eq. (3.64). A more classical approach using conservation of wave action density reproduces the instability domain in wavenumber space, underlining the crucial dependence of drift wave aspect ratio for zonal flow formation. The physical reason for this constraint intuitively follows from Figure 3.1.

Chapter 4

Drift wave energetics

We start by deriving various integral quantities characteristic for the OHW and MHW systems, which give insight to the energy flow intrinsic to the systems. In the simulation these integrals are computed such that we may confirm the analytically predicted energy flow in favor of zonal flow generation by means of numerical results.

Energetics of the ordinary Hasegawa - Wakatani model

Recall the OHW eqs. :

$$\frac{\partial \Omega}{\partial t} + \{\phi, \Omega\} = \alpha\left(\phi - n\right) + D^{\Omega}\nabla_{\perp}^{2}\Omega \tag{4.1a}$$

$$\frac{\partial n}{\partial t} + \{\phi, n\} = \alpha\left(\phi - n\right) - \kappa\frac{\partial \phi}{\partial y} + D^{n}\nabla_{\perp}^{2} n. \tag{4.1b}$$

Following the procedure from section (Energy transfer) we multiply Eq. (4.1a) by ϕ and integrate over coordinate space to get an evolution equation for the total kinetic energy,

$$\frac{\partial}{\partial t}\int d\mathbf{x}\ \frac{1}{2}\left(\nabla_{\perp}\phi\right)^{2} = -\alpha\int d\mathbf{x}\ \phi\left(\phi - n\right) - \int d\mathbf{x}\ \phi D^{\Omega}\nabla_{\perp}^{2}\Omega. \tag{4.2}$$

Averaging Eq. (4.1a) in the zonal direction yields

$$\frac{\partial}{\partial t}\overline{\Omega} - \frac{\partial}{\partial x}\overline{\left(\Omega\frac{\partial \phi}{\partial y}\right)} = \alpha\left(\overline{\phi} - \overline{n}\right) + \frac{1}{L_y}\int_{0}^{L_y} dy\ D^{\Omega}\nabla_{\perp}^{2}\Omega. \tag{4.3}$$

We shall use $D_0^{\Omega} = D^{\Omega}\nabla_{\perp}^{2}\Omega$ for notational convenience. Multiplying through by $\overline{\phi}$ and integrating also over y then gives the evolution of the zonal flow kinetic energy,

$$\frac{d}{dt}\int d\mathbf{x}\ \frac{1}{2}\left(\nabla\overline{\phi}\right)^{2} = \int d\mathbf{x}\ \overline{\phi}\frac{\partial}{\partial x}\overline{\left(\Omega\frac{\partial \phi}{\partial y}\right)} - \alpha\int d\mathbf{x}\ \overline{\phi}\left(\overline{\phi} - \overline{n}\right) - \int d\mathbf{x}\ \overline{\phi}D_0^{\Omega}. \tag{4.4}$$

As previously shown, subtracting the zonal flow kinetic energy evolution equation from the total kinetic energy evolution equation results in an evolution equation for the kinetic energy contained in the fluctuating motions, cf. Eq. (3.25).

$$\begin{aligned}\frac{\partial}{\partial t}\int d\mathbf{x}\ \frac{1}{2}\left(\nabla\widetilde{\phi}\right)^{2} = &-\int d\mathbf{x}\ \overline{\phi}\frac{\partial}{\partial x}\overline{\left(\Omega\frac{\partial \phi}{\partial y}\right)} \\ &+\alpha\int d\mathbf{x}\ \left[\overline{\phi}\left(\overline{\phi} - \overline{n}\right) - \phi\left(\phi - n\right)\right] + \int d\mathbf{x}\ \left[\overline{\phi}D_0^{\Omega} - \phi D_0^{\Omega}\right].\end{aligned} \tag{4.5}$$

Note that

$$\begin{aligned}\left(\overline{\phi}-\overline{n}\right)-\phi\left(\phi-n\right) &= \overline{\phi}(\overline{\phi}-\overline{n})-\left[(\overline{\phi}+\widetilde{\phi})(\overline{\phi}+\widetilde{\phi}-\overline{n}-\widetilde{n})\right] \\ &= -\widetilde{\phi}(\widetilde{\phi}-\widetilde{n})-\overline{\phi}(\widetilde{\phi}-\widetilde{n})-\widetilde{\phi}(\overline{\phi}-\overline{n}),\end{aligned}$$

and the last two therm vanish when integrating over y by definition of the average of fluctuating quantities upon moving the averaged quantities out of the y integral. We thus have

$$\begin{aligned}\frac{\partial}{\partial t}\int d\mathbf{x}\ \frac{1}{2}\left(\nabla\widetilde{\phi}\right)^2 = &-\int d\mathbf{x}\ \overline{\phi}\frac{\partial}{\partial x}\overline{\left(\Omega\frac{\partial\phi}{\partial y}\right)} \\ &-\alpha\int d\mathbf{x}\ \widetilde{\phi}\left(\widetilde{\phi}-\widetilde{n}\right)+\int d\mathbf{x}\ \left[\overline{\phi}D_0^{\Omega}-\phi D_0^{\Omega}\right].\end{aligned}\tag{4.6}$$

Multiplying Eq. (4.1) by n and integrating over coordinate space yields the evolution equation for the potential energy.

$$\frac{\partial}{\partial t}\int d\mathbf{x}\ \frac{1}{2}n^2 = -\kappa\int d\mathbf{x}\ n\frac{\partial\phi}{\partial y}+\alpha\int d\mathbf{x}\ n\left(\phi-n\right)+D^n\int d\mathbf{x}\ n\nabla_\perp^2 n,\tag{4.7}$$

where we have used Eq. (3.4) with ϕ replaced by n in the calculation leading to the above. Writing out the full density and potential in the first and second term on the RHS then gives

$$\begin{aligned}\frac{\partial}{\partial t}\int d\mathbf{x}\ \frac{1}{2}n^2 = &-\kappa\int d\mathbf{x}\ \widetilde{n}\frac{\partial\widetilde{\phi}}{\partial y}+\alpha\int d\mathbf{x}\ \overline{n}\left(\overline{\phi}-\overline{n}\right) \\ &+\alpha\int d\mathbf{x}\ \widetilde{n}\left(\widetilde{\phi}-\widetilde{n}\right)+D^n\int d\mathbf{x}\ n\nabla_\perp^2 n.\end{aligned}\tag{4.8}$$

The total energy is the sum of potential and kinetic energy of fluctuating motions and the zonal flow. Hence,

$$\begin{aligned}&\frac{\partial}{\partial t}\int d\mathbf{x}\ \left[\frac{1}{2}n^2+\frac{1}{2}\left(\nabla\phi\right)^2\right] = -\kappa\int d\mathbf{x}\ \widetilde{n}\frac{\partial\widetilde{\phi}}{\partial y}+\alpha\int d\mathbf{x}\ \overline{n}\left(\overline{\phi}-\overline{n}\right) \\ &+\alpha\int d\mathbf{x}\ \widetilde{n}\left(\widetilde{\phi}-\widetilde{n}\right)+D^n\int d\mathbf{x}\ n\nabla_\perp^2 n-\alpha\int d\mathbf{x}\ \overline{\phi}\left(\overline{\phi}-\overline{n}\right) \\ &-\alpha\int d\mathbf{x}\ \widetilde{\phi}\left(\widetilde{\phi}-\widetilde{n}\right)-\int d\mathbf{x}\ \phi D^{\Omega}\nabla_\perp^2\Omega,\end{aligned}\tag{4.9}$$

which may be simplified to

$$\begin{aligned}&\frac{\partial}{\partial t}\int d\mathbf{x}\ \left[\frac{1}{2}n^2+\frac{1}{2}\left(\nabla\phi\right)^2\right] = -\kappa\int d\mathbf{x}\ \widetilde{n}\frac{\partial\widetilde{\phi}}{\partial y}-\alpha\int d\mathbf{x}\ \left(\overline{n}-\overline{\phi}\right)^2 \\ &-\alpha\int d\mathbf{x}\ \left(\widetilde{n}-\widetilde{\phi}\right)^2+D^n\int d\mathbf{x}\ n\nabla_\perp^2 n-\int d\mathbf{x}\ \phi D^{\Omega}\nabla_\perp^2\Omega.\end{aligned}\tag{4.10}$$

The complete energy characteristics of the ordinary Hasegawa - Wakatani Equations is consequently

$$\begin{aligned}\frac{dE}{dt} &= \widetilde{\Gamma}_n-\mathcal{J}_0-\widetilde{\mathcal{J}}+\Delta^n-\Delta^{\Omega}, \\ \frac{dK}{dt} &= -\widetilde{\mathcal{A}}-\Pi-\Delta^{\Omega}+\Delta_0^{\Omega}, \\ \frac{dU}{dt} &= -\mathcal{A}_0+\Pi-\Delta_0^{\Omega}, \\ \frac{dP}{dt} &= \widetilde{\Gamma}_n+\mathcal{B}_0+\widetilde{\mathcal{B}}+\Delta^n,\end{aligned}$$

where

$$\widetilde{\Gamma}_n = -\kappa \int d\mathbf{x}\ \widetilde{n}\frac{\partial \widetilde{\phi}}{\partial y},$$

$$\mathcal{J}_0 = \alpha \int d\mathbf{x}\ \left(\overline{n} - \overline{\phi}\right)^2,$$

$$\widetilde{\mathcal{J}} = \alpha \int d\mathbf{x}\ \left(\widetilde{n} - \widetilde{\phi}\right)^2,$$

$$\mathcal{A}_0 = \alpha \int d\mathbf{x}\ \overline{\phi}\left(\overline{\phi} - \overline{n}\right),$$

$$\widetilde{\mathcal{A}} = \alpha \int d\mathbf{x}\ \widetilde{\phi}\left(\widetilde{\phi} - \widetilde{n}\right),$$

$$\mathcal{B}_0 = \alpha \int d\mathbf{x}\ \overline{n}\left(\overline{\phi} - \overline{n}\right),$$

$$\widetilde{\mathcal{B}} = \alpha \int d\mathbf{x}\ \widetilde{n}\left(\widetilde{\phi} - \widetilde{n}\right),$$

$$\Pi = \int d\mathbf{x}\ \overline{\phi}\frac{\partial}{\partial x}\overline{\left(\Omega\frac{\partial \phi}{\partial y}\right)} = -\int d\mathbf{x}\ v_0\frac{\partial}{\partial x}\left(\widetilde{v}_x\widetilde{v}_y\right),$$

$$\Delta^{\Omega} = D^{\Omega}\int d\mathbf{x}\ \phi\nabla_{\perp}^2\Omega,$$

$$\Delta^{n} = D^{n}\int d\mathbf{x}\ n\nabla_{\perp}^2 n,$$

$$\Delta_0^{\Omega} = D^{\Omega}\int d\mathbf{x}\ \overline{\phi}\nabla_{\perp}^2\overline{\Omega}.$$

Note that $-\mathcal{A}_0 + \mathcal{B}_0 = -\mathcal{J}_0$ and $-\widetilde{\mathcal{A}} + \widetilde{\mathcal{B}} = -\widetilde{\mathcal{J}}$. Neglecting diffusion we see that the turbulent radial flux, which can extract free energy from the density gradient (i.e., the density gradient drives the radial flux) may act as a source for the total energy, whereas the resistive dissipation of fluctuating and zonal flow energy acts as a sink for the total energy since the integrals are positive definite. It is clear that the turbulent flux and the resistive dissipation of fluctuating motions vanish in the adiabatic, i.e., Boltzmann distributed density, limit ($\widetilde{n} \to \widetilde{\phi}$). This is in fact a tautology since Boltzmann distribution means nothing but that we may neglect parallel particle motion in the momentum equations, thus there cannot be any resistivity along the magnetic field. The greater the phase lag between density and potential, the stronger we expect the total energy to respond.

Energetics of the modified Hasegawa - Wakatani model

The energetics are readily found analogous to the previous section. Multiplying the vorticity equation by ϕ and integrating over coordinate space gives the equation for the total kinetic energy

$$\frac{\partial}{\partial t}\int d\mathbf{x}\ \frac{1}{2}\left(\nabla_{\perp}\phi\right)^2 = -\alpha\int d\mathbf{x}\ \widetilde{\phi}\left(\widetilde{\phi} - \widetilde{n}\right) - D^{\Omega}\int d\mathbf{x}\ \phi\nabla_{\perp}^2\Omega. \tag{4.13}$$

Integrating Eq. (2.74a) in the y direction, multiplying by $\overline{\phi}$ and integrating also over x gives the equation for the kinetic energy contained in the zonal flow

$$\frac{\partial}{\partial t}\int d\mathbf{x}\ \frac{1}{2}\left(\nabla_{\perp}\overline{\phi}\right)^2 = \int d\mathbf{x}\ \overline{\phi}\frac{\partial}{\partial x}\overline{\left(\Omega\frac{\partial \phi}{\partial y}\right)} - D^{\Omega}\int d\mathbf{x}\ \overline{\phi}\nabla_{\perp}^2\Omega. \tag{4.14}$$

Subtracting Eq. (4.14) from Eq. (4.13) yields the kinetic energy contained in the fluctuating motions

$$\frac{\partial}{\partial t}\int d\mathbf{x}\ \frac{1}{2}\left(\nabla_\perp\widetilde{\phi}\right)^2 = \alpha\int d\mathbf{x}\ \widetilde{\phi}\left(\widetilde{\phi}-\widetilde{n}\right) - \int d\mathbf{x}\ \overline{\phi}\frac{\partial}{\partial x}\overline{\left(\Omega\frac{\partial\phi}{\partial y}\right)} + D^\Omega\int d\mathbf{x}\ (\phi+\overline{\phi})\nabla_\perp^2\Omega. \tag{4.15}$$

Muliplying Eq. (2.74) by n and integrating over coordinate space derives an expression for the potential energy

$$\frac{\partial}{\partial t}\int d\mathbf{x}\ \frac{1}{2}n^2 = -\kappa\int d\mathbf{x}\ \widetilde{n}\frac{\partial\widetilde{\phi}}{\partial y} + \alpha\int d\mathbf{x}\ \widetilde{n}\left(\widetilde{\phi}-\widetilde{n}\right) + D^n\int d\mathbf{x}\ n\nabla_\perp^2 n. \tag{4.16}$$

The evolution of total energy is found upon adding the potential energy to the total kinetic energy, Eq. (4.16) + Eq. (4.13)

$$\frac{\partial}{\partial t}\int d\mathbf{x}\ \frac{1}{2}\left[(\nabla_\perp\phi)^2+n^2\right] = -\kappa\int d\mathbf{x}\ \widetilde{n}\frac{\partial\widetilde{\phi}}{\partial y} - \alpha\int d\mathbf{x}\ \left(\widetilde{n}-\widetilde{\phi}\right)^2 - D^\Omega\int d\mathbf{x}\ \phi\nabla_\perp^2\Omega + D^n\int d\mathbf{x}\ n\nabla_\perp^2 n. \tag{4.17}$$

The energetics are consequently

$$\begin{aligned}
\frac{dE}{dt} &= \widetilde{\Gamma}_n - \widetilde{\mathcal{J}} + \Delta^n - \Delta^\Omega,\\
\frac{dK}{dt} &= \widetilde{\mathcal{A}} - \Pi + \Delta^\Omega + \Delta_0^\Omega,\\
\frac{dU}{dt} &= \Pi - \Delta_0^\Omega,\\
\frac{dP}{dt} &= \widetilde{\Gamma}_n + \widetilde{\mathcal{B}} + \Delta^n,
\end{aligned}$$

and the integrals are defined in the previous section. We note that in the modified Hasegawa - Wakatani model the resistive dissipation is only due to the phase lag between the fluctuating components, as the zonal components have $k_y = 0 = k_z$. Note also that in the collision-less limit, $\alpha\to\infty$ with $\widetilde{n}\to\widetilde{\phi}$ which recovers the modified Hasegawa - Mima equation, we have $\widetilde{\mathcal{A}} = \widetilde{\mathcal{B}} = \widetilde{\mathcal{J}} = 0 = \widetilde{\Gamma}_n$. Thus, the adiabatic limit in the modified Hasegawa - Wakatani equations corresponds to the formalism of the modified Hasegawa - Mima equation and we have previously shown that a similar correspondence is true for the ordinary HW and HM equations.

Chapter 5

Numerical simulations

5.1 The code - 2dads

The OHW and MHW models are solved by a two-dimensional diffusion-advection solver (2dads) written by Garcia and modified to include the MHW model by Kube. The code uses a spectral Fourier-Galerkin method combined with a third order stiffly stable time integrator scheme. The equations are solved on a box of size $[-20, 20] \times [-20, 20]$ in physical space. The fields are expanded by truncated Fourier-series with 256 modes in both radial and poloidal direction, giving a spacial resolution of $\Delta x = \Delta y = 40/256 \approx 0.156$. Derivatives are evaluated in spectral space, where the error involved is faster than exponential, hence derivation in spectral space can be thought of as exact. Evaluating the nonlinear terms in spectral space corresponds to convolution, which due to the Fourier series being truncated, introduces an aliasing error. Following [21] a hyper-viscosity coefficient of order 6 ($\alpha\nabla^6\Omega$ and $\alpha\nabla^6 n$ with $\alpha = 0.0001$)is implemented to dissipate energy at small-scales. The discretization in time is $\Delta t = 0.001$ which introduces an error of $(\Delta t)^3$ for the third order time integrator. Full field output in physical space is written every for every 500th time step. Output to the probes is written every time step, resulting in 20,000 full physical fields for n, ϕ and Ω and 1,000,000 data points for various probe quantities. There are 8 probes placed equidistantly on the diagonal from the top left to the bottom right of the simulation domain. Unless otherwise stated, we use the probe located at the center of the domain. Initial conditions are a single density perturbation mode with amplitude 1,600, $k_x = 0$ and $k_y = 2$ and vorticity identical to zero throughout the domain. In order to speed up the mixing of different wavelengths initially, a Gaussian bell around the mode $(0, 2)$ in Fourier space is also excited, leading to the initial density perturbation shown in the contour-plots. We have performed simulations for C = 0.1, C = 1, C = 5 and C = 10 for both OHW and MHW. Perpendicular viscosity for vorticity and density is taken to be 0.001, which leads to quenching of turbulent kinetic energy for C = 5 and C = 10 in the MHW simulations. Simulations are performed until $t = 10,000$, which gives saturated time-series over at least 8,000 time units. Runs until $t = 20,000$ are performed for C = 10 in OHW and C = 5 in MHW in order to achieve sufficient long saturated state (OHW) and to investigate whether the strong zonal flow is eventually damped in order to get statistics from this run. In general the saturated state is achieved later for high adiabacity, which is associated with density and potential being more in - phase and hence decreasing the drift wave instability growth rate.
As can be seen from the plots of the linear instability growth rate, the code works with sufficient accuracy for our purposes.

Note the normalized density gradient is not really a free parameter of the models

at hand, it can be taken into the normalization of the Hasegawa Wakatani equations by means of

$$\frac{1}{\kappa}\frac{\partial}{\partial t} \to \frac{\partial}{\partial t} \quad , \quad \frac{\phi}{\kappa} \to \phi \quad , \quad \frac{n}{\kappa} \to n$$

and redefining the true free parameters

$$\frac{\mathcal{C}}{\kappa} \to \mathcal{C} \quad , \quad \frac{\varpi}{\kappa} \to \varpi \quad , \quad \frac{D_{\text{classical}}}{\kappa} \to D_{\text{classical}}.$$

5.2 Linear Stability Analysis of the ordinary Hasegawa Wakatani model

As a first check for our code (written by Garcia, modified by Kube) we perform a linear stability analysis of the ordinary Hasegawa-Wakatani Equations, Eqs. (4.1), and compare the growth rate with numerical results for selected wave-numbers. To this end, neglect the nonlinear electric drift term and consider density and potential variations of the form

$$\left(\widetilde{\phi}, \widetilde{n}\right) \sim \left(\widehat{\phi}, \widehat{n}\right) e^{i\mathbf{k}\cdot\mathbf{x} - i\omega t}. \tag{5.1}$$

Inserting into Eqs. (4.1) we obtain

$$i\omega k^2 \widehat{\phi} + Dk^2 \widehat{\phi} = \alpha(\widehat{\phi} - \widehat{n}) \tag{5.2a}$$

$$-i\omega \widehat{n} + Dk^2 \widehat{n} + \alpha \widehat{n} = \alpha \widehat{\phi} - ik_y \widehat{\phi}, \tag{5.2b}$$

where now for convenience have set $D^\Omega = D^n \equiv D$ for the perpendicular diffusion coefficients. The equations above are readily combined to yield the complex dispersion relation

$$\omega^2 k^2 + i\omega(\alpha k^2 + Dk^4 - Dk^2 + \alpha) + D^2 k^4 - i\alpha k_y = 0. \tag{5.3}$$

An analytic expression for the growth rate of the unstable branch is found in Camargo *et al.* [17],

$$\gamma = -\frac{1}{2}\left[\frac{\alpha(1+k^2)}{k^2} + 2Dk^2\right] + \frac{1}{2\sqrt{2}}\frac{\alpha(1+k^2)}{k^2}\sqrt{\sqrt{1 + \frac{16\alpha^2 k_y^2/k^4}{\alpha^4(1+k^2)^4/k^8}} - 1} \tag{5.4}$$

Note that we have considered only the case $k_x = 0$ which corresponds to maximum growth. We initialize different perturbations in the y-direction with $k_x = 0$ and compute the slope of the time-evolution of the corresponding Fourier-amplitude. Since $k_x = 0$ it is sufficient to consider the mean-value of the computed field in the x-direction and then Fourier-transform to find the Fourier-amplitude of $(k_x, k_y) = (0, \widehat{k_y})$. Figures 5.1 - 5.3 show plots of numerical results versus the analytical growth rate, Eq. (5.4). The analytic predictions are good, yet there is some deviation for C = 0.1 on the high k side and for C = 10 for low k. We note that the Hasegawa Wakatani system allows for non-modal behavior [28] which may result in deviations from the analytic growth rate we employ. However, the key feature is that Figures 5.1 - 5.3 prove that our code works to a sufficient degree of precision.

5.3 Data analysis methods

There are a number of statistical tools that we shall employ to uncover features of the turbulent dynamics. Here we give a brief overview. In general we will use temporal and spatial autocorrelation functions (ACFs) to determine the time

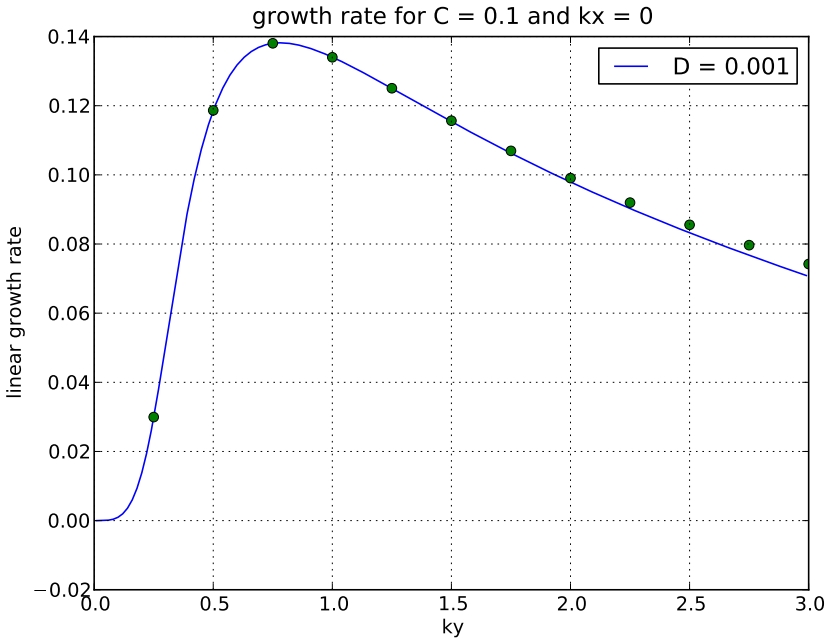

Figure 5.1: Growth rate for C = 0.1

scales and spatial correlation lengths involved. The time scales may also be found from the rescaled range analysis and structure function considerations. Spatial correlations will help us understand the role of the *aspect ratio* of the nonlinear structures, which we may compare with the instability domains found analytically in the adiabatic regime, cf. Parametric Instability, Modulational Instability, Wave-Kinetic Equation. Probability density functions (PDF) supplemented by kurtosis and skewness are calculated to compare with known PDF's.

Kurtosis and Skewness

Introduce the ith central moment in the following way

$$m_i = \frac{1}{N}\sum_{j=1}^{N}(x_j - \overline{x})^i, \tag{5.5}$$

where $\overline{x}$ is the sample mean and N the sample size. Note that the second moment is simply the variance. The estimator for skewness and kurtosis used are then given by

$$g_{\text{skewness}} = \frac{m_3}{m_2^{3/2}}, \tag{5.6}$$

and

$$g_{\text{kurtosis}} = \frac{m_4}{m_2^2} - 3. \tag{5.7}$$

Self - similarity

Consider a stochastic process, $X(t)$. Following Rypdal [18] we have the following definitions.

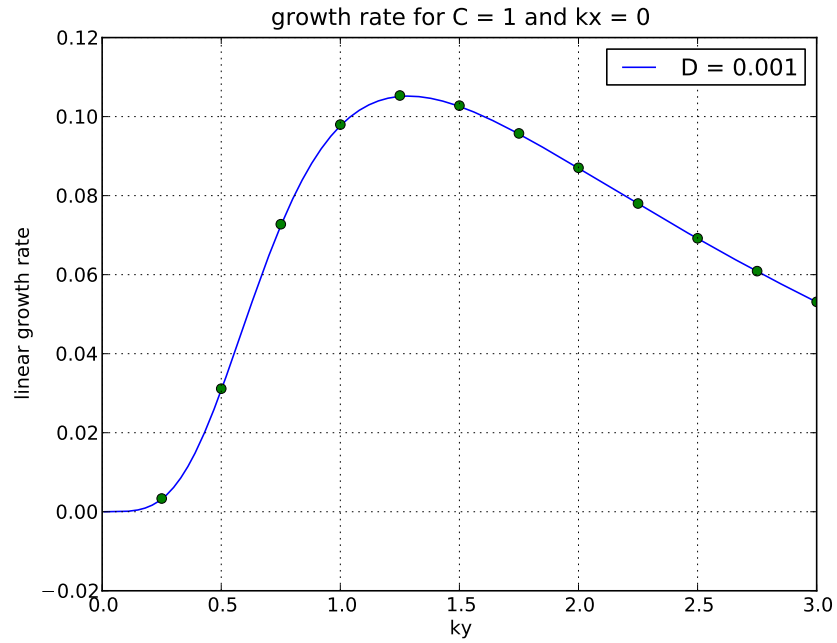

Figure 5.2: Growth rate for C = 1

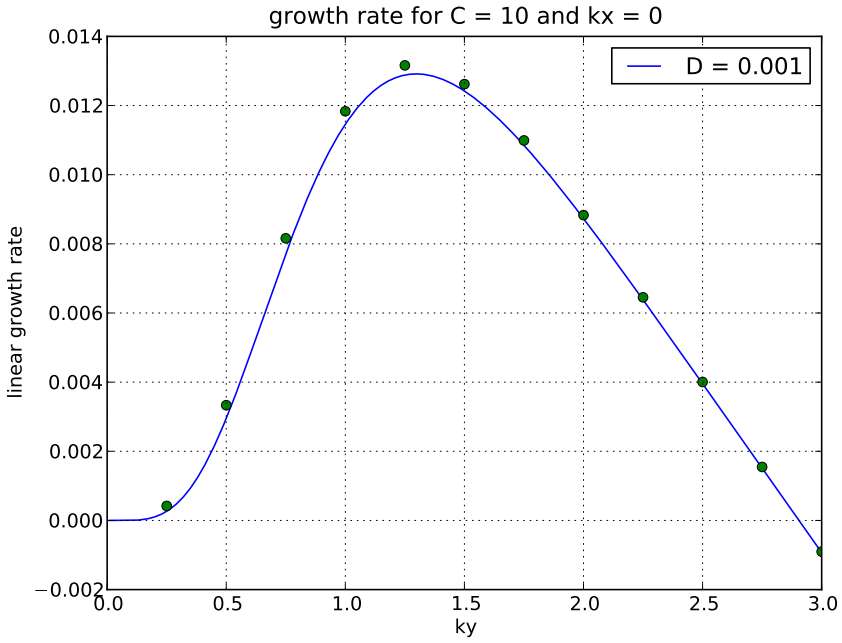

Figure 5.3: Growth rate for C = 10

A process is stationary if $X(t_0 + t) \stackrel{d}{=} X(t)$ for all fixed t_0.

The process inherits stationary increments if $X(t_0 + t) - X(t_0) \stackrel{d}{=} X(t) - X(0)$ for all fixed t_0.

For $H \geq 0$, the process is called H-self-similar if $X(at) \stackrel{d}{=} a^H X(t)$ for all $a > 0$.

Here, $\stackrel{d}{=}$ should be understood as "equal in distribution", i.e., statistical distributions exhibit translational symmetry with respect to time. The self-similar, stationary, process has the following covariance function, Rypdal [18], Melzani [19]:

$$\langle X(t)X(s)\rangle = \frac{1}{2}\left\langle X(1)^2\right\rangle \left(t^{2H} + s^{2H} - |t-s|^{2H}\right), \tag{5.8}$$

where the angle brackets denote expectation values. Introduce the increments of the process X, $Y(t_0) = X(t_0 + t) - X(t_0)$, which by self-similarity gives $Y(t_0) = X(t) - X(0)$. We may then compute the autocorrelation function of the increments at lag n, where $n \to \infty$,

$$C_X(n) = \langle X_n X_1\rangle = \left\langle Y_1^2\right\rangle H(2H-1)n^{2H-2}. \tag{5.9}$$

Since the above relation holds for long time lags, we readily associate the similarity parameter, H, with the decay of the ACF at large lags,

$$C_X(\tau) \sim (2H-1)\tau^{-\alpha_X}\ ,\ \alpha_X = 2 - 2H. \tag{5.10}$$

We also see that $C_X(\tau \to \infty) > 0$ if $H > 1/2$ and $C_X(\tau \to \infty) < 0$ if $H < 1/2$. Clearly, $C_X(\tau \to \infty) = 0$ is the case for random walks with uncorrelated increments, $H = 1/2$ in this case. For $H > 1/2$ there is a positive correlation at long lags and also a slower decay compared to anti-correlation at large lags ($H < 1/2$) with a faster decay. For H close to 1 we note that there is only a weak decay in the ACF, indicating that regions in the R/S-plot (see below) following such H-dependence are strongly correlated. $H = 1$ is the signature of a deterministic signal (or at least a deterministic, coherent mode with period given by the length of the sample region for which $H = 1$).

Rescaled Range Analysis and Hurst exponent

The self-similarity parameter H introduced above is commonly referred to as the *Hurst exponent*, after the British hydrologist Edwin Hurst. For a self-similar signal $Y(t)$, the rescaled range as a function of sample size has the dependence $R/S(n) \sim n^H$. The rescaled-range can be thought of as a normalized standard deviation with respect to the deviation in maximum and minimum of the cumulated sum for a piece of the original sample. The algorithm is as follows, divide the signal in pieces of length n for which the standard deviation is to be computed. Then calculate the difference between the maxima and minima in the cumulated, mean adjusted series for this part of the original signal. The rescaled range is then given by the ratio of the difference in extrema from the cumulated, mean adjusted series to the standard deviation corresponding to this sample. To improve statistics the mean over the rescaled range for all other samples of equal size, n, is computed. One visualizes by means of a R/S vs. n loglog-plot.
To be more precise, for each sample piece of size n consisting of the elements $X_1, X_2, ..., X_n$ we compute the mean adjusted cumulative sum,

$$Y_k = \sum_{j=1}^{k}\left(X_j - \frac{1}{n}\sum_{i=1}^{n} X_i\right). \tag{5.11}$$

We then find the range, given by the difference between the extrema in the mean adjusted cumulative sum,

$$R_k = \max(Y_l) - \min(Y_l),\ l = 1, 2, ..., n. \tag{5.12}$$

Using the standard deviation for the sample of size n, S_n the rescaled range for sample size n is given by $R/S\ (n)$, which is proportional to the similarity parameter as described earlier ($R/S(n) \sim n^H$). To improve statistics we calculate the rescaled range for the $\mathcal{N}$ pieces of length n (the total size of the signal is $N = \mathcal{N}\ n$) and average.

Structure function analysis

For a stochastic process $X(t)$ the structure function of order q is defined according to

$$S(t_0, \tau) = \langle |X(t_0 + \tau) - X(t_0)|^q \rangle\,, \tag{5.13}$$

where $\langle ... \rangle$ denotes an ensemble average, which we shall take to be the mean of the signal. For a stationary (statistically speaking) signal or a signal with stationary increments, the structure function clearly does not depend on t_0. An estimator for this case is given by

$$\widehat{S}_q(\tau) = \sum_{i=1}^{N-\tau} \frac{|X_{i+\tau} - X_i|^q}{N - \tau}, \tag{5.14}$$

where N is the number of sample points and τ is the (integer) lag. When plotting the structure function, if there exist a region where the structure function saturates, the interpretation is that the signal is stationary at those time-lags. The time-lag found by structure function analysis may be compared to the correlation time found from ACF-analysis.

Note that the structure function is related to the similarity parameter of an inertial range can be identified; $S_q(\tau) \propto \tau^{\zeta(q)}$, where $\zeta(q) = Hq$. This only holds if there is no intermittency present (and the PDF associated with the quantity under consideration is not dominated by heavy tails).

Chapter 6

Results

In this section we show results of the numerical simulations performed. Trends or results are described. For interpretation and relation to Part I, see chapter Discussion.

6.1 Typical time - series and contour - plots

We start out by presenting typical time-series for the ordinary- and modified Hasegawa Wakatani system for different adiabacity parameters. Figures 6.1 and 6.3 are for the ordinary and Figures 6.2 and 6.4 for the modified system respectively. In Chapter 7 and 8 we found that if the transfer term is positive, the energy is transfered from the fluctuating motions to the zonal flows, which we also observe when studying the lower subplots of Figures 6.1 - 6.4. Note that for $C = 1$ in the modified system, the zonal flows contain considerably more energy than the fluctuating motions. Figure 6.5 shows the saturated state of the turbulence. Note that the time-series really are as bursty as Figures 6.1 - 6.4, but the logarithmic scale suppresses this effect. Clearly the MHW system allows more energy to be contained in zonal structures as theoretically proposed earlier. Figures 6.34 - 6.27 show the emergence of zonal structures in the modified system with increasing adiabacity. From Figure 6.6 we see directly the confining effect of zonal flows, the radial flux is substantially reduced compared to the ordinary system with no zonal flows. Finally, Figure 6.9 confirms the obvious notion that elongated structures in the poloidal direction act as to break the isotropy of the turbulence.

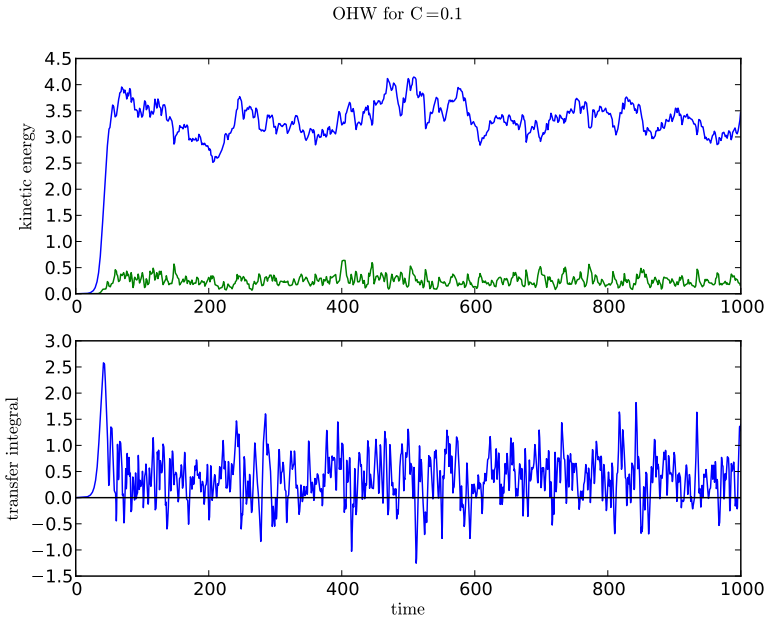

Figure 6.1: Top: Kinetic energy contained in fluctuating motions (blue) and zonal structures (green). Bottom: Transfer integral Π

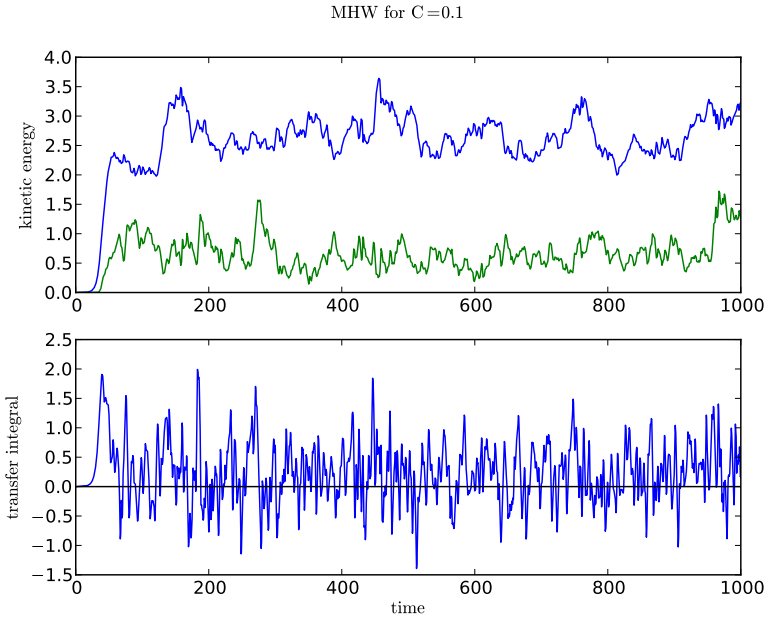

Figure 6.2: Top: Kinetic energy contained in fluctuating motions (blue) and zonal structures (green). Bottom: Transfer integral Π

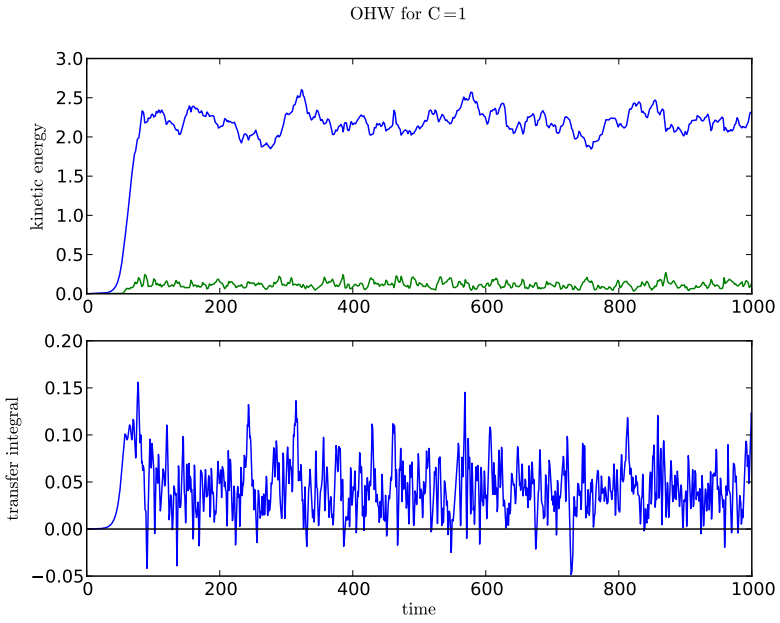

Figure 6.3: Top: Kinetic energy contained in fluctuating motions (blue) and zonal structures (green). Bottom: Transfer integral Π

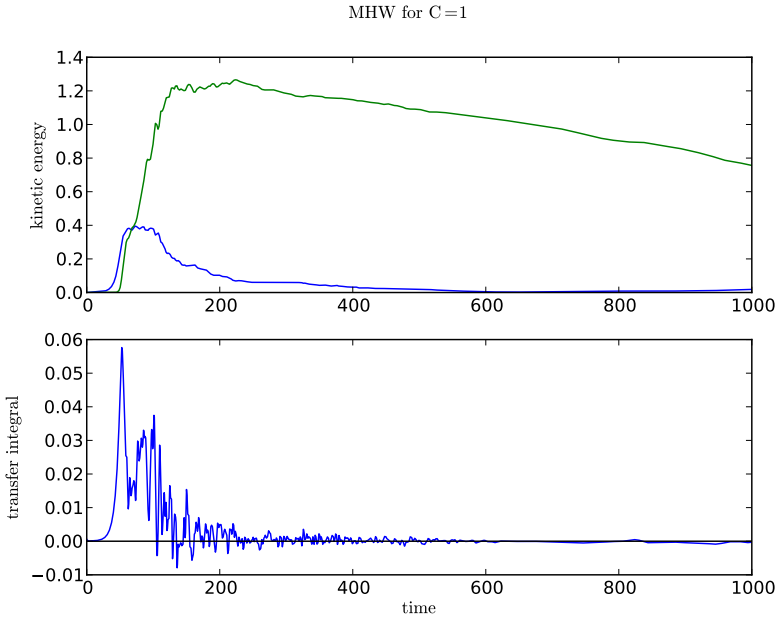

Figure 6.4: Top: Kinetic energy contained in fluctuating motions (blue) and zonal structures (green). Bottom: Transfer integral Π

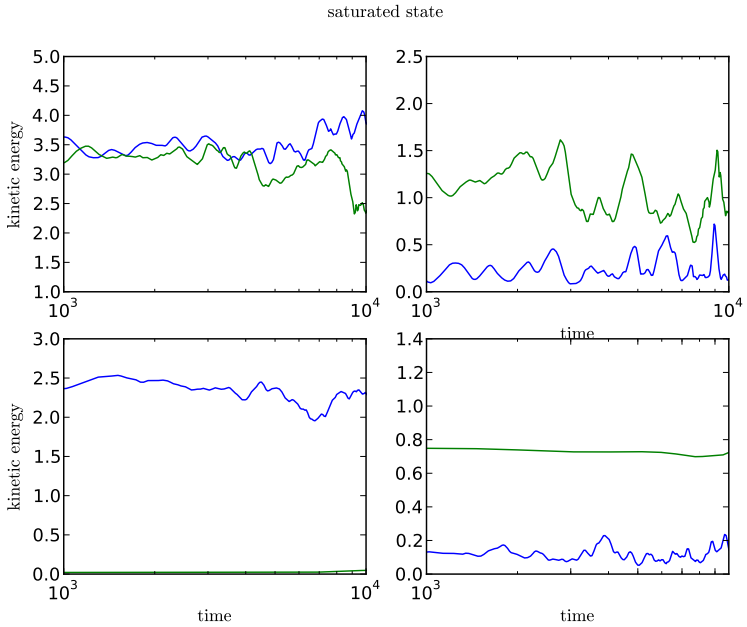

Figure 6.5: Top left: Kinetic energy contained in fluctuating motions for C = 0.1, OHW (blue) and MHW (green). Top right: Kinetic energy contained in zonal structures for C = 0.1, OHW (blue) and MHW (green). Bottom left: Kinetic energy contained in fluctuating motions for C = 1, OHW (blue) and MHW (green). Bottom right: Kinetic energy contained in zonal structures for C = 1, OHW (blue) and MHW (green). Logarithmic time-axis.

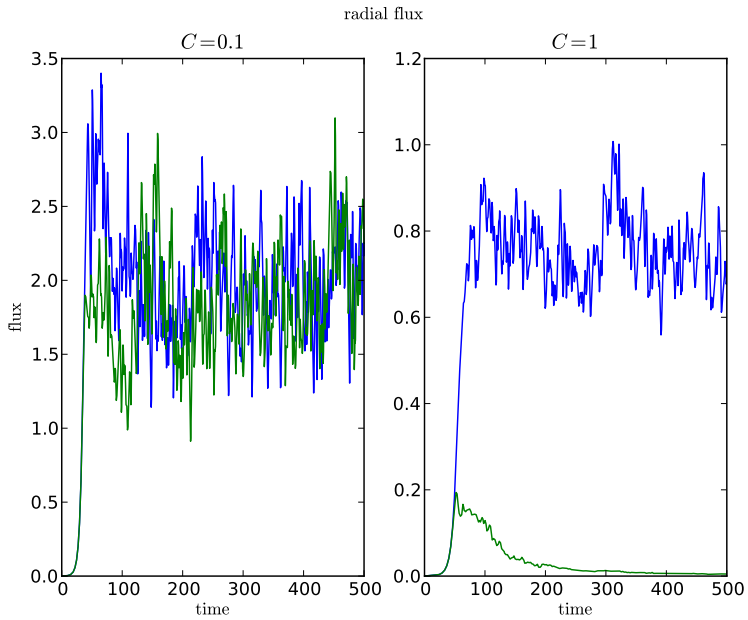

Figure 6.6: Radial flux for OHW (blue) and MHW (green).

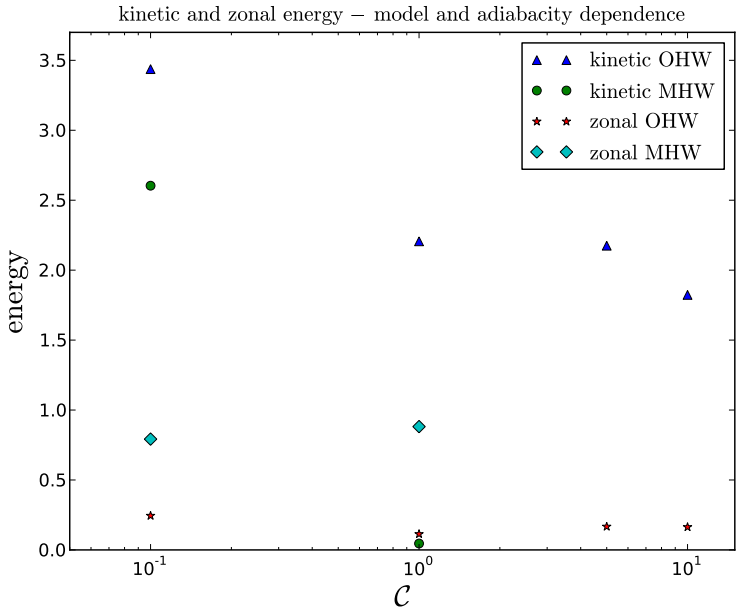

Figure 6.7: Kinetic and zonal energy integrals for OHW and MHW vs. adiabacity parameter.

In Figure 6.7 the dependence of zonal and turbulent kinetic energy on model and adiabacity is shown. We have performed simulations for C = 0.1, 1, 5 and 10 but the arising zonal flows aren't damped quick enough to give meaningful time-series for C = 5 and 10 in the MHW runs. Figure 6.8 shows the strong intermittency for the turbulent kinetic energy, being quenched for long time intervals. This is, of course, a direct consequence of the strong and persistent occurrence of zonal flows in these runs, which flatten the turbulence almost entirely for energy. Consequently

we shall not use data from those runs with a few exceptions which are explicitely mentioned later on.

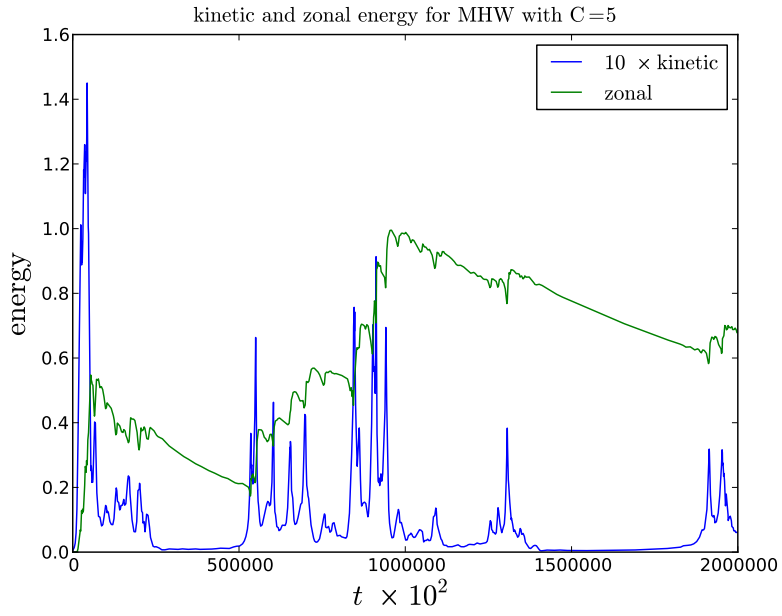

Figure 6.8: Quenching and turbulence suppression due to strong zonal flows in MHW with C = 5. The turbulent kinetic energy is magnified by a factor 10 for visualization purposes.

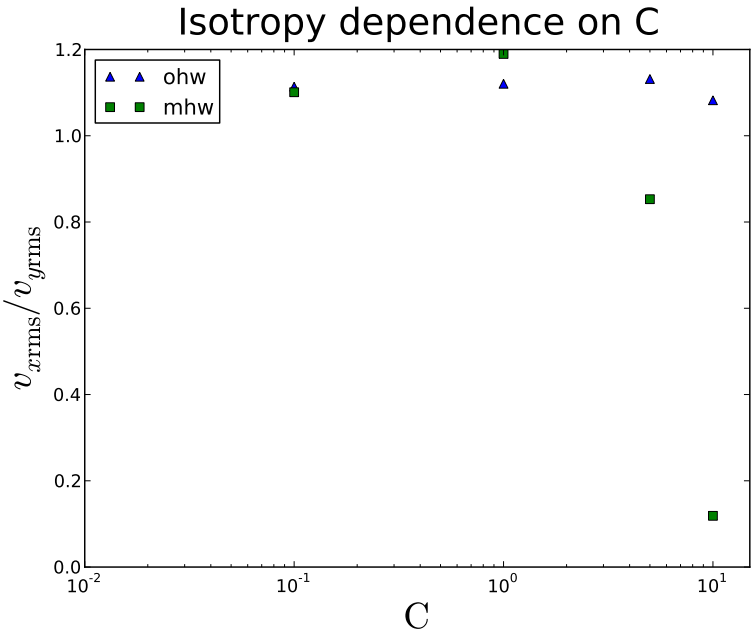

Figure 6.9: Adiabacity and model dependence of the root mean-square velocities.

Typical contours of the field quantities $\widetilde{n}$, $\overline{n}$,$\widetilde{\phi}$, $\overline{\phi}$, $\widetilde{\Omega}$ and $\overline{\Omega}$ are shown below. In

the absence of zonal flows, i.e., OHW with C = 0.1 and C = 1, there is no significant difference between turbulent and full quantities, hence we only show plots for the full fields in those cases. The turbulent fields are the difference of the total fields and zonal, i.e., poloidally averaged, fields.

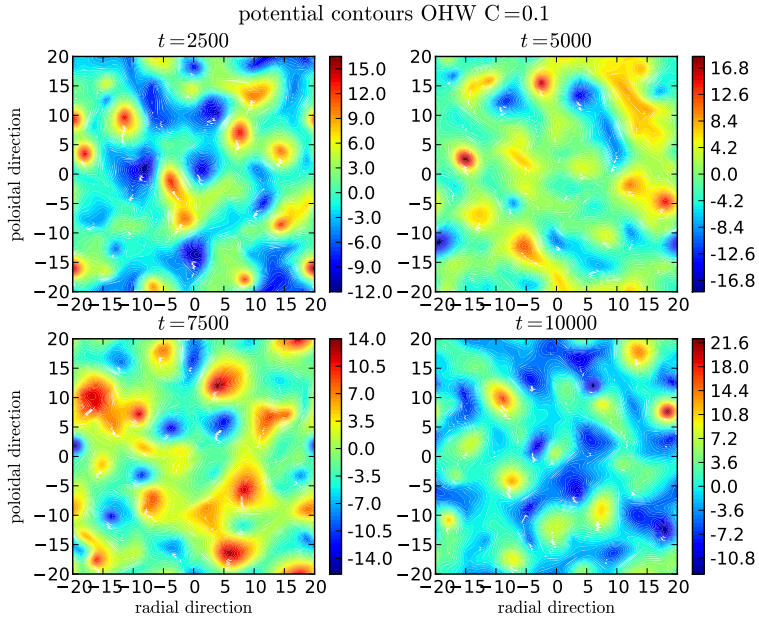

Figure 6.10: Full potential contours for OHW with C = 0.1.

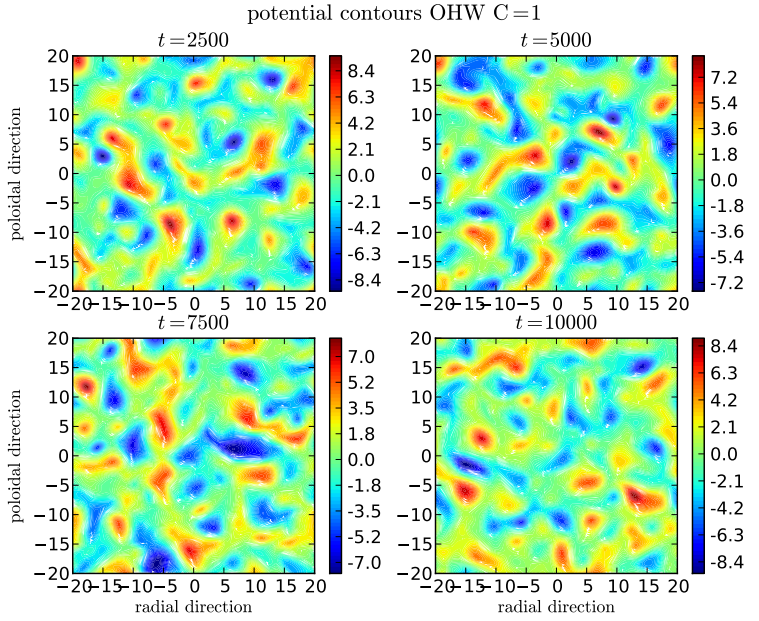

Figure 6.11: Full potential contours for OHW with C = 1.

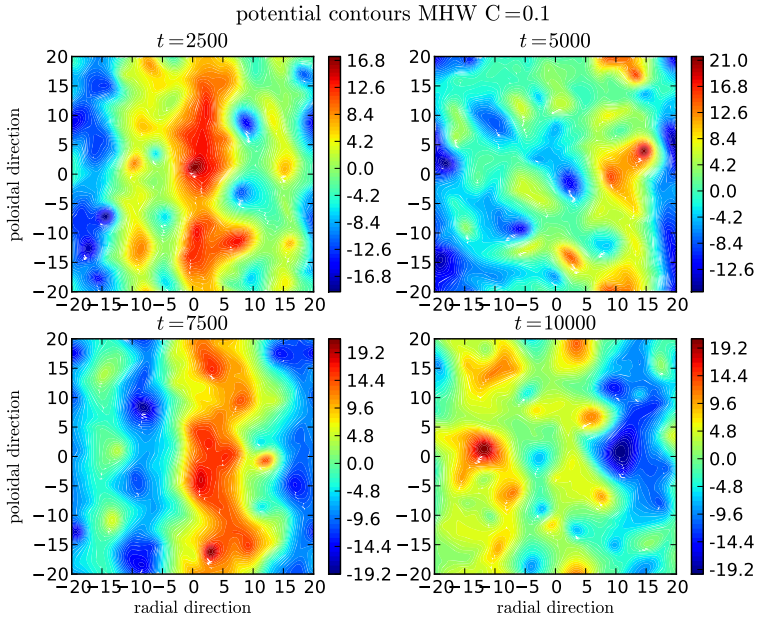

Figure 6.12: Full potential contours for MHW with C = 0.1.

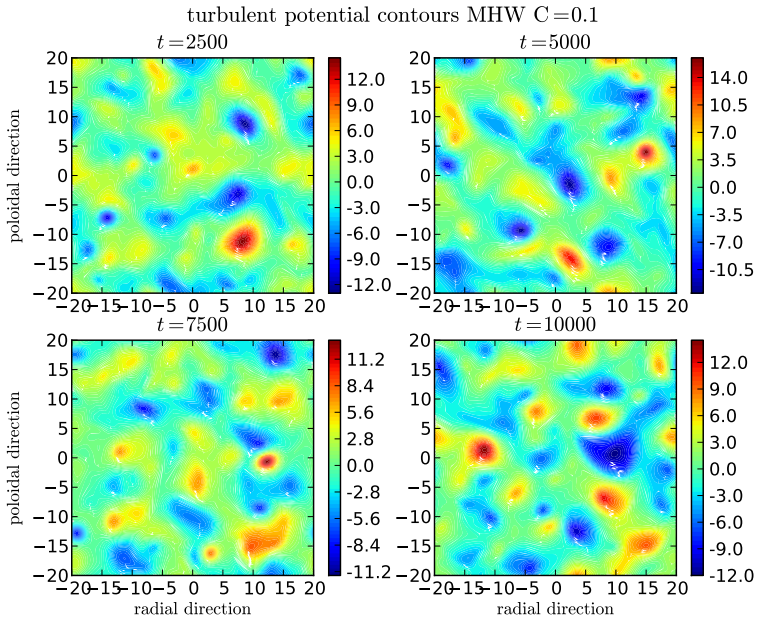

Figure 6.13: Turbulent potential contours for MHW with C = 0.1.

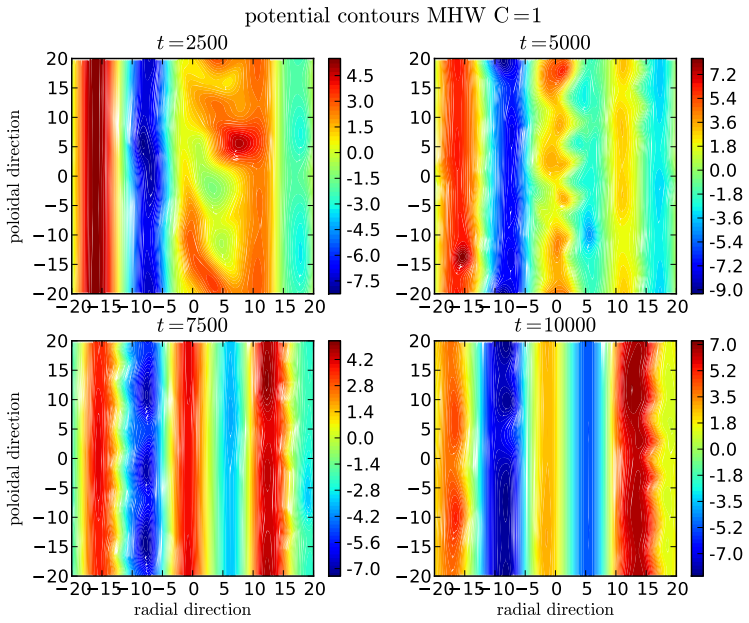

Figure 6.14: Full potential contours for MHW with C = 1.

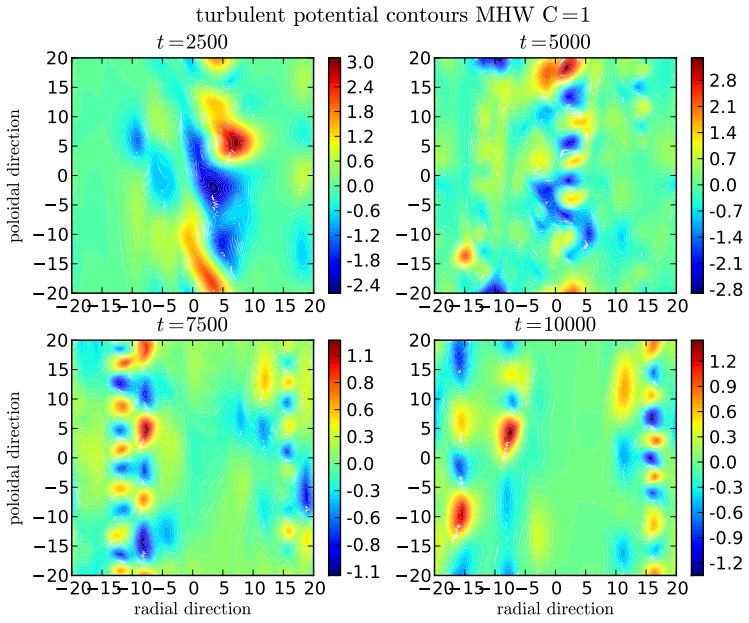

Figure 6.15: Turbulent potential contours for MHW with C = 1.

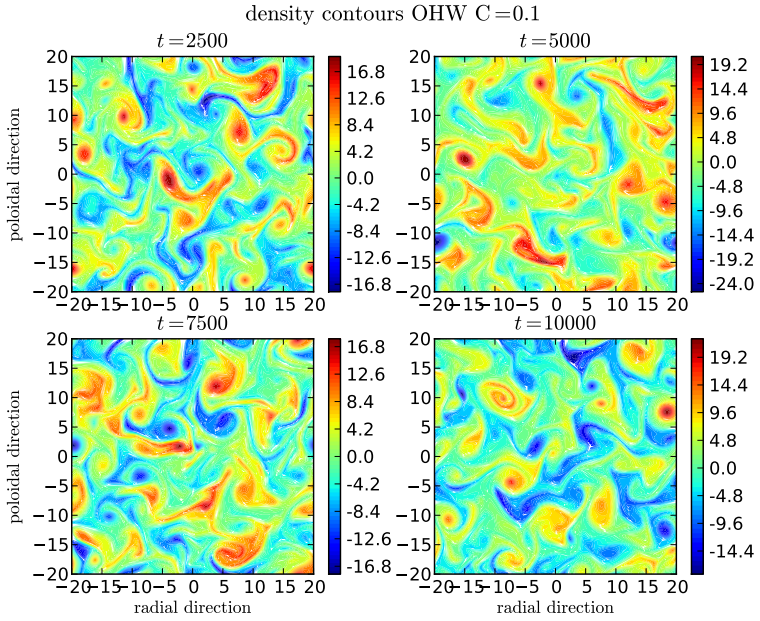

Figure 6.16: Full density contours for OHW with C = 0.1.

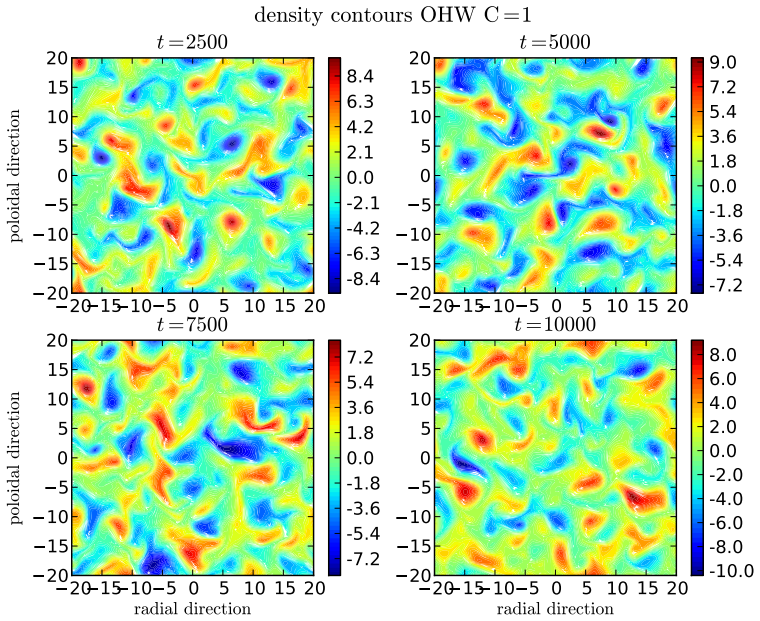

Figure 6.17: Full density contours for OHW with C = 1.

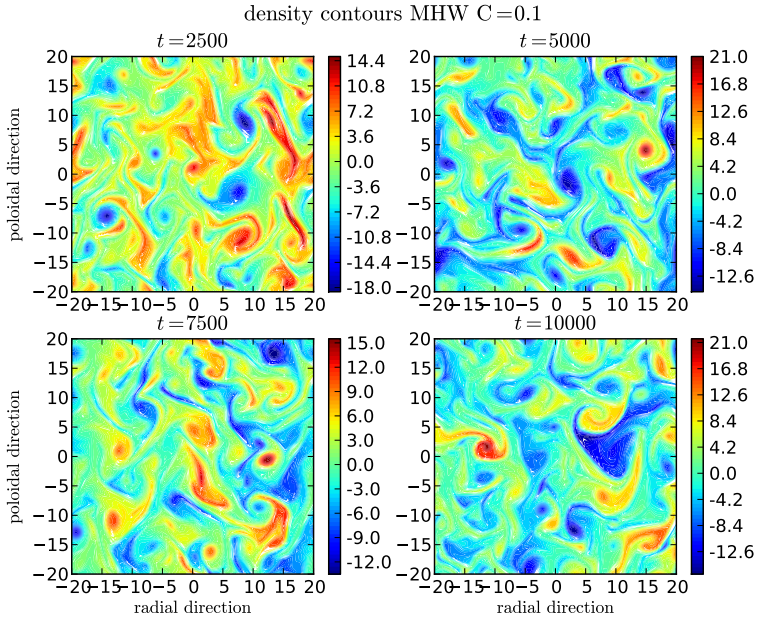

Figure 6.18: Full density contours for MHW with C = 0.1.

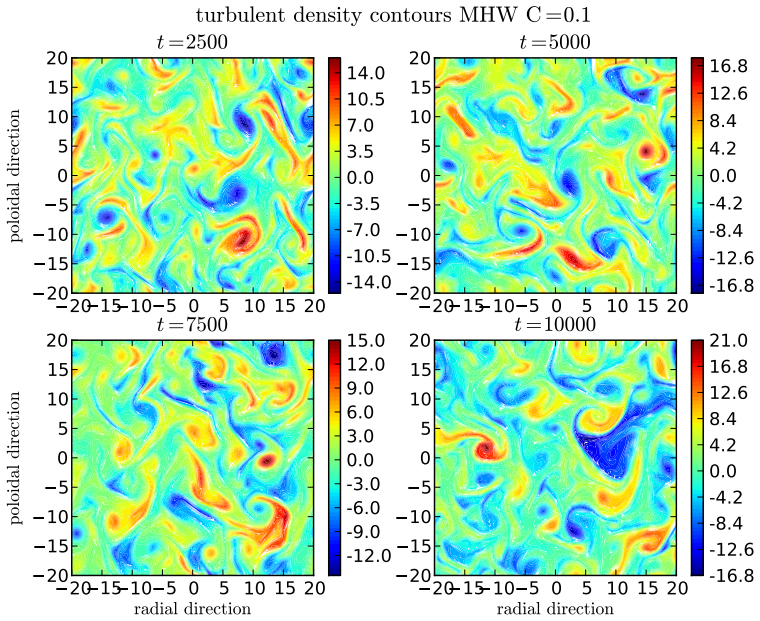

Figure 6.19: Turbulent density contours for MHW with C = 0.1.

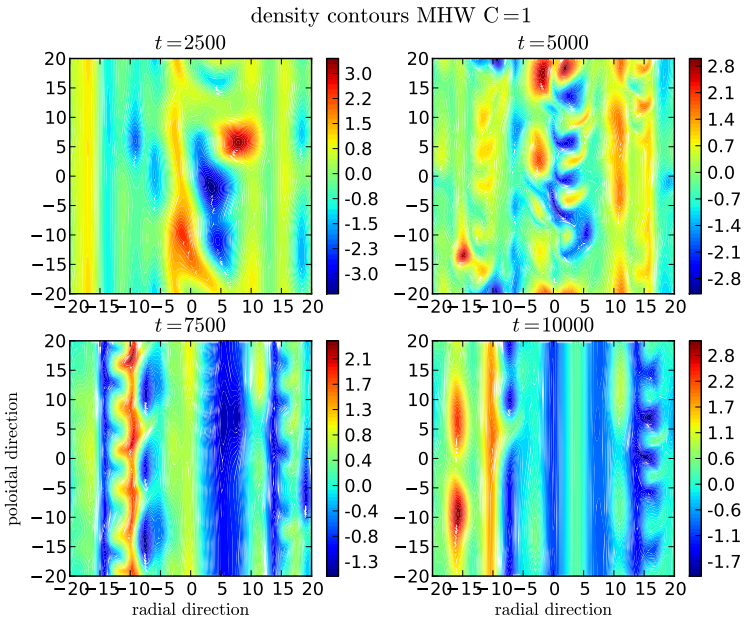

Figure 6.20: Full density contours for MHW with C = 1.

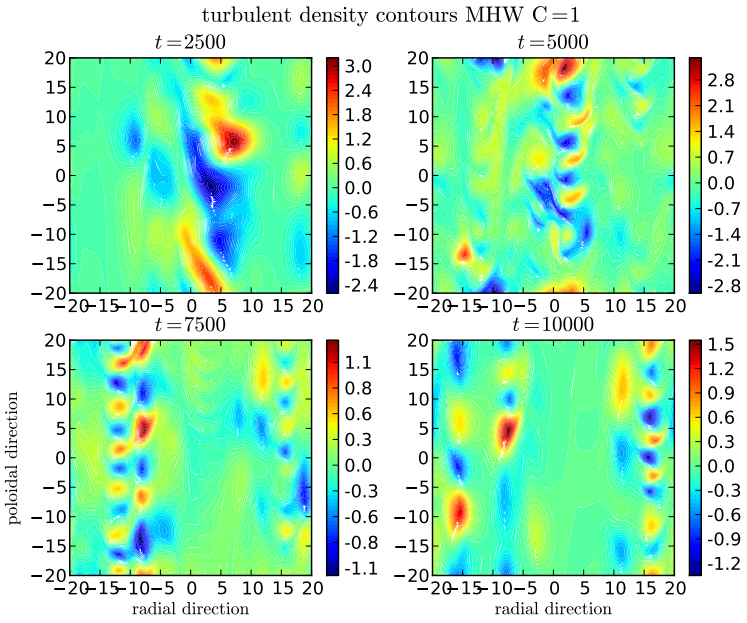

Figure 6.21: Turbulent density contours for MHW with C = 1.

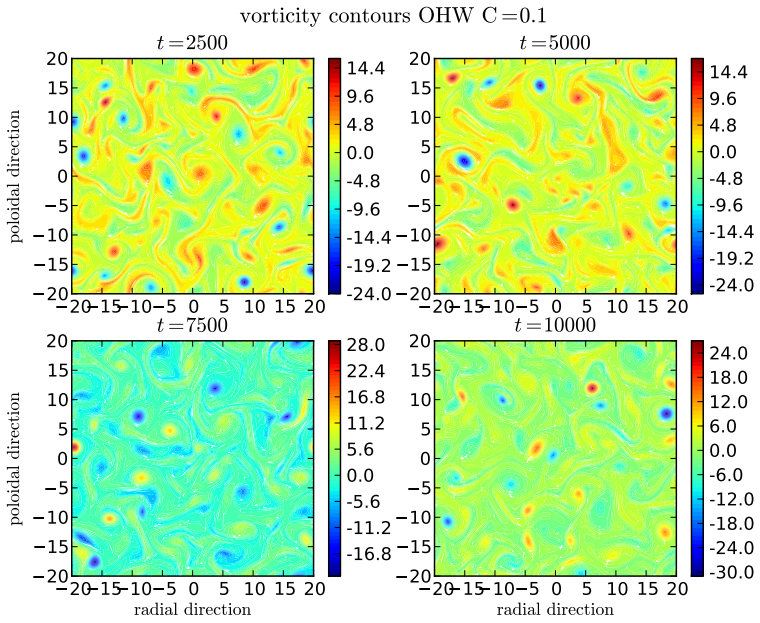

Figure 6.22: Full vorticity contours for OHW with C = 0.1.

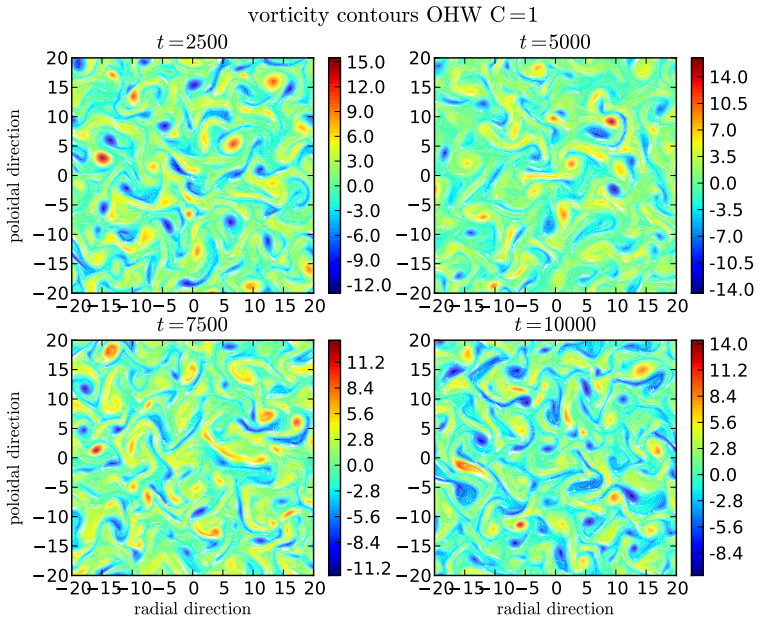

Figure 6.23: Full vorticity contours for OHW with C = 1.

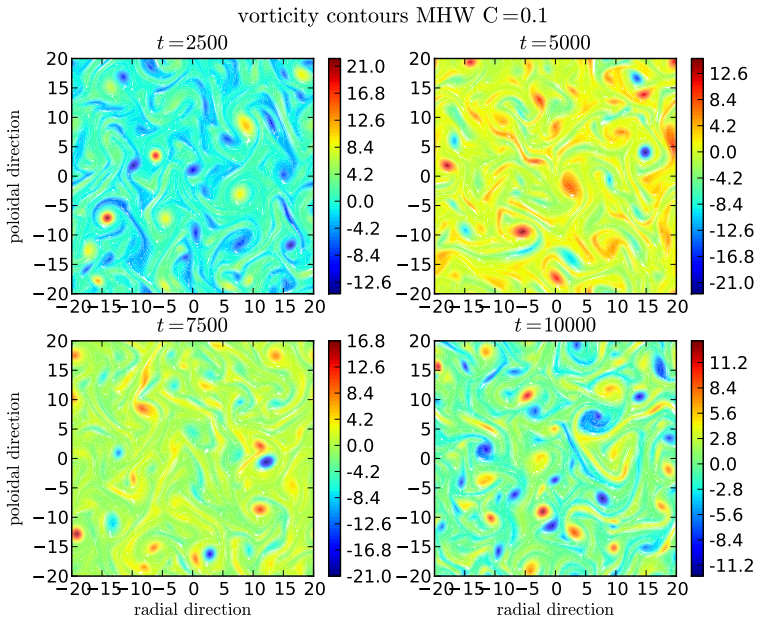

Figure 6.24: Full vorticity contours for MHW with C = 0.1.

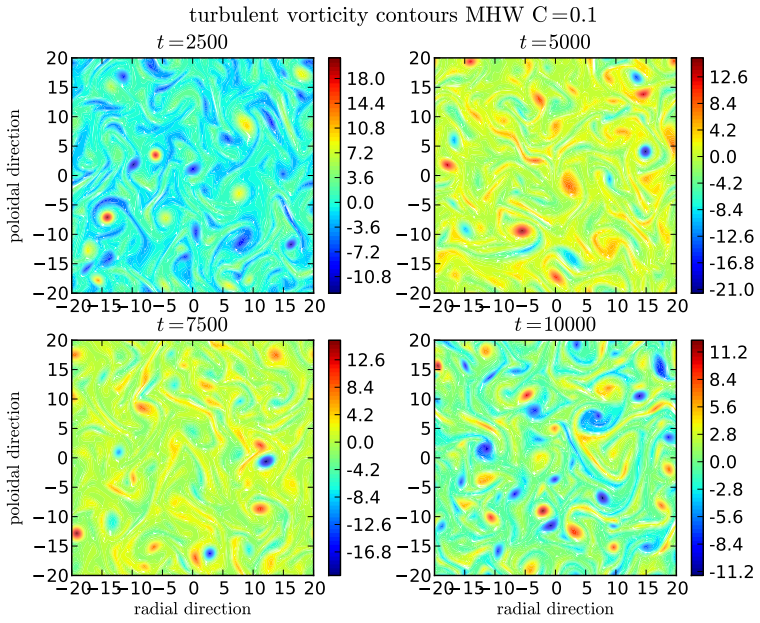

Figure 6.25: Turbulent vorticity contours for OHW with C = 0.1.

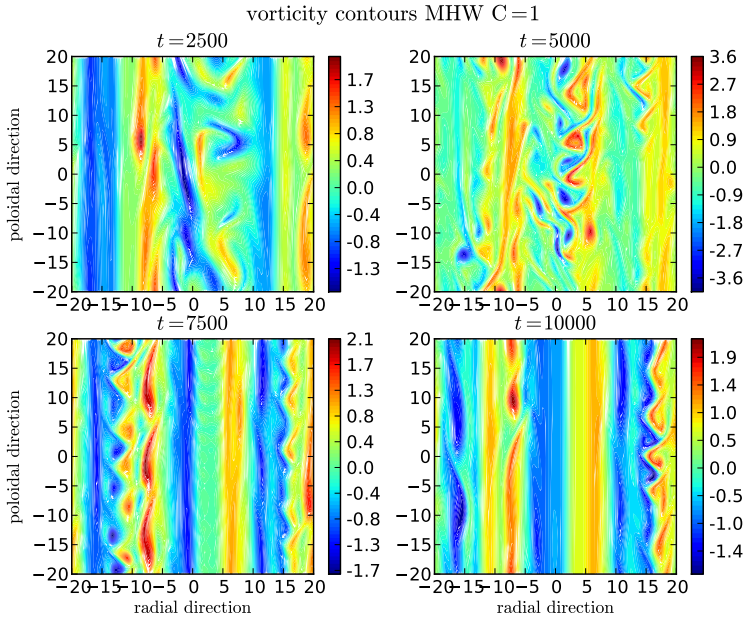

Figure 6.26: Full vorticity contours for MHW with C = 1.

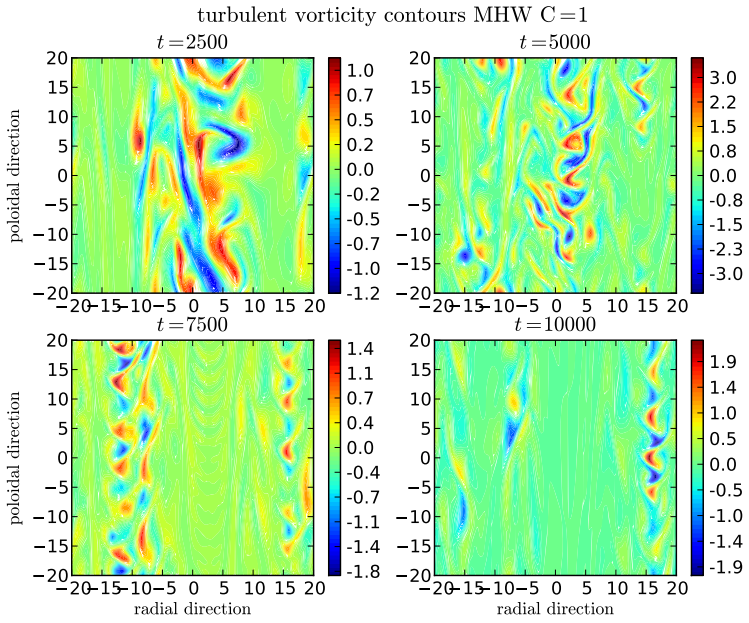

Figure 6.27: Turbulent potential contours for MHW with C = 1.

To show that the zonal flow in the MHW model with C = 1 is indeed persistent, we average the zonal flows over the saturated state and obtain Figure 6.28 for the potential structure and Figure 6.29 for the density. We have also computed the root-mean square deviation of the instantaneous profiles, the gray-shaded area shows the deviation from the red line, which is the time-averaged profile. We see that fluctuations for the potential structure are less than for density, still we may state that the zonal flows are persistent at all times, since the averages not not vanish. This is non-trivial, since one may suspect zonal flows to spontaneously arise, than be

destroyed by dissipation and arise again some place else in the simulation domain, possibly with reversed polarity. A check of instantaneous averages, not shown here, revels that the zonal flows do *emph* change polarization. Thus, we find that once a zonal flow is excited in the MHW with C = 1 model, it stays, on average, at a fixed position, and it does not oscillate in strength about some value. The zonal flows, especially for potential structures, are persistent.
We read off a wavelength of about 13 radial length units for the potential zonal flow, which gives a wavenumber of $q = 2\pi/13 \approx 0.5$. In our theoretical considerations we have assumed $q \ll k$; since $k \sim 1$ we find that this is not the case and we have to admit that our theoretical predictions are not necessarily precise, but they give a good indication of what we observe in our numerical experiments. On the other hand, the assumption that zonal components vary on a much slower time-scale than turbulent components is justified by the persistence of the zonal flows.

Radial and poloidal velocities at the center of the simulation domain

Here we show a brief overview of the measured turbulent radial and poloidal velocity measured at the center of the simulation domain.

	$\langle\tilde{v}_x\rangle_{\mathrm{rms}}$	$\langle\tilde{v}_y\rangle_{\mathrm{rms}}$
OHW C = 0.1	1.92	1.75
MHW C = 0.1	1.67	1.54
OHW C = 1	1.54	1.43
MHW C = 1	0.18	0.24

Table 6.1: Radial and poloidal velocities at the domain center. OHW/MHW for C = 0.1 and C =1.

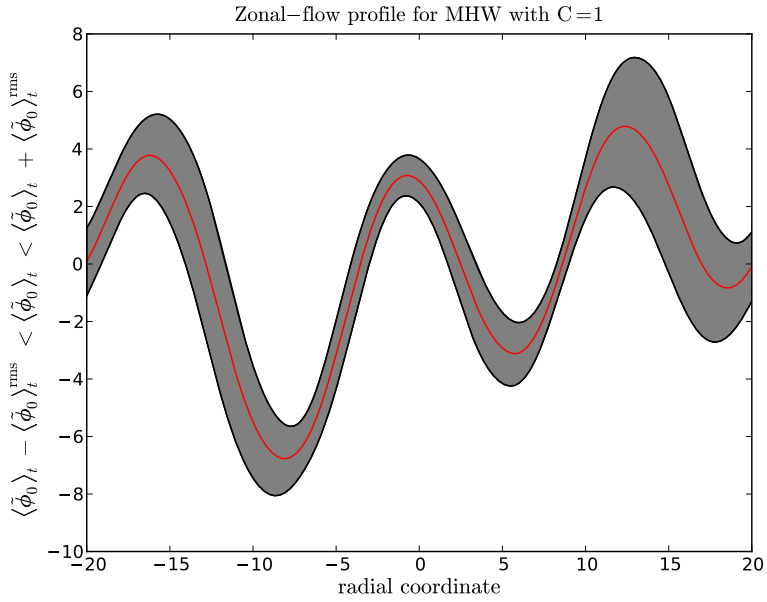

Figure 6.28: Time averaged zonal potential profile in MHW with C = 1.

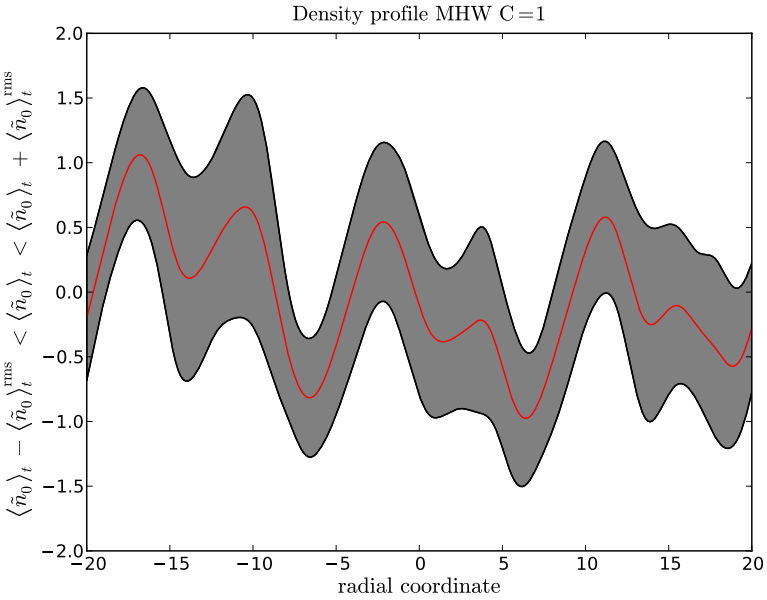

Figure 6.29: Time averaged zonal density profile in MHW with C = 1.

6.2 Autocorrelation functions

Spatial and temporal autocorrelation functions (ACFs) for selected quantities are shown in this section. We use time-series from the domain centered probe for temporal ACFs. To determine the spatial correlations, we have considered fluctuating field quantities along x = -10,0,10 and y = -10,0,10 in the simulation domain respectively. Since the radial correlation length is about 5 length units, fluctuations on those "cuts" are uncorrelated and we are allowed to form averages over ACFs on each line to improve statistics. The instantaneous spatial ACFs are averaged over the saturated state in order to compare with the temporal correlations.

For the OHW we find for the temporal correlation of $\widetilde{\phi}$ that an increase in C leads to a decrease in correlation time, whereas $\widetilde{\Omega}$ exhibits approximately unchanged temporal correlation in OHW with respect to C. For the MHW both increase their temporal correlation. For fixed C, the correlation time is longer for the MHW than for the OHW, regardless whether $\widetilde{\phi}$ or $\widetilde{\Omega}$ is considered. This may be understood as structures spending more time at the probe position, which in turn is related to a lower velocity in both radial and poloidal direction in the MHW system compared to the OHW model.
Increase in C leads to a decrease in radial and poloidal correlation for the OHW system and the turbulent potential, whereas the radial and poloidal correlation is approximately constant for the vorticity. The radial and poloidal rms velocities are approximately unchanged with respect to C in the OHW system, hence, when correlation time decreases, so should the correlation length. This is indeed the case for the potential in the OHW case. The radial correlation length for the vorticity is approximately unchanged since velocities and its temporal correlation are approximately constant. The effect of the zonal flows in the MHW model is to elongate turbulent structures in the poloidal direction, this is seen in an increased poloidal correlation length for both potential and vorticity for C = 1. The radial correlation is approximately unchanged as C increases in the MHW case. Zonal flows are present for both C = 0.1 and C = 1 and as discussed earlier, the zonal flow induced velocity is in the poloidal direction. Clearly the poloidal correlation length is larger in the MHW than in the OHW system since zonal flows are absent there. Radial correlation length are approximately the same in both systems for fixed C.

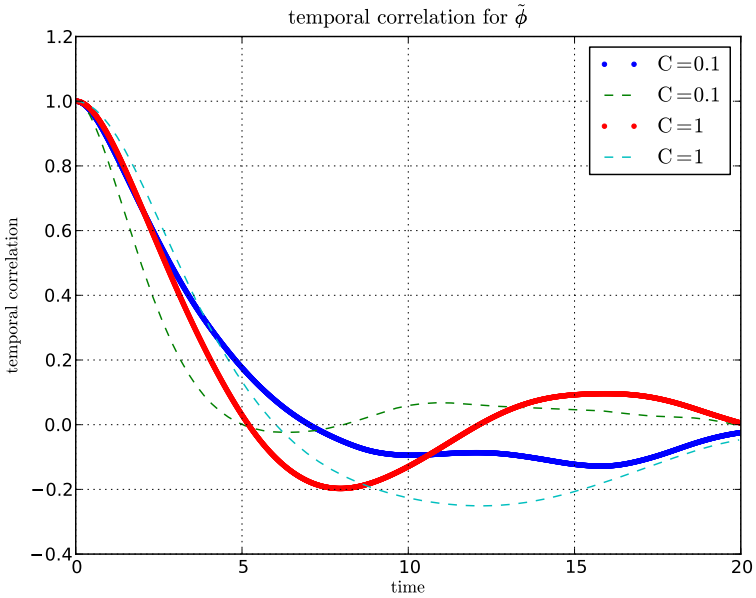

Figure 6.30: Temporal autocorrelation function for $\widetilde{\phi}$ in OHW (dotted) and MHW (broken line) for C = 0.1 and C = 1 .

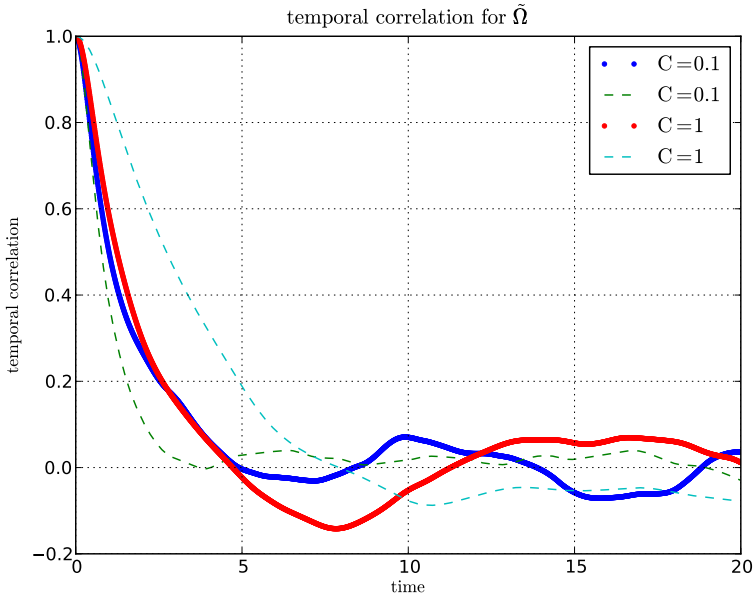

Figure 6.31: Temporal autocorrelation function for $\widetilde{\Omega}$ in OHW (dotted) and MHW (broken line) for C = 0.1 and C = 1 .

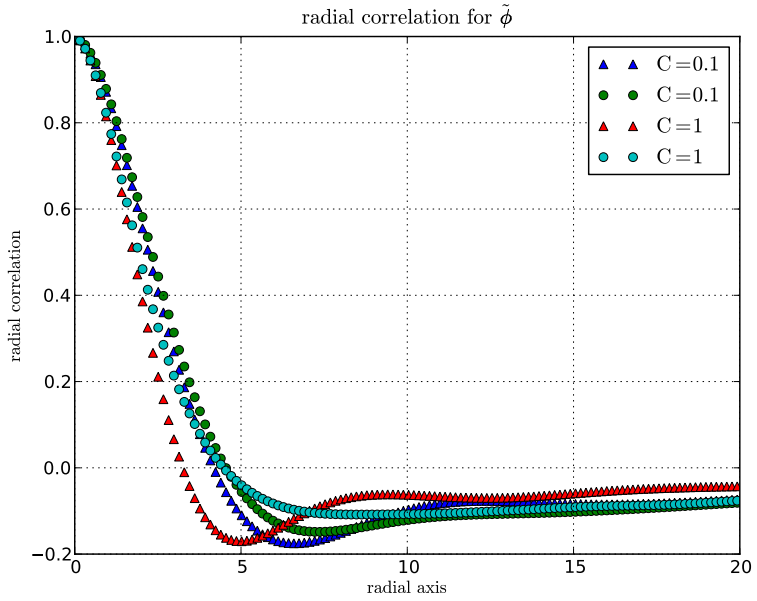

Figure 6.32: Radial autocorrelation function for $\widetilde{\phi}$ in OHW (triangles) and MHW (circles) for C = 0.1 and C = 1 .

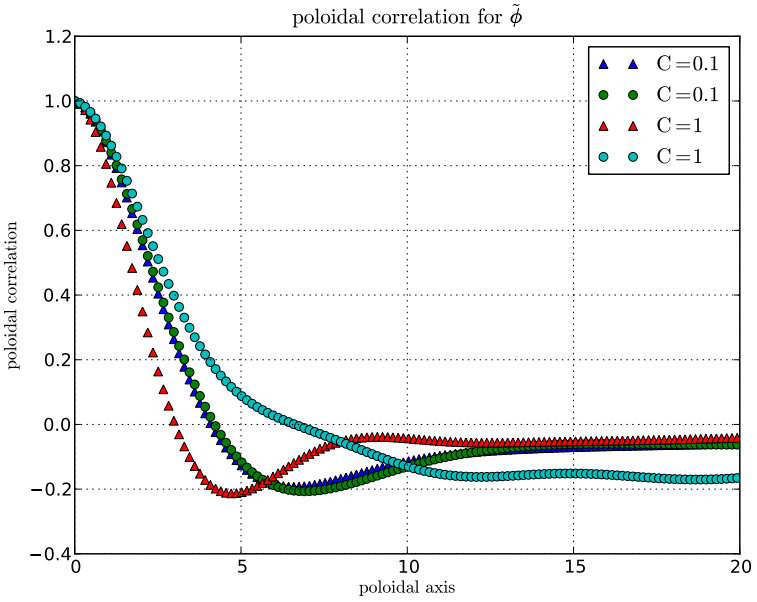

Figure 6.33: Poloidal autocorrelation function for $\widetilde{\phi}$ in OHW (triangles) and MHW (circles) for C = 0.1 and C = 1 .

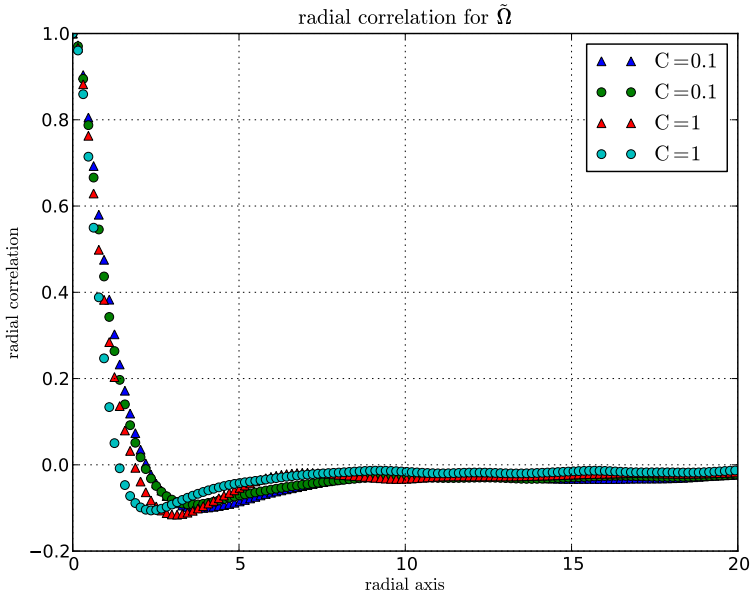

Figure 6.34: Radial autocorrelation function for $\widetilde{\Omega}$ in OHW (triangles) and MHW (circles) for C = 0.1 and C = 1 .

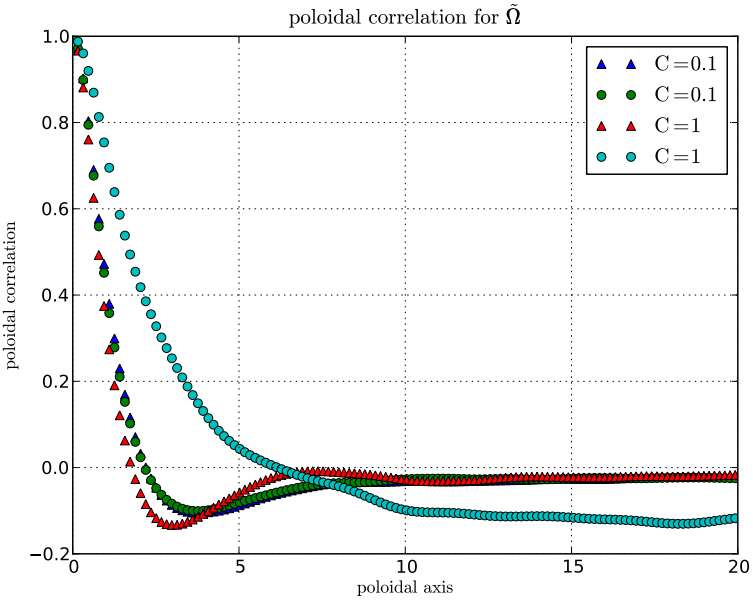

Figure 6.35: Poloidal autocorrelation function for $\widetilde{\Omega}$ in OHW (triangles) and MHW (circles) for C = 0.1 and C = 1 .

6.3 Flux scaling

Figure 6.36 shows the integrated radial flux in the saturated state for different adiabacity parameters. Note that the MHW & C = 5 run is only of illustrative value here, the zonal flows are too present and zonal flow damping occurs over a

too large time-span for the run to yield any significant statistics that can be used to compare it to the corresponding runs in of the OHW model. Figure 6.37 summarizes the essential physics in this work. There are two dependencies of the radial plasma transport, suppression by zonal flows and adiabacity. For an interpretation we refer to the Discussion chapter below.

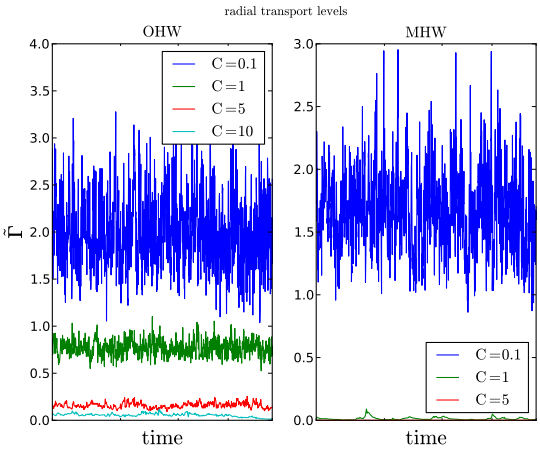

Figure 6.36: Radial flux from $t = 5000$ to $t = 9000$ for OHW and MHW.

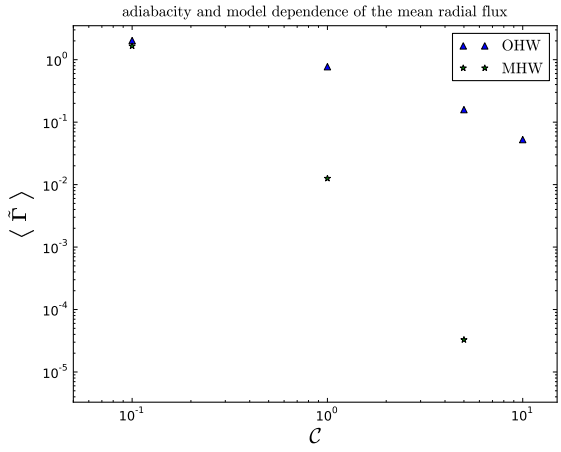

Figure 6.37: Adiabacity and model dependence of the mean radial flux.

6.4 Energy spectra

We present partial wave-number spectra, similarly to [4]. The energy-distribution as a function of radial wave-number, k_x, is given as

$$E(k_x) = \sum_{k_y} \frac{1}{2} k_\perp^2 \left| \widetilde{\phi}_k \right|^2, \tag{6.1}$$

and equivalently for the poloidal distribution

$$E(k_y) = \sum_{k_x} \frac{1}{2} k_\perp^2 \left| \widetilde{\phi}_k \right|^2. \tag{6.2}$$

In order to compare with contour plots, we shall use both full and turbulent potential in the expressions above.

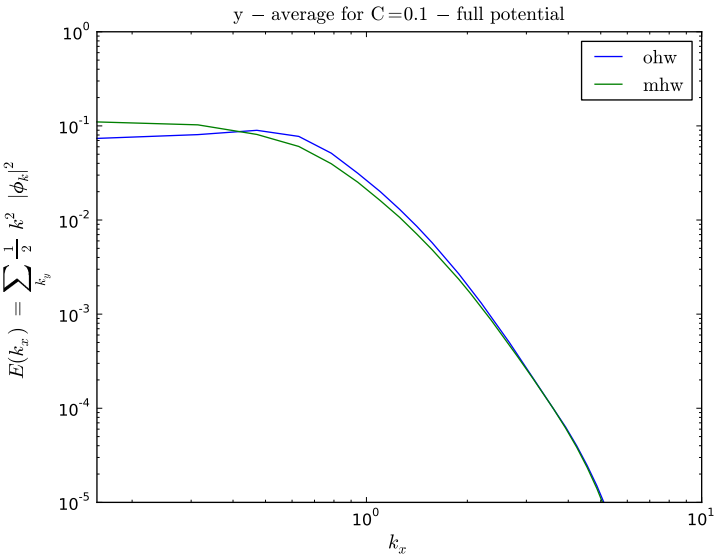

Figure 6.38: Radial energy distribution for full potential and C = 0.1. OHW vs. MHW.

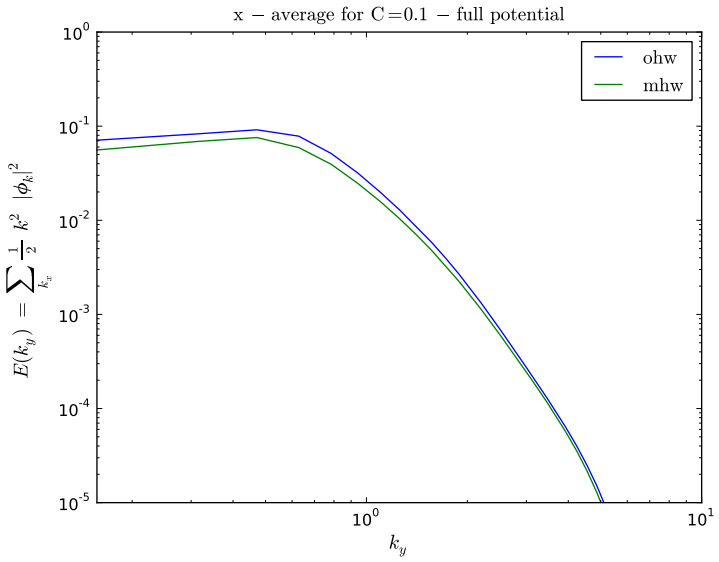

Figure 6.39: Poloidal energy distribution for full potential and C = 0.1. OHW vs. MHW.

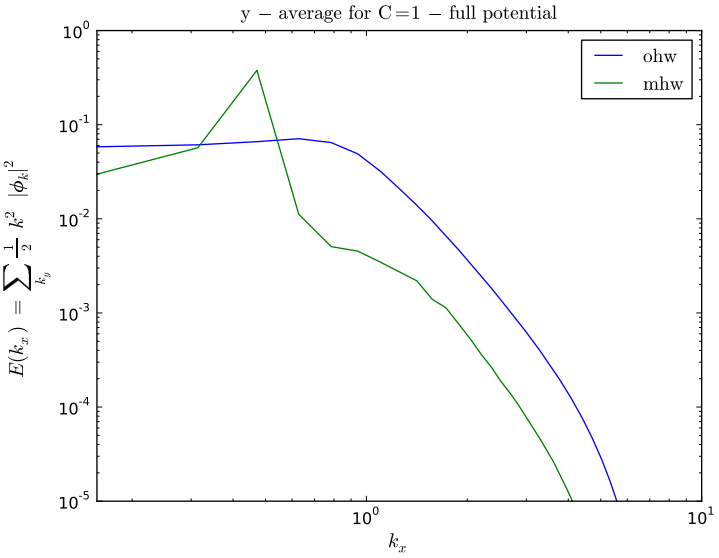

Figure 6.40: Radial energy distribution for the full potential and C = 1. OHW vs. MHW.

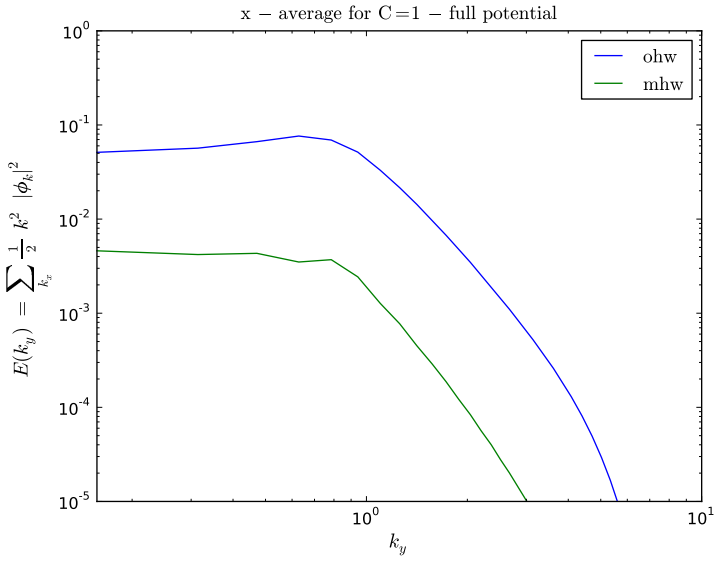

Figure 6.41: Poloidal energy distribution for the full potential and C = 1. OHW vs. MHW.

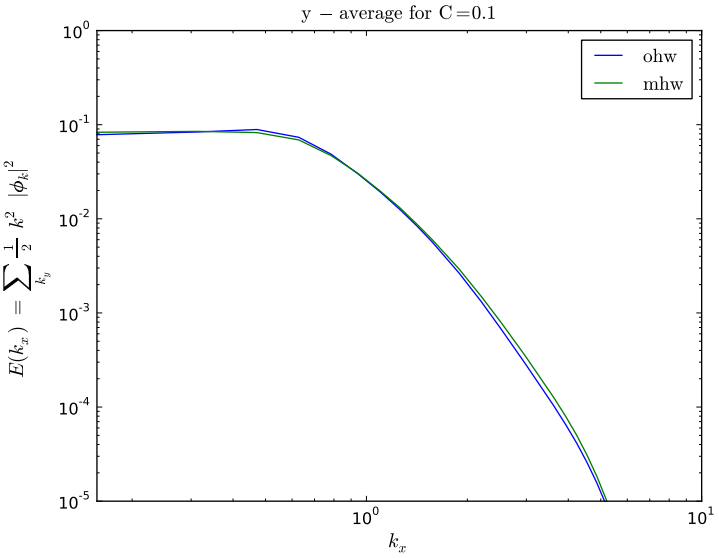

Figure 6.42: Radial energy distribution for the turbulent potential and C = 0.1. OHW vs. MHW.

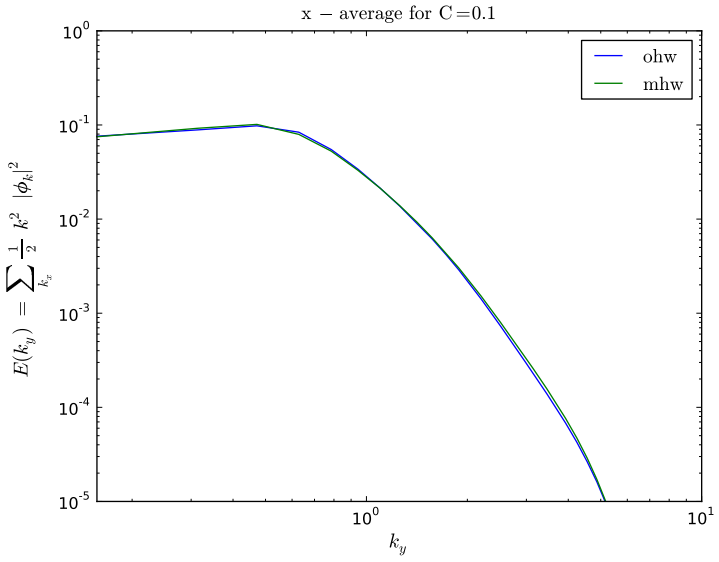

Figure 6.43: Poloidal energy distribution for the turbulent potential and C = 0.1. OHW vs. MHW.

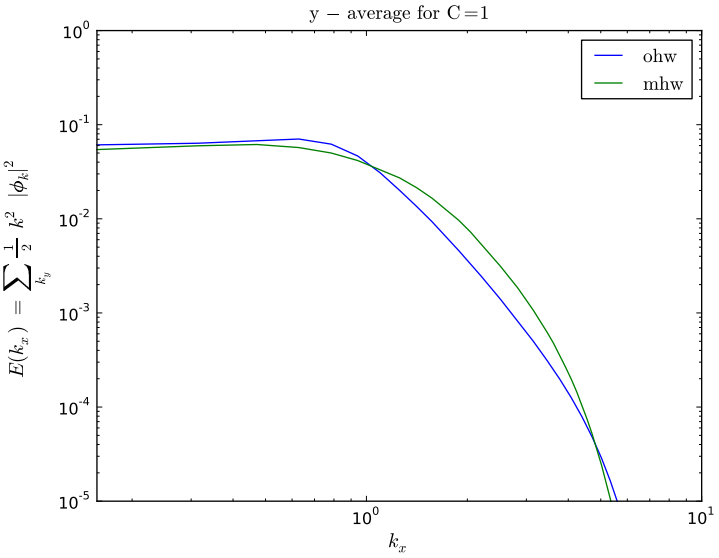

Figure 6.44: Radial energy distribution for the turbulent potential and C = 1. OHW vs. MHW.

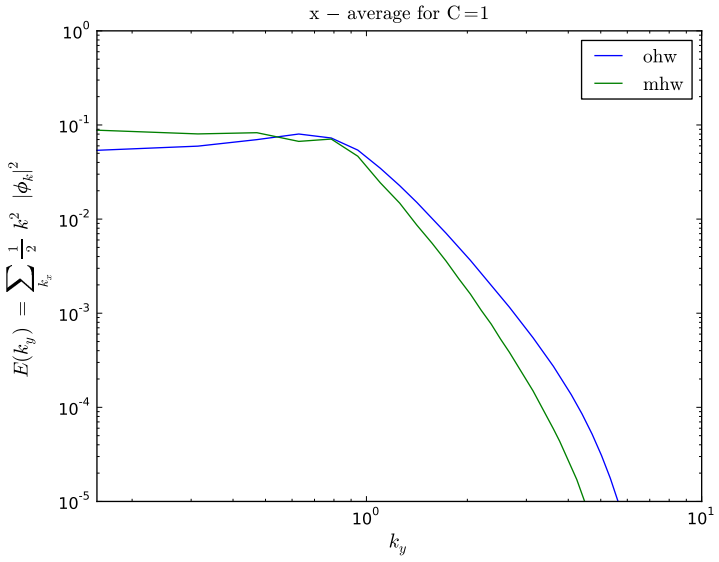

Figure 6.45: Poloidal energy distribution for the turbulent potential and C = 1. OHW vs. MHW.

Figure 6.38 - 6.41 show no significant difference in energy distribution for C = 0.1, whence the zonal flow is clearly distinguished for C = 1 in the MHW radial energy distribution. The peak is located at $k_x \approx 0.4$ which corresponds to a wavelength of $\lambda_x \approx 16$ and clearly confirms Figure 2.51 where a zonal flow of approximately the same wavelength is present. In the poloidal direction, there is less energy contained in the total field with zonal flows than in the OHW.
The turbulent energy distribution is almost identical for C = 0.1 in OHW and MHW, whereas the radial energy contained in small radial structures is a little higher in the zonal flows state compared to the OHW and the poloidal energy contained in large poloidal structures is slightly higher in the MHW than in the OHW.

This reflects the shearing of the turbulent potential by the emerging zonal flow. Consistent with both contour plots and theory.

6.5 Hurst exponents

6.5.1 Rescaled - range analysis

Rescaled range plots are shown for selected quantities. We note that the fit over the non-deterministic inertial range is in general not over a full decade in R/S, thus we have to be careful when drawing statistically significant predictions. Yet, we emphasize that this is due to the shortness of our time-series, which is the data we have available and hence the best we can do. Table 6.2 shows that the parameters lie approximately between 0.4 and 0.6 for turbulent quantities, except for the zonal part of the potential, which is evident from the persistence of the potential zonal structure (see Figure 6.28). Thus the probe "sees" the potential structure over significant time spans, and the associated signal is nearly deterministic. Note that Table 6.2 is the first evidence of the *absence* of long-range correlations in the OHW but also the zonal flow governed MHW system.

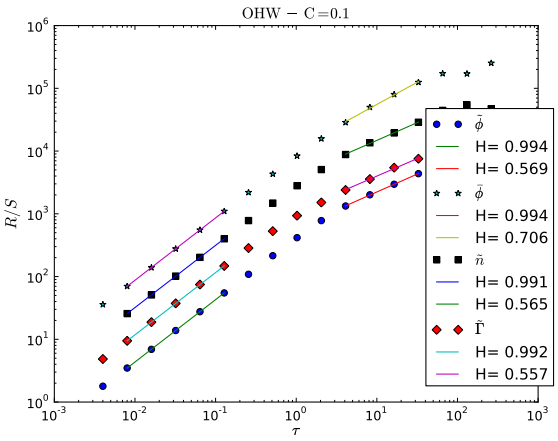

Figure 6.46: Rescaled range for $\widetilde{n}$, $\widetilde{\Gamma}$, $\widetilde{\phi}$ and $\overline{\phi}$ in OHW with C = 0.1.

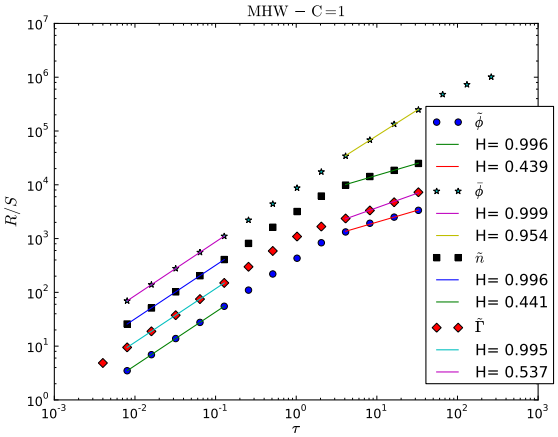

Figure 6.47: Rescaled range for $\widetilde{n}$, $\widetilde{\Gamma}$, $\widetilde{\phi}$ and $\overline{\phi}$ in MHW with C = 1.

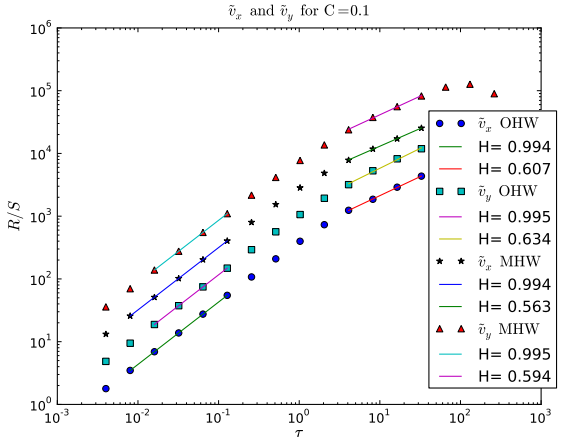

Figure 6.48: Rescaled range for $\widetilde{v}_x$ and $\widetilde{v}_y$ OHW and MHW with C = 0.1.

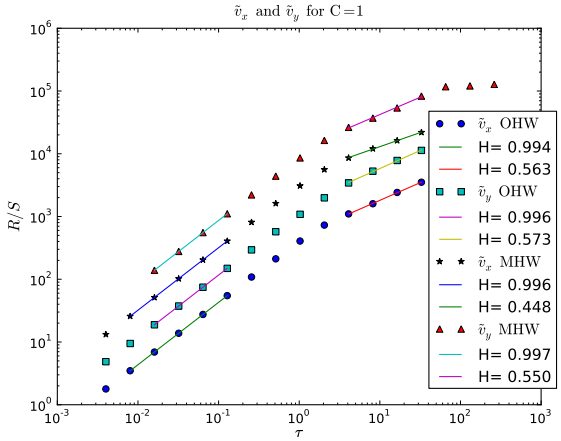

Figure 6.49: Rescaled range for $\widetilde{v}_x$ and $\widetilde{v}_y$ OHW and MHW with C = 1.

The Hurst exponents shown in the plots above are summarized in the table below. H_C^{model} stands for "Hurst exponent in the inertial range for OHW/MHW with adiabacity C".

	$\widetilde{\phi}$	$\widetilde{n}$	$\widetilde{\Gamma}$	$\widetilde{\Omega}$	$\widetilde{v}_x$	$\widetilde{v}_y$	$\overline{\phi}$
$H_{0.1}^O$	0.569	0.565	0.557	0.592	0.607	0.634	0.706
H_1^O	0.551	0.571	0.583	0.538	0.563	0.573	0.723
$H_{0.1}^M$	0.540	0.566	0.551	0.574	0.563	0.594	0.963
H_1^M	0.439	0.441	0.537	0.523	0.448	0.550	0.954

Table 6.2: Summarized Hurst-exponents from the rescaled-range method.

6.5.2 Structure functions and variogram

In this section we calculate the Hurst - exponent by means of the variogram and also directly from the scaling-exponents of the structure functions.

The variogram is the second order structure function and its relation to the Hurst-exponent in the similarity-range is given by

$$S_2(\tau) \sim \tau^{2H}. \tag{6.3}$$

In Figures 6.50 - 6.51 we have indicated the fit over the similarity range and also labeled the corresponding Hurst-exponent for the ordinary Hasegawa Wakatani model (H_C^O) and the modified model (H_C^M) where C is the coupling - parameter as before. Note that all structure functions shown are normalized by its first lag value, denoted by Δ.

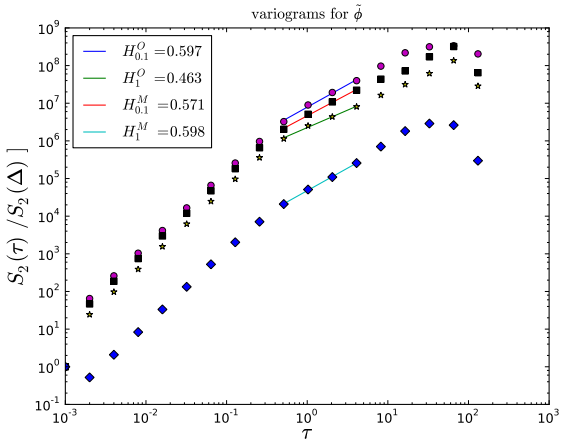

Figure 6.50: $S_2(\tau)$ for $\widetilde{\phi}$ in OHW with C = 0.1 (circles), OHW with C = 1 (stars), MHW with C = 0.1 (squares) and MHW with C = 1 (diamonds).

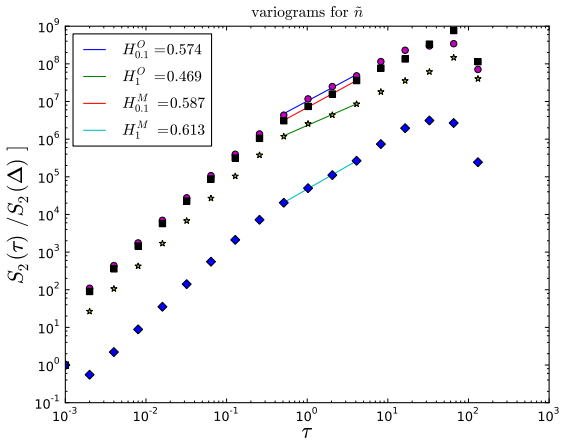

Figure 6.51: $S_2(\tau)$ for $\widetilde{n}$ in OHW with C = 0.1 (circles), OHW with C = 1 (stars), MHW with C = 0.1 (squares) and MHW with C = 1 (diamonds).

The variogram method gives no significant improvement over the rescaled range method since it is rather difficult to identify a proper inertial scaling range, as can be

seen from the figures above; to be consistent we present computed Hurst exponents over what comes closest to an inertial range in Table 6.4.

	$\widetilde{\phi}$	$\widetilde{n}$	$\widetilde{\Gamma}$	$\widetilde{\Omega}$
$H_{0.1}^{O}$	0.597	0.575	0.634	0.574
H_{1}^{O}	0.463	0.469	0.460	0.512
$H_{0.1}^{M}$	0.571	0.587	0.541	0.607
H_{1}^{M}	0.598	0.613	0.374	0.436

Table 6.3: Summarized Hurst-exponents from the variogram method.

	$\overline{\phi}$	$\widetilde{v}_x$	$\widetilde{v}_y$
$H_{0.1}^{O}$	0.730	0.646	0.588
H_{1}^{O}	0.758	0.463	0.593
$H_{0.1}^{M}$	0.977	0.549	0.587
H_{1}^{M}	0.994	0.295	0.491

Table 6.4: Summarized Hurst-exponents from the variogram method continued.

The Hurst exponents shown here are to be taken with even more caution than those obtained from the R/S analysis since the inertial range in the second order structure function has wavy tendencies, which is bad. However, also by applying this method we find no significant evidence of long-range correlations, since parameters scatter from 0.4 to 0.6 with the (obvious) exception of the zonal potential as explained in the previous section.

6.5.3 Structure - function inertial range scaling

In the following we obtain the scaling exponents for the structure functions directly from the slope in the inertial range. Figure 6.52 includes two regions where we have fitted the slopes, the deterministic range, where the Hurst parameter is 1, and the self-similarity range (or inertial-range), where the Hurst parameter is lower than 1 but varying for the variables under consideration.

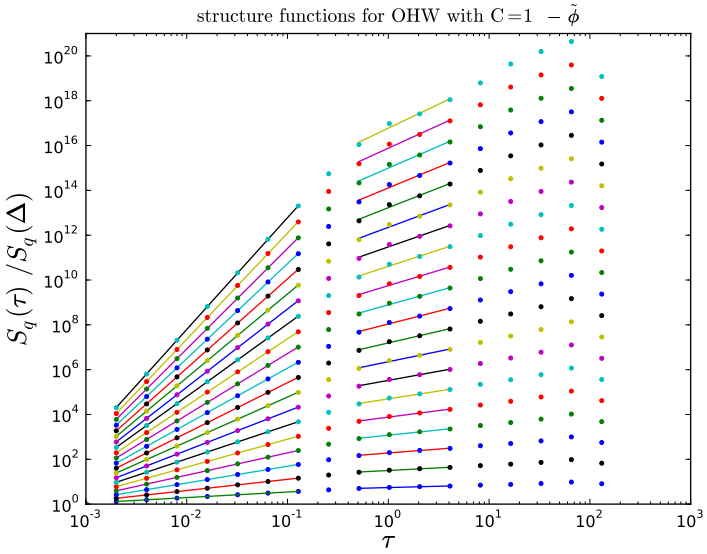

Figure 6.52: Structure functions for the fluctuating potential in OHW with C = 1. Increasing order from below q = 0.25 up to q = 5 in steps of 0.25.

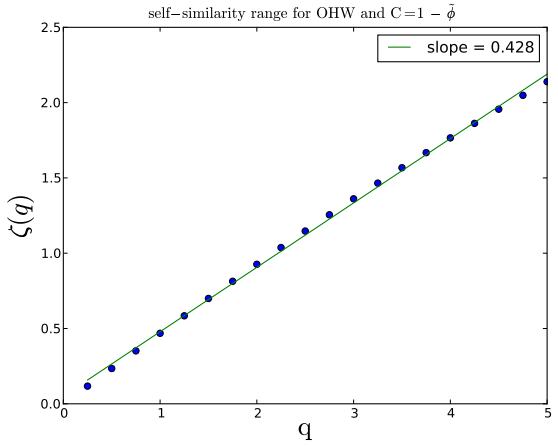

Figure 6.53: Hurst exponent inferred from the self-similarity range of Figure 6.52.

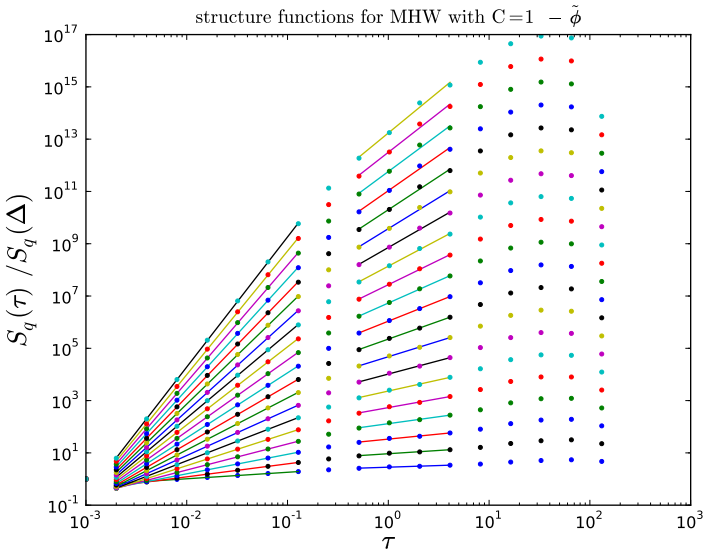

Figure 6.54: Structure functions for the fluctuating potential in OHW with C = 1. Increasing order from below q = 0.25 up to q = 5 in steps of 0.25.

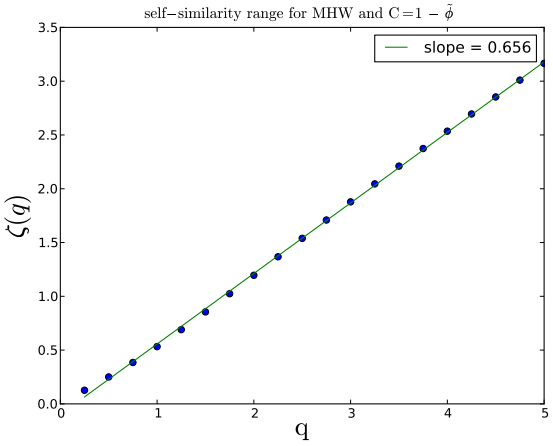

Figure 6.55: Hurst exponent inferred from the self-similarity range of Figure 6.54.

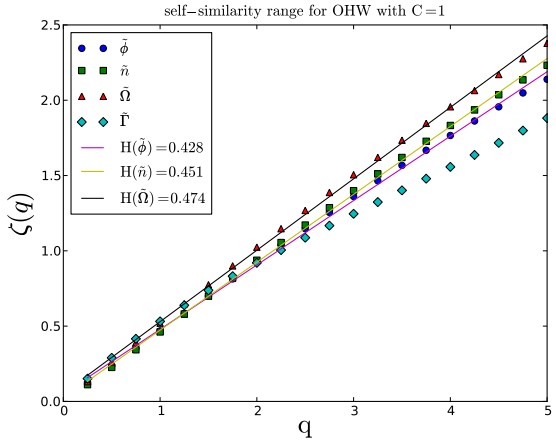

Figure 6.56: Structure function scaling exponents for $\widetilde{n}$, $\widetilde{\phi}$, $\widetilde{\Omega}$ and $\widetilde{\Gamma}$ in the quasi-adiabatic state for OHW.

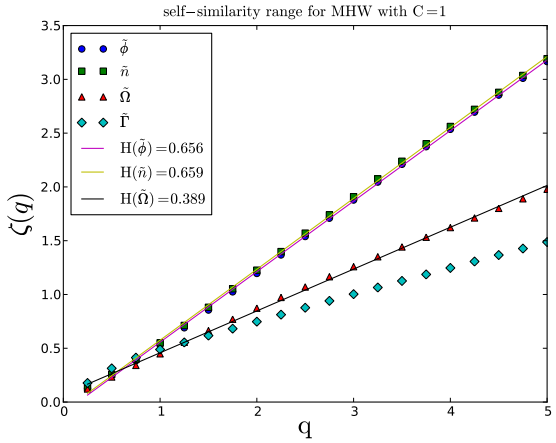

Figure 6.57: Structure function scaling exponents for $\widetilde{n}$, $\widetilde{\phi}$, $\widetilde{\Omega}$ and $\widetilde{\Gamma}$ in the quasi-adiabatic state for MHW.

Figures 6.56 and 6.57 reproduce the tendency from the rescaled range analysis that long-range correlations are absent in the OHW model. The presence of zonal flows in the MHW model does not significantly alter this tendency. Similar results to the above are obtained for C = 0.1 not shown here.

6.6 Probability distributions

The figures in this section show the computed histograms at the domain centered probe. As expected, variables follow approximately a normal-distribution for the ordinary model for both C = 0.1, C = 1 as well as for C = 0.1 in the modified equations. In the modified model for C = 1 the fluctuations are not Gaussian.

Assuming that density and radial-velocity fluctuations are Gaussian and correlated to some extend, we may compute the resulting probability distribution for the flux, given as the product of those stochastic variables. As can be seen from Figures 6.61 and Figures 6.65, the flux is consistently modeled. We may normalize in

a statistical sense by subtracting mean values and dividing by standard deviations,

$$\mathrm{V} = \frac{v_x - \langle v_x \rangle}{\sigma_{v_x}} \qquad \mathrm{N} = \frac{n - \langle n \rangle}{\sigma_n}.$$

It can then be shown (f.ex. Carreras et. al. [22]) that the probability distribution for the flux is given by

$$f_\Gamma(\Gamma) = \frac{1}{\pi}\sqrt{1-\gamma^2}\exp(\gamma\Gamma)K_0(|\Gamma|), \tag{6.4}$$

where K_0 is the modified Bessel function of the second kind with base-number 0 and the cross-correlation between $\widetilde{n}$ and $\widetilde{v}_x$ is quantified by

$$\gamma = \langle NV \rangle.$$

It should be noted that the expression above, of course, changes when the variables are not normalized.

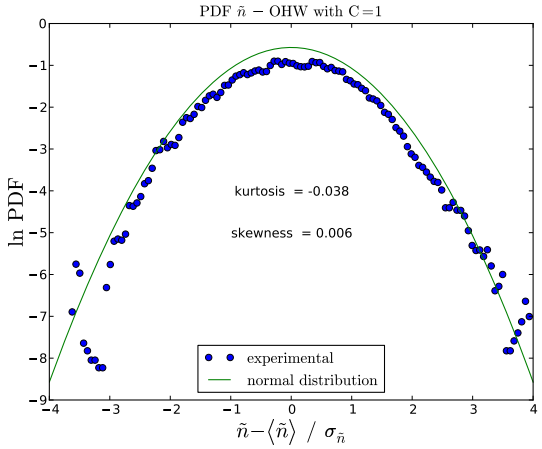

Figure 6.58: Fluctuating density PDF compared to normal distribution for OHW with C = 1.

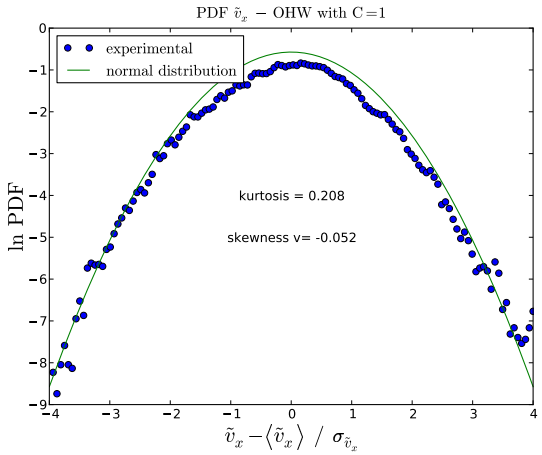

Figure 6.59: Fluctuating radial-velocity PDF compared to normal distribution for OHW with C = 1.

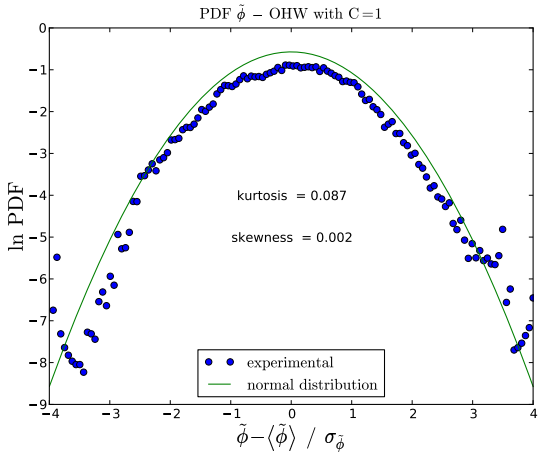

Figure 6.60: Fluctuating potential PDF compared to normal distribution for OHW with C = 1.

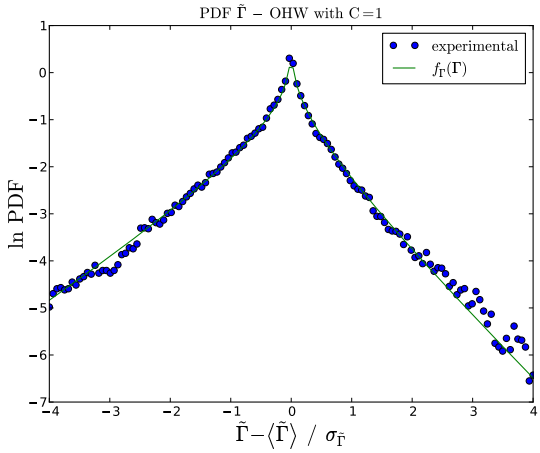

Figure 6.61: Radial-flux PDF compared to analytical expression for OHW with C = 1

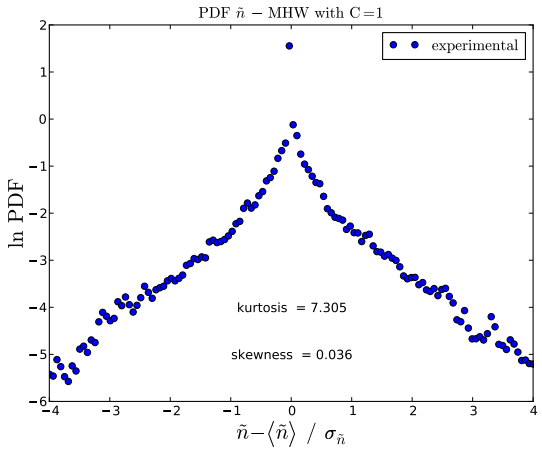

Figure 6.62: Fluctuating density PDF compared to normal distribution for MHW with C = 1.

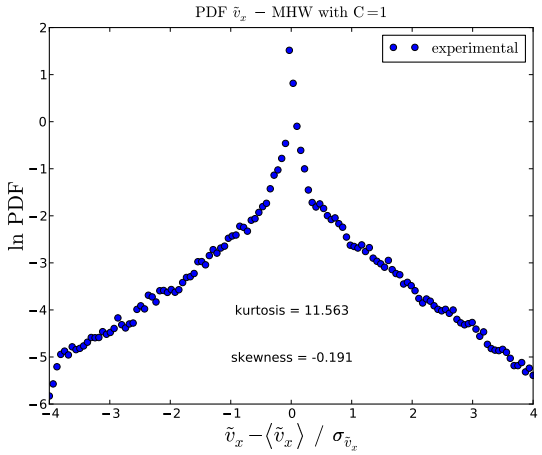

Figure 6.63: Fluctuating radial-velocity PDF compared to normal distribution for MHW with C = 1.

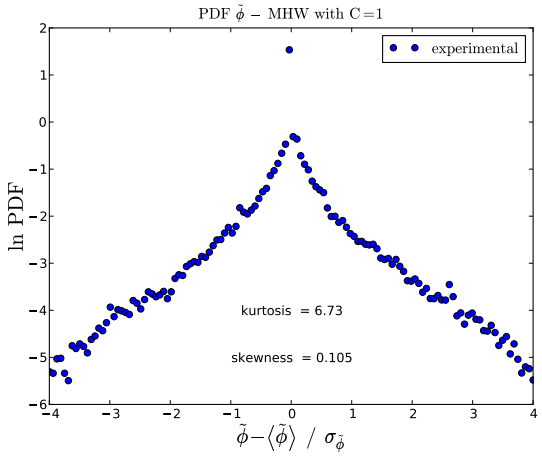

Figure 6.64: Fluctuating potential PDF compared to normal distribution for MHW with C = 1.

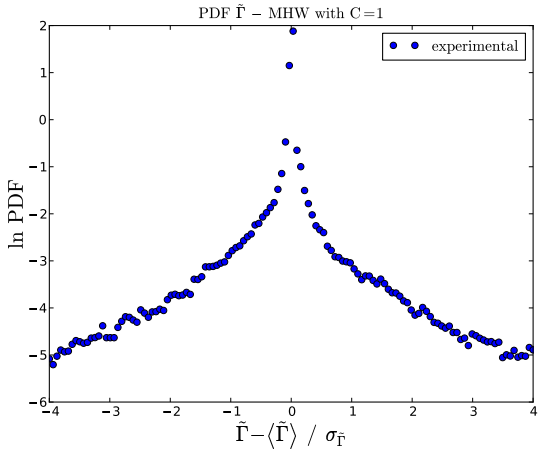

Figure 6.65: Radial-flux PDF compared to analytical expression for MHW with C = 1

Chapter 7

Discussion

Aspect ratio

In chapter 6 we found important constraints on the aspect ratio for the underlying drift wave turbulence to self-consistently form zonal flows. The instability domain for beating of drift waves to resonate and form zonal flows as well as the assumed functional form of wave kinetic energy perturbations associated with a zonal flow is

$$1 + k_y^2 - 3k_x^2 > 0.$$

We also found that drift waves satisfying the above can grow unstable by means of the modulational instability, as was shown by the reductive perturbation multi-scale expansion method. Cf. Figure 3.4 for the aspect ratio dependence in the modified Hasegawa Mima equation, which we recall to be the adiabatic limit of the modified Hasegawa Wakatani model. We may compare with Figure 7.1 which gives the ratio of radial to poloidal correlation length for the turbulent potential and vorticity in the different cases. This gives an indication that our predictions point in the correct direction - we see that turbulent structures in cases where zonal flows are allowed and excited indeed tend to be tilted. Furthermore, Figure 6.9 reflects that the turbulent velocities cease to be isotropic when zonal flows are present. This may also be seen from contour plots of the turbulent fields.

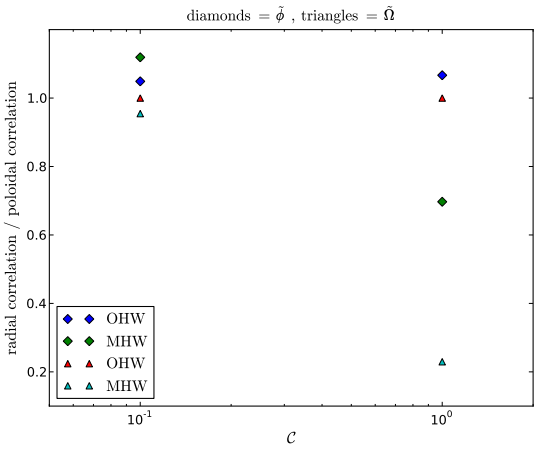

Figure 7.1: Ratio of radial to poloidal correlation length for turbulent potential and vorticity.

Flux scaling

As discussed earlier, the zonal flows that arise in the modified Hasegawa-Wakatani eqs. act as a transport barrier by means of forming an energy reservoir for the kinetic energy contained in the turbulent, fluctuating motions. As the zonal flows grow, the drift-wave turbulence is suppressed. It is indeed the turbulent drift-waves that transport plasma down the equilibrium background gradient, hence, as fluctuation levels go down, so does the radial flux.
By the same reasoning we deduce the adibacity dependence of the radial flux. The couplings-parameter, $\mathcal{C}$, is inversely proportional to the electron resistivity along the magnetic field lines and thus directly proportional to electron conductivity along $\mathbf{B}$. The electron conductivity along the field lines gives the density response to potential fluctuations as shown in the section on resistive drift waves, which in turn relates to the growth rate of the drift-wave instability. The more adiabatic the (electron) density response is, the less pronounced is the turbulence, see Eq. (2.24). Consequently, the (turbulent) transport levels down the equilibrium background density gradient decrease as the systems adiabacity is increased. This is precisely what we observe from Figure 6.37. From the energetics of the Hasegawa Wakatani models we learned that only the turbulent flux can act as a sink term for the total energy. Recalling what we just discussed and referring to Figure 6.7, we see that the total energy, which is the sum of kinetic and zonal energy, shows the same sensitivity to model and adiabacity, just as it should. The more adiabatic the system, the less is the flux and consequently the less energy is brought into the system from regions of higher plasma density, i.e., core regions. Also, zonal flows can be thought of as transport barriers such as to suppress radial transport which again results in less energy being transported into the system.

Gaussian fluctuations

The PDFs shown confirm that fluctuations in the hydrodynamic and quasi-adiabatic OHW system are Gaussian. There are no zonal flows and the turbulence is isotropic, such that there is no mechanism that should give deviation from a normal distribution. The theoretical model for the stochastic variable formed by multiplying the turbulent density and radial velocity reproduces the numerical flux to good agreement. In the quasi-adiabatic zonal flow case (MHW with C = 1), the turbulent density appears more structured due to the shearing effect of the zonal flow on the turbulent field, resulting in flattened PDFs for density and hence also for the flux. The PDFs for the zonal flow case consist of heavy exponential tails which is due to large bursts events. Comparing with MHW and C = 0.1, we find near Gaussian fluctuations. This is readily understood from the contour plots, where the density shows no zonal structure. The suppressing effect of the zonal flow on the turbulent radial transport causes the PDF for the flux in this case to become almost symmetric about zero with considerably lower probability of high amplitude bursts, compared to the other cases. Note also that density and potential show similar skewness and kurtosis in the quasi-adiabatic state in OHW, which is to be expected since the correlation between them is significant.

Validity of analytic work

We have considered the adiabatic limit in the modified Hasegawa Wakatani equation, resulting in the modified Hasegawa Mima equation, to get analytical results for drift wave dynamics. In order to interpret the obtained equations, we needed to assume that drift wave turbulence occurs on much smaller spatial scales than zonal flow dynamics, as well as longer time scales for zonal flows than for drift waves.

The persistence of zonal structures as shown in Figure 6.28 is highly non-trivial, since this actually corresponds to zero frequency modes. The correlation times for turbulent quantities are of about 3 - 5 normalized time units, so this assumption is justified by our numerical computations. Note that the deviation $H = 1$ in rescaled range plots coincides roughly with this. From Figure 6.28 we also found the potential zonal flow wavenumber to be approximately one half. It is not obvious what the turbulent wavelengths really are. Omni-directional wavenumber spectra show a peak around $k \sim 1$. We have chosen to only present the partial energy spectra since omni-directional spectra due to our computation algorithm turn out to be very bursty. If we take radial and poloidal correlation length to be a very rough estimate for corresponding wavelengths, we find $k \sim \sqrt{\left(\frac{2\pi}{7}\right)^2 + \left(\frac{2\pi}{4}\right)^2} \approx 1.8$ for the turbulent potential in the MHW and C = 1 state. Considering contour plots again, we see that the actual wavelengths are longer, hence the above can be thought of as an upper limit for the turbulent wavenumber. As mentioned earlier, $k \sim 1$ is the mode with largest growth rate in the HW system. In conclusion, we find that $q \ll k$ seems to be invalid and our theoretical discussions are (obviously) very approximative only. Note, however, even if the *actual* instability domains might differ from what we predicted, obtaining the same instability region for different physical phenomenon, i.e., modulation of drift wave envelope and modulation of wave kinetic energy coinciding with the region for zonal growth by parametric instability, is indication of a physical connection between them. Indeed, zonal flow formation is favorably thought of as being generated by edge localized drift-wave turbulence. See also [5].

Absence of long - range correlations

Referring to the section on rescaled - range analysis, there seems to be no significant evidence of long - range correlations in neither OHW or MHW. The zonal flows present in this work are persistent and only weakly damped, hence our result does not necessarily apply to changing zonal flow configurations which occur when viscosity is increased. Structure function analysis reveals Hurst exponents corresponding to fractional Gaussian noise in the absence of zonal flows, whereas the in the case of zonal flow (MHW, C = 1) the Hurst parameter appears to be increased. This is not necessarily an indication of long range correlations since the PDFs clearly are not Gaussian in this case. The presence of power law tails in PDFs can lead to an overestimated Hurst exponent in structure function analysis compared to rescaled range considerations, which effectively removes the heavy tail impact due to its "ranging" algorithm. Note again that self-similarity ranges for R/S and structure function analysis are too short to draw statistically significant conclusions from our findings. It is essential to run simulations much longer to clarify this issue.

Chapter 8

Conclusion

In the adiabatic limit of the modified Hasegawa Wakatani equations, small-scale electrostatic turbulence is adequately described by the modified Hasegawa Mima equation. For this limit, we have shown how zonal generation from small-scale electrostatic drift wave turbulence may occur from a parametric beating of resonant drift waves. Drift wave envelope modulations, governed by the cubic nonlinear Schrödinger equation, are unstable in the same wavenumber regime as the parametric zonal flow generation mechanism, suggesting a causality between those phenomena. The instability domain is confirmed by considering perturbations to the wave action density in the presence of zonal flows.

Numerical simulations show the emergence of persistent zonal structures in the quasi-adiabatic modified Hasegawa Wakatani model, as predicted by theory. We find that zonal flows increase poloidal correlation lengths for both turbulent potential and vorticity. Temporal correlation of vorticity is increased by zonal flows which is connected with zonal flows appearing persistent, hence corresponding to zero frequency modes.
Partial energy spectra show no significant difference in the hydrodynamic limit, whereas the radial energy distribution in the presence of zonal flows contains more energy at small scale whence energy is distributed over larger poloidal scales.
Radial transport levels are suppressed by adiabacity and zonal structures acting as transport barriers. Turbulence is reduced in the quasi-adiabatic MHW state with zonal structures containing most of the energy. The zonal structures induce velocity shears that causes anisotropy of the underlying turbulence.
Probability distribution functions are Gaussian in the absence of zonal flows which induce exponential tails. The turbulent radial flux follows theoretical predictions for whenever fluctuations are Gaussian. Turbulent density and potential are correlated in the quasi-adiabatic state.

Rescaled range analysis gives Hurst exponents between 0.4 and 0.6, yielding no indication of long range correlations. Structure function analysis confirms the findings where fluctuations follow Gaussian PDFs, whereas Hurst exponents are increased for the quasi-adiabatic MHW case. This is not necessarily an indication of long-range correlations since heavy exponential tails in PDFs tend to increase the self-similarity exponent found from structure functions compared to the rescaled range analysis. Longer time-series are needed to confirm the statistical significance of our findings since inertial-ranges span less than one decade in both rescaled range and structure function analysis.

Chapter 9

Outlook

The apparent absence of long-range correlations in both the ordinary and modified Hasegawa - Wakatani equations should be confirmed by extending self-similarity ranges in R/S and structure function analysis by means of significantly longer time series to at least three decades.

Runs for $C = 5$ and $C = 10$ show that zonal-flows are persistent over long time intervals, thus essentially suppressing turbulence. Longer time-series are needed to obtain turbulence statistics in the adiabatic regime, and also to investigate whether zonal-flows arise quasi-periodically. We have seen one event of rapid zonal-flow destruction for $C = 5$ which could be associated with a Kevin-Helmholtz type instability. This should be investigated in depth by viscosity scans in the adiabatic regime to make sure that this is indeed not associated with the systems viscosity. If statistics are to be carried out on this type of events, we again point out the need for much longer time-series, hoping to reproduce several of such events.

The influence of boundary conditions on the unphysical mode $k_x = 0$ should be investigated. Note that it is an inherent property of the Hasegawa - Wakatani equations that this mode is associated with the largest growth rate. Clearly no such mode can exist in Tokamak plasmas where density gradients in the edge are present.

Chapter 10

Appendix A

In this section we show some of the more cumbersome derivations used in the text. This is in order to guarantee a more fluent reading without too many technical interruptions.

10.1 Eq. (3.17)

The first equality on the LHS may be derived upon introducing

$$\widetilde{\Omega} = \frac{\partial^2 \widetilde{\phi}}{\partial x^2} + \frac{\partial^2 \widetilde{\phi}}{\partial y^2},$$

and

$$\overline{\Omega} = \frac{\partial^2 \overline{\phi}}{\partial x^2}.$$

We then have

$$(\Omega \partial_y \phi)_0 = \int dy \ \left(\widetilde{\Omega} \partial_y \widetilde{\phi}\right) + \int dy \ \left(\overline{\Omega} \partial_y \widetilde{\phi}\right) = \left(\widetilde{\Omega} \partial_y \widetilde{\phi}\right)_0,$$

and the first equality follows.
To arrive at the second equality we first note that

$$\begin{aligned}
\left(\widetilde{\Omega} \partial_y \widetilde{\phi}\right)_0 &= \frac{1}{L_y} \int_0^{L_y} dy \ \left[\frac{\partial^2 \widetilde{\phi}}{\partial x^2} \frac{\partial \widetilde{\phi}}{\partial y} + \frac{1}{2} \frac{\partial}{\partial y} \left(\frac{\partial \widetilde{\phi}}{\partial y} \right)^2 \right] \\
&= \frac{1}{L_y} \int_0^{L_y} dy \ \left[\frac{\partial}{\partial x} \left(\frac{\partial \widetilde{\phi}}{\partial x} \frac{\partial \widetilde{\phi}}{\partial y} \right) - \frac{\partial \widetilde{\phi}}{\partial x} \frac{\partial^2 \widetilde{\phi}}{\partial x \partial y} \right] \\
&= \frac{\partial}{\partial x} \left(\frac{\partial \widetilde{\phi}}{\partial x} \frac{\partial \widetilde{\phi}}{\partial y} \right)_0 - \frac{1}{L_y} \int_0^{L_y} dy \ \frac{\partial \widetilde{\phi}}{\partial x} \frac{\partial^2 \widetilde{\phi}}{\partial x \partial y} \\
&= \frac{\partial}{\partial x} \left(\frac{\partial \widetilde{\phi}}{\partial x} \frac{\partial \widetilde{\phi}}{\partial y} \right)_0 - \frac{1}{L_y} \int_0^{L_y} dy \ \frac{1}{2} \frac{\partial}{\partial y} \left(\frac{\partial \widetilde{\phi}}{\partial x} \right)^2 \\
&= \frac{\partial}{\partial x} \left(\frac{\partial \widetilde{\phi}}{\partial x} \frac{\partial \widetilde{\phi}}{\partial y} \right)_0,
\end{aligned}$$

due to the periodicity of $\partial\widetilde{\phi}/\partial x$ and $\partial\widetilde{\phi}/\partial y$.
Trivially we also have

$$\left(\widetilde{\Omega}\partial_y\widetilde{\phi}\right) = \frac{\partial}{\partial x}\left(\frac{\partial\widetilde{\phi}}{\partial x}\frac{\partial\widetilde{\phi}}{\partial y}\right).$$

The x and y components of the fluctuating electric drift are readily computed,

$$\widetilde{\mathbf{v}}_x = \widehat{\mathbf{z}} \times \nabla\widetilde{\phi} \cdot \widehat{\mathbf{x}} = -\partial_y\widetilde{\phi}\widehat{\mathbf{x}}$$
$$\widetilde{\mathbf{v}}_y = \widehat{\mathbf{z}} \times \nabla\widetilde{\phi} \cdot \widehat{\mathbf{y}} = \partial_x\widetilde{\phi}\widehat{\mathbf{y}},$$

and we find

$$(\Omega\partial_y\phi) = -\frac{\partial}{\partial x}\left(\widetilde{v}_x\widetilde{v}_y\right).$$

Rewriting the middle term of Eq. (3.17) and computing shows that

$$\begin{aligned}
\int d\mathbf{x}\ \overline{\phi}\left(\widetilde{\Omega}\partial_y\widetilde{\phi}\right) &= -\int d\mathbf{x}\ \overline{\phi}\frac{\partial}{\partial x}\left(\frac{\partial\widetilde{\phi}}{\partial x}\frac{\partial\widetilde{\phi}}{\partial y}\right) \\
&= \int d\mathbf{x}\ \frac{\partial\overline{\phi}}{\partial x}\frac{\partial}{\partial x}\left(\frac{\partial\widetilde{\phi}}{\partial x}\frac{\partial\widetilde{\phi}}{\partial y}\right) - \int d\mathbf{x}\ \frac{\partial}{\partial x}\left(\overline{\phi}\frac{\partial\widetilde{\phi}}{\partial x}\frac{\partial\widetilde{\phi}}{\partial y}\right) \\
&= \int d\mathbf{x}\ \frac{\partial\overline{\phi}}{\partial x}\frac{\partial}{\partial x}\left(\frac{\partial\widetilde{\phi}}{\partial x}\frac{\partial\widetilde{\phi}}{\partial y}\right) + \int dy\ \left(\overline{\phi}\frac{\partial\widetilde{\phi}}{\partial y}\frac{\partial\widetilde{\phi}}{\partial x}\right)^{|\mathrm{bdx}} \\
&= -\int d\mathbf{x}\ v_0\frac{\partial}{\partial x}\left(\widetilde{v}_x\widetilde{v}_y\right),
\end{aligned}$$

which is what we wanted to show. Q.E.D.

Chapter 11

Appendix B

In the following we shall derive the dispersion relation given by [11] in a detailed fashion. Consider again the nonlinear, cubic, Schrödinger equation

$$i\frac{\partial A}{\partial t} + P\frac{\partial^2 A}{\partial x^2} + Q\left|A\right|^2 A = 0. \tag{11.1}$$

Let us seek a solution on the form

$$A_0 = a_0 e^{i\omega t},$$

where a_0 is a complex constant. Inserting into the equation we find

$$\omega = \left|a_0\right|^2 Q.$$

The NLS can be linearized upon assuming a small perturbation to the solution on the form

$$A = [a_0 + \epsilon(x,t)]e^{i|a_0|^2 Qt},$$

where $|\epsilon/a_0| \ll 1$.

Plugging into the equation and carefully evaluating the nonlinear term we have

$$i\frac{\partial \epsilon}{\partial t} - a_0\left|a_0\right|^2 Q - \epsilon\left|a_0\right|^2 Q + P\frac{\partial^2 \epsilon}{\partial x^2} + Q\left|a_0\right|^2 a_0 + Qa_0^2(2\epsilon+\epsilon^*) + Q(2a_0\left|\epsilon\right|^2 + a_0^*\epsilon^2 + \epsilon\left|\epsilon\right|^2) = 0.$$

Now, there is no loss in generality if we assume a_0 to be real (neglecting the phase information). Doing so and discarding terms proportional to ϵ^2 we find

$$i\frac{\partial \epsilon}{\partial t} + P\frac{\partial^2 \epsilon}{\partial x^2} + Qa_0^2(\epsilon + \epsilon^*) = 0.$$

A general, wave - like, perturbation is expressed as

$$\epsilon = a_1 e^{ikx - i\Omega t} + a_2 e^{-ikx + i\Omega t},$$

where a_1 and a_2 are again taken to be real without loss of generality and k and Ω are the wavenumber and frequency of the perturbation. Inserting for ϵ in Eq. (11) and collecting terms we arrive at

$$\begin{aligned} &e^{ikx - i\Omega t}\left(\Omega a_1 - Pk^2 a_1 + Qa_0^2 a_1 + Qa_0^2 a_2\right) \\ &+ e^{-ikx + i\Omega t}\left(-\Omega a_2 - Pk^2 a_2 + Qa_0^2 a_2 + Qa_0^2 a_1\right) = 0. \end{aligned}$$

This equation is supposed to hold for all k and all Ω, thus the terms proportional to the exponentials must vanish and we have the equivalent matrix equation

$$\begin{pmatrix} \Omega - Pk^2 + Qa_0^2 & Qa_0^2 \\ Qa_0^2 & -\Omega - Pk^2 + Qa_0^2 \end{pmatrix} \begin{pmatrix} a_1 \\ a_2 \end{pmatrix} = \begin{pmatrix} 0 \\ 0 \end{pmatrix}.$$

For the solutions to be nontrivial we require the 2×2 matrix to be singular which is the case when its determinant vanishes. We therefore have

$$-\Omega^2 - 2Pk^2Qa_0^2 + (Pk^2)^2 = 0,$$

which gives the dispersion relation that we use in the text

$$\Omega^2 = P^2k^4 - 2PQk^2a_0^2 = P^2k^4 - 2PQk^2 \left|A_0\right|^2. \tag{11.2}$$

Chapter 12

Appendix C

In this section we present the detailed calculations leading to the results shown in the section Modulational instability. Consider again Eq. (3.51) ,

$$(\partial_t + \kappa\partial_y)\widetilde{\phi} + \partial_x\overline{\phi}\partial_y\widetilde{\phi} - (\partial_t + \partial_x\phi\partial_y - \partial_y\phi\partial_x)(\partial_x^2 + \partial_y^2)\phi = 0. \tag{12.1}$$

We use the expansion to fourth order,

$$\phi = \epsilon(\widetilde{\phi}_1 + \overline{\phi}_1) + \epsilon^2(\widetilde{\phi}_2 + \overline{\phi}_2) + \epsilon^3(\widetilde{\phi}_3 + \overline{\phi}_3) + \epsilon^4(\widetilde{\phi}_4 + \overline{\phi}_4),$$

where we have taken the expansion of ϕ to start at order ϵ. As is shown in Appendix B, including ϕ_0 only adds a Doppler shift to the observed frequency in addition to complicating the calculations. The differential operators to fourth order ϵ are

$$\begin{aligned}
\partial_\sigma &= \partial_{\sigma_0} + \epsilon\partial_{\sigma_1} + \epsilon^2\partial_{\sigma_2} + \epsilon^3\partial_{\sigma_3} + \epsilon^4\partial_{\sigma_4} \\
\partial_\sigma^2 &= \partial_\sigma\partial_\sigma = \partial_{\sigma_0}^2 + 2\epsilon\partial_{\sigma_0\sigma_1}^2 + \epsilon^2(2\partial_{\sigma_0\sigma_2}^2 + \partial_{\sigma_1}^2) \\
&\quad + \epsilon^3(2\partial_{\sigma_0\sigma_3}^2 + 2\partial_{\sigma_1\sigma_2}^2) + \epsilon^4(2\partial_{\sigma_0\sigma_4}^2 + 2\partial_{\sigma_1\sigma_3}^2 + \partial_{\sigma_2}^2),
\end{aligned}$$

where $\sigma = x, y, t$. We now proceed to evaluate Eq. (12.1) term by term.

$$\begin{aligned}
&(\partial_t + \kappa\partial_y)\widetilde{\phi} = [\partial_{t_0} + \epsilon\partial_{t_1} + \epsilon^2\partial_{t_2} + \epsilon^3\partial_{t_3} + \epsilon^4\partial_{t_4} + \kappa(\partial_{y_0} + \epsilon\partial_{y_1} + \epsilon^2\partial_{y_2} + \epsilon^3\partial_{y_3} + \epsilon^4\partial_{y_4})] \\
&[\epsilon\widetilde{\phi}_1 + \epsilon^2\widetilde{\phi}_2 + \epsilon^3\widetilde{\phi}_3 + \epsilon^4\widetilde{\phi}_4] \\
&= \epsilon[(\partial_{t_0} + \kappa\partial_{y_0})\widetilde{\phi}_1] \\
&+ \epsilon^2[(\partial_{t_0} + \kappa\partial_{y_0})\widetilde{\phi}_2 + (\partial_{t_1} + \kappa\partial_{y_1})\widetilde{\phi}_1] \\
&+ \epsilon^3[(\partial_{t_0} + \kappa\partial_{y_0})\widetilde{\phi}_3 + (\partial_{t_1} + \kappa\partial_{y_1})\widetilde{\phi}_2 + (\partial_{t_2} + \kappa\partial_{y_2})\widetilde{\phi}_1] \\
&+ \epsilon^4[(\partial_{t_0} + \kappa\partial_{y_0})\widetilde{\phi}_4 + (\partial_{t_1} + \kappa\partial_{y_1})\widetilde{\phi}_3 + (\partial_{t_2} + \kappa\partial_{y_2})\widetilde{\phi}_2 \\
&+ (\partial_{t_3} + \kappa\partial_{y_3})\widetilde{\phi}_1].
\end{aligned}$$

$$\begin{aligned}
\partial_x\overline{\phi}\partial_y\widetilde{\phi} &= (\partial_{x_0} + \epsilon\partial_{x_1} + \epsilon^2\partial_{x_2} + \epsilon^3\partial_{x_3} + \epsilon^4\partial_{x_4})(\epsilon\overline{\phi}_1 + \epsilon^2\overline{\phi}_2 + \epsilon^3 + \overline{\phi}_3 + \epsilon^4 + \overline{\phi}_4) \\
&\quad (\partial_{y_0} + \epsilon\partial_{y_1} + \epsilon^2\partial_{y_2} + \epsilon^3\partial_{y_3} + \epsilon^4\partial_{y_4})(\epsilon\widetilde{\phi}_1 + \epsilon^2\widetilde{\phi}_2 + \epsilon^3 + \widetilde{\phi}_3 + \epsilon^4 + \widetilde{\phi}_4) \\
&= \epsilon^2(\partial_{x_0}\overline{\phi}_1\partial_{y_0}\widetilde{\phi}_1) + \epsilon^3[\partial_{x_0}\overline{\phi}_1(\partial_{y_0}\widetilde{\phi}_2 + \partial_{y_1}\widetilde{\phi}_1) + \partial_{y_0}\widetilde{\phi}_1(\partial_{x_0}\overline{\phi}_2 + \partial_{x_1}\overline{\phi}_1)] \\
&+ \epsilon^4[\partial_{x_0}\overline{\phi}_1(\partial_{y_0}\widetilde{\phi}_3 + \partial_{y_1}\widetilde{\phi}_2 + \partial_{y_2}\widetilde{\phi}_2) + \partial_{x_0}\overline{\phi}_2(\partial_{y_0}\widetilde{\phi}_2 + \partial_{y_1}\widetilde{\phi}_1) \\
&+ \partial_{x_1}\overline{\phi}_1(\partial_{y_0}\widetilde{\phi}_2 + \partial_{y_1}\widetilde{\phi}_1) + \partial_{y_0}\widetilde{\phi}_1(\partial_{x_0}\overline{\phi}_3 + \partial_{x_1}\overline{\phi}_2 + \partial_{x_2}\overline{\phi}_1)].
\end{aligned}$$

We continue by calculating $\partial_x^2\phi$, $\partial_t\partial_x^2\phi$ and $\partial_x\phi\partial_y\partial_x^2\phi$. The other terms are then easily found by changing indices to y where necessary, due to the symmetry of the equation.

$$\begin{aligned}
\partial_x^2\phi &= [\partial_{x_0}^2 + 2\epsilon\partial_{x_0x_1}^2 + \epsilon^2(2\partial_{x_0x_2}^2 + \partial_{x_1}^2) + \epsilon^3(2\partial_{x_0x_3}^2 + 2\partial_{x_1x_2}^2) + \epsilon^4(2\partial_{x_0x_4}^2 + 2\partial_{x_1x_3}^2 + \partial_{x_2}^2)] \\
&\quad [\epsilon(\widetilde{\phi}_1 + \overline{\phi}_1) + \epsilon^2(\widetilde{\phi}_2 + \overline{\phi}_2) + \epsilon^3(\widetilde{\phi}_3 + \overline{\phi}_3) + \epsilon^4(\widetilde{\phi}_4 + \overline{\phi}_4)] \\
&\quad = \epsilon[\partial_{x_0}^2(\widetilde{\phi}_1 + \overline{\phi}_1)] + \epsilon^2[\partial_{x_0}^2(\widetilde{\phi}_2 + \overline{\phi}_2) + 2\partial_{x_0x_1}^2(\widetilde{\phi}_1 + \overline{\phi}_1)] \\
&\quad + \epsilon^3[\partial_{x_0}^2(\widetilde{\phi}_3 + \overline{\phi}_3) + 2\partial_{x_0x_1}^2(\widetilde{\phi}_2 + \overline{\phi}_2) + 2\partial_{x_0x_2}^2(\widetilde{\phi}_1 + \overline{\phi}_1) + \partial_{x_1}^2(\widetilde{\phi}_1 + \overline{\phi}_1)] \\
&\quad + \epsilon^4[\partial_{x_0}^2(\widetilde{\phi}_4 + \overline{\phi}_4) + 2\partial_{x_0x_1}^2(\widetilde{\phi}_3 + \overline{\phi}_3) + 2\partial_{x_0x_2}^2(\widetilde{\phi}_2 + \overline{\phi}_2) + \partial_{x_1}^2(\widetilde{\phi}_2 + \overline{\phi}_2) \\
&\quad + 2\partial_{x_0x_3}^2(\widetilde{\phi}_1 + \overline{\phi}_1) + 2\partial_{x_1x_2}^2(\widetilde{\phi}_1 + \overline{\phi}_1)].
\end{aligned}$$

$$\begin{aligned}
\partial_t\partial_x^2\phi &= (\partial_{t_0} + \epsilon\partial_{t_1} + \epsilon^2\partial_{t_2} + \epsilon^3\partial_{t_3} + \epsilon^4\partial_{t_4})\partial_x^2\phi \\
&\quad = \epsilon[\partial_{t_0}\partial_{x_0}^2(\widetilde{\phi}_1 + \overline{\phi}_1)] + \epsilon^2[\partial_{t_0}\partial_{x_0}^2(\widetilde{\phi}_2 + \overline{\phi}_2) + \partial_{t_0}2\partial_{x_0x_1}^2(\widetilde{\phi}_1 + \overline{\phi}_1) + \partial_{t_1}\partial_{x_0}^2(\widetilde{\phi}_1 + \overline{\phi}_1)] \\
&\quad + \epsilon^3[\partial_{t_0}\partial_{x_0}^2(\widetilde{\phi}_3 + \overline{\phi}_3) + \partial_{t_0}2\partial_{x_0x_1}^2(\widetilde{\phi}_2 + \overline{\phi}_2) + \partial_{t_0}2\partial_{x_0x_2}^2(\widetilde{\phi}_1 + \overline{\phi}_1) + \partial_{t_0}\partial_{x_1}^2(\widetilde{\phi}_1 + \overline{\phi}_1) \\
&\quad + \partial_{t_1}\partial_{x_1}^2(\widetilde{\phi}_2 + \overline{\phi}_2) + \partial_{t_1}2\partial_{x_0x_1}^2(\widetilde{\phi}_1 + \overline{\phi}_1) + \partial_{t_2}\partial_{x_1}^2(\widetilde{\phi}_1 + \overline{\phi}_1)] \\
&\quad + \epsilon^4[\partial_{t_0}\partial_{x_0}^2(\widetilde{\phi}_4 + \overline{\phi}_4) + \partial_{t_0}2\partial_{x_0x_1}^2(\widetilde{\phi}_3 + \overline{\phi}_3) + \partial_{t_0}2\partial_{x_0x_2}^2(\widetilde{\phi}_2 + \overline{\phi}_2) + \partial_{t_0}2\partial_{x_1}^2(\widetilde{\phi}_2 + \overline{\phi}_2) \\
&\quad + \partial_{t_0}2\partial_{x_0x_3}^2(\widetilde{\phi}_1 + \overline{\phi}_1) + \partial_{t_0}2\partial_{x_1x_2}^2(\widetilde{\phi}_1 + \overline{\phi}_1) + \partial_{t_1}\partial_{x_0}^2(\widetilde{\phi}_3 + \overline{\phi}_3) + \partial_{t_1}2\partial_{x_0x_1}^2(\widetilde{\phi}_2 + \overline{\phi}_2) \\
&\quad + \partial_{t_1}2\partial_{x_0x_2}^2(\widetilde{\phi}_1 + \overline{\phi}_1) + \partial_{t_1}\partial_{x_1}^2(\widetilde{\phi}_1 + \overline{\phi}_1) + \partial_{t_2}\partial_{x_0}^2(\widetilde{\phi}_2 + \overline{\phi}_2) \\
&\quad + \partial_{t_2}2\partial_{x_0x_1}^2(\widetilde{\phi}_1 + \overline{\phi}_1) + \partial_{t_3}\partial_{x_0}^2(\widetilde{\phi}_1 + \overline{\phi}_1)].
\end{aligned}$$

$$\begin{aligned}
\partial_x\phi\partial_y &= (\partial_{x_0} + \epsilon\partial_{x_1} + \epsilon^2\partial_{x_2} + \epsilon^3\partial_{x_3} + \epsilon^4\partial_{x_4})[\epsilon(\widetilde{\phi}_1 + \overline{\phi}_1) + \epsilon^2(\widetilde{\phi}_2 + \overline{\phi}_2) + \epsilon^3(\widetilde{\phi}_3 + \overline{\phi}_3) + \epsilon^4(\widetilde{\phi}_4 + \overline{\phi}_4)] \\
&\quad (\partial_{y_0} + \epsilon\partial_{y_1} + \epsilon^2\partial_{y_2} + \epsilon^3\partial_{y_3} + \epsilon^4\partial_{y_4}) \\
&\quad = \epsilon[\partial_{x_0}(\widetilde{\phi}_1 + \overline{\phi}_1)\partial_{y_0}] + \epsilon^2[\partial_{x_0}(\widetilde{\phi}_1 + \overline{\phi}_1)\partial_{y_1} + \partial_{x_0}(\widetilde{\phi}_2 + \overline{\phi}_2)\partial_{y_0} + \partial_{x_1}(\widetilde{\phi}_1 + \overline{\phi}_1)\partial_{y_0}] \\
&\quad + \epsilon^3[\partial_{x_0}(\widetilde{\phi}_1 + \overline{\phi}_1)\partial_{y_2} + \partial_{x_0}(\widetilde{\phi}_2 + \overline{\phi}_2)\partial_{y_1} + \partial_{x_1}(\widetilde{\phi}_1 + \overline{\phi}_1)\partial_{y_1} + \partial_{x_0}(\widetilde{\phi}_3 + \overline{\phi}_3)\partial_{y_0} \\
&\quad + \partial_{x_1}(\widetilde{\phi}_2 + \overline{\phi}_2)\partial_{y_0} + \partial_{x_2}(\widetilde{\phi}_1 + \overline{\phi}_1)\partial_{y_0}] \\
&\quad + \epsilon^4[\partial_{x_0}(\widetilde{\phi}_1 + \overline{\phi}_1)\partial_{y_3} + \partial_{x_0}(\widetilde{\phi}_2 + \overline{\phi}_2)\partial_{y_2} + \partial_{x_1}(\widetilde{\phi}_1 + \overline{\phi}_1)\partial_{y_2} + \partial_{x_0}(\widetilde{\phi}_3 + \overline{\phi}_3)\partial_{y_1} \\
&\quad + \partial_{x_1}(\widetilde{\phi}_2 + \overline{\phi}_2)\partial_{y_1} + \partial_{x_2}(\widetilde{\phi}_1 + \overline{\phi}_1)\partial_{y_1} + \partial_{x_0}(\widetilde{\phi}_4 + \overline{\phi}_4)\partial_{y_0} + \partial_{x_1}(\widetilde{\phi}_3 + \overline{\phi}_3)\partial_{y_0} + \partial_{x_2}(\widetilde{\phi}_2 + \overline{\phi}_2)\partial_{y_0} \\
&\quad + \partial_{x_3}(\widetilde{\phi}_1 + \overline{\phi}_1)\partial_{y_0}].
\end{aligned}$$

$$\begin{aligned}
\partial_x\phi\partial_y\partial_x^2\phi &= \epsilon^2[\partial_{x_0}(\widetilde{\phi}_1 + \overline{\phi}_1)\partial_{y_0}\partial_{x_0}^2(\widetilde{\phi}_1 + \overline{\phi}_1)] \\
&\quad = \epsilon^3[+2\partial_{x_0}(\widetilde{\phi}_1 + \overline{\phi}_1)\partial_{y_0}\partial_{x_0x_1}^2(\widetilde{\phi}_1 + \overline{\phi}_1) + \partial_{x_0}(\widetilde{\phi}_1 + \overline{\phi}_1)\partial_{y_1}\partial_{x_0}^2(\widetilde{\phi}_1 + \overline{\phi}_1) \\
&\quad + \partial_{x_0}(\widetilde{\phi}_2 + \overline{\phi}_2)\partial_{y_0}\partial_{x_0}^2(\widetilde{\phi}_1 + \overline{\phi}_1) + \partial_{x_1}(\widetilde{\phi}_1 + \overline{\phi}_1)\partial_{y_0}\partial_{x_0}^2(\widetilde{\phi}_1 + \overline{\phi}_1)] \\
&\quad + \epsilon^4\{\partial_{x_0}(\widetilde{\phi}_1 + \overline{\phi}_1)\partial_{y_0}[\partial_{x_0}^2(\widetilde{\phi}_3 + \overline{\phi}_3) + 2\partial_{x_0x_1}^2(\widetilde{\phi}_2 + \overline{\phi}_2) + 2\partial_{x_0x_2}^2(\widetilde{\phi}_1 + \overline{\phi}_1) \\
&\quad + \partial_{x_1}^2(\widetilde{\phi}_1 + \overline{\phi}_1)] + \partial_{x_0}(\widetilde{\phi}_1 + \overline{\phi}_1)\partial_{y_1}[\partial_{x_0}^2(\widetilde{\phi}_2 + \overline{\phi}_2) + 2\partial_{x_0x_1}^2(\widetilde{\phi}_1 + \overline{\phi}_1)] \\
&\quad + \partial_{x_0}(\widetilde{\phi}_2 + \overline{\phi}_2)\partial_{y_0}[\partial_{x_0}^2(\widetilde{\phi}_2 + \overline{\phi}_2) + 2\partial_{x_0x_1}^2(\widetilde{\phi}_1 + \overline{\phi}_1)] \\
&\quad + \partial_{x_1}(\widetilde{\phi}_1 + \overline{\phi}_1)\partial_{y_0}[\partial_{x_0}^2(\widetilde{\phi}_2 + \overline{\phi}_2) + 2\partial_{x_0x_1}^2(\widetilde{\phi}_1 + \overline{\phi}_1)] \\
&\quad + \partial_{x_0}(\widetilde{\phi}_1 + \overline{\phi}_1)\partial_{y_2}\partial_{x_0}^2(\widetilde{\phi}_1 + \overline{\phi}_1) + \partial_{x_0}(\widetilde{\phi}_2 + \overline{\phi}_2)\partial_{y_1}\partial_{x_0}^2(\widetilde{\phi}_1 + \overline{\phi}_1) \\
&\quad + \partial_{x_1}(\widetilde{\phi}_1 + \overline{\phi}_1)\partial_{y_1}\partial_{x_0}^2(\widetilde{\phi}_1 + \overline{\phi}_1) + \partial_{x_0}(\widetilde{\phi}_3 + \overline{\phi}_3)\partial_{y_0}\partial_{x_0}^2(\widetilde{\phi}_1 + \overline{\phi}_1) \\
&\quad + \partial_{x_1}(\widetilde{\phi}_2 + \overline{\phi}_2)\partial_{y_0}\partial_{x_0}^2(\widetilde{\phi}_1 + \overline{\phi}_1) + \partial_{x_2}(\widetilde{\phi}_1 + \overline{\phi}_1)\partial_{y_0}\partial_{x_0}^2(\widetilde{\phi}_1 + \overline{\phi}_1)\}.
\end{aligned}$$

To first order in ϵ we read off

$$\partial_{t_0}(\widetilde{\phi}_1+\overline{\phi}_1)+\kappa\partial_{y_0}(\widetilde{\phi}_1+\overline{\phi}_1)-[\partial^2_{x_0}+\partial^2_{y_0}]\partial_{t_0}(\widetilde{\phi}_1+\overline{\phi}_1)=0,$$

which is precisely Eq. (3.53) since $\overline{\phi}_1$ does not depend on any y_i coordinate, furtheremore we assume that the zonal components vary on spatial scales at least one order in ϵ larger than fluctuating components, $\partial_{x_0}\overline{\phi}_1/\partial_{x_0}\widetilde{\phi}_1 \ll 1$, and also on a slower time scale, $\partial_{t_0}\overline{\phi}_1/\partial_{t_0}\widetilde{\phi}_1 \ll 1$.
We find to second order in ϵ

$$\begin{aligned}
&\left[1-\left(\partial^2_{x_0}+\partial^2_{y_0}\right)\right]\partial_{t_0}\left(\widetilde{\phi}_2+\overline{\phi}_2\right)+\kappa\partial_{y_0}\left(\widetilde{\phi}_2+\overline{\phi}_2\right)\\
&+\left[1-\left(\partial^2_{x_0}+\partial^2_{y_0}\right)\right]\partial_{t_1}\left(\widetilde{\phi}_1+\overline{\phi}_1\right)+\kappa\partial_{y_1}\left(\widetilde{\phi}_1+\overline{\phi}_1\right)-2\left(\partial^2_{x_0x_1}+\partial^2_{y_0y_1}\right)\left(\widetilde{\phi}_1+\overline{\phi}_1\right)\\
&-\left[\partial_{x_0}(\widetilde{\phi}_1+\overline{\phi}_1)\partial_{y_0}\left(\partial^2_{x_0}+\partial^2_{y_0}\right)(\widetilde{\phi}_1+\overline{\phi}_1)-\partial_{y_0}(\widetilde{\phi}_1+\overline{\phi}_1)\partial_{x_0}\left(\partial^2_{x_0}+\partial^2_{y_0}\right)(\widetilde{\phi}_1+\overline{\phi}_1)\right]\\
&=0.
\end{aligned}$$

Again assuming that the characteristic time- and spatial scales of the zonal flow are at least one order in ϵ larger than the corresponding scales for the fluctuating motions, we arrive at Eq. (3.56) when inserting the assumed wave-form of $\widetilde{\phi}_1$ given by Eq. (3.54). Equations at third- and fourth order in ϵ are readily read-off from the above and the discussion in section Modulational Instability is already sufficiently explanatory at those orders.

As indicated previously, taking the whole expansion of the potential down to order ϵ^0 gives f.ex. at order zero

$$\begin{aligned}
(\partial_{t_0}+\kappa\partial_{y_0})\widetilde{\phi}_0+\partial_{x_0}\overline{\phi}_0\partial_{y_0}\widetilde{\phi}_0-\partial_{t_0}(\partial^2_{x_0}+\partial^2_{y_0})(\widetilde{\phi}_0+\overline{\phi}_0)-\partial_{x_0}(\widetilde{\phi}_0+\overline{\phi}_0)\partial_{y_0}(\partial^2_{x_0}+\partial^2_{y_0})(\widetilde{\phi}_0+\overline{\phi}_0)\\
+\partial_{y_0}(\widetilde{\phi}_0+\overline{\phi}_0)\partial_{x_0}(\partial^2_{x_0}+\partial^2_{y_0})(\widetilde{\phi}_0+\overline{\phi}_0)=0,
\end{aligned}$$

which upon assuming $\widetilde{\phi}_0$ of the form

$$\widetilde{\phi}_0 \sim A(x_1,x_2,...,y_1,y_2,...,t_1,t_2,...)\exp^{ik_xx_0+ik_yy_0-i\omega t_0}+c.c,$$

results in the promised

$$\omega=\frac{\kappa k_y}{1+k^2}+k_y\partial_{x_0}\overline{\phi}_0=\frac{\kappa k_y}{1+k^2}+k_y\overline{v}_x, \tag{12.2}$$

where the zonal flow velocity is given by $\overline{v}_x=\partial_{x_0}\overline{\phi}_0$ and the last term on the RHS above is the zonal flow induced Doppler shift.

Chapter 13

Bibliography

[1] H.L. Pécseli. *Waves and Oscillations in Plasmas*, Taylor and Francis Ltd. , 2012.

[2] F.F. Chen. *Plasma Physics and controlled Fusion. Volume 1: Plasma Physics. 2nd edition*, Springer, 2006.

[3] P.M. Bellan. *Fundamentals of Plasma Physics*, Cambridge University Press, 2006.

[4] A.Hasegawa and M.Wakatani. *Plasma edge turbulence*, Physical Review Letters, 50 (1983), pp. 682-686.

[5] P.H. Diamond, S.-I. Itoh, K. Itoh and T. S. Hahm. *Zonal flows in plasma - a review*, Plasma Physics and Controlled Fusion, 47 (2005), R35-R161.

[6] T.D. Kaladze, D.J. Wu, O.A. Pokhotelov, R.Z. Sagdeev, L.Stenflo and P.K. Shukla. *Drift wave driven zonal flows in plasmas*, Physics of Plasmas, 12, 122311 (2005).

[7] G. Manfredi, C.M. Roach and R.O. Dendy. *Zonal flow and streamer generation in drift turbulence*, Plasma Physics and Controlled Fusion, 43 (2001), pp. 825-837.

[8] C. Holland, P.H. Diamond, S. Champeux, E. Kim, O. Gurcan, M.N. Rosenbluth, G.R. Tynan, N. Crocker, W. Nevins and J.Candy. *Investigations of the role of nonlinear couplings in structure formation and transport regulation: experiment, simulation, and theory*, Nuclear Fusion 43 (2003), pp. 761-780.

[9] R.F. Abdullatif and R.L. Dewar. *Derivation of the Nonlinear Schrödinger Equation by The Derivative Perturbation Expansion Method*, International Journal of Basic and Applied Sciences, Vol:11 No: 02.

[10] S. Champeux and P.H. Diamond. *Streamer and zonal flow generation from envelope modulations in drift wave turbulence*, Physics Letters A 288 (2001), pp. 214-219.

[11] D.G. Swanson. *Plasma Waves*, Academic Press Inc., 1998.

[12] G. Witham. *Linear and Nonlinear Waves*, Wiley Interscience ,1999.

[13] A.I. Smolyakov, P.H. Diamond and V.I. Shevchenko. *Zonal flow generation by parametric instability in magnetized plasmas and geostrophic fluids*, Physics of Plasmas, 7, 1349 (2000).

[14] W.D. Hayes. *Conservation of Action and Modal Wave Action*, Proceedings of the Royal Society of London. Series A, Mathematical and Pysical Sciences, Vol. 320, No. 1541 (Dec. 15, 1970), pp. 187-208.

[15] O.E. Garcia, N.H. Bian, V. Naulin, A.H. Nielsen and J. Juul Rasmussen. *Two-dimensional convection and interchange motions in fluids and magnetized plasmas*, Physica Scripta, T122 (2006), pp. 104-124.

[16] S.W. McDonald. *Phase-space representations of wave equations with applications to the eikonal approximation for short-wavelength waves*, Physics Reports, 158, No. 6 (1988), pp. 337-416.

[17] S.J. Camargo, D. Biskamp and B.D. Scott. *Resistive drift-wave turbulence*, American Institute of Physics, 1995.

[18] M. Rypdal. *Lecture notes on stochastic processes with scaling properties*, January 2010.

[19] M. Melzani. *Blob statistics in the scrape-off layer of tokamaks*, July 2011.

[20] M. Gilmore, C.X. Yu, T.L. Rhodes and W.A. Peebles. *Investigation of rescaled range analysis, the Hurst exponent, and long-time correlations in plasma turbulence*, Physics of Plasmas, Vol. 9, No. 4 (2002).

[21] R. Numata, R. Ball, R.L. Dewar. *Nonlinear simulation of drift wave turbulence*, 2008.

[22] R. Benzi, S. Ciliberto, R. Tripiccione, C. Baudet, F. Massaioli and S. Succi. *Extended self-similarity in turbulent flows*, Physical Review E, Vol. 48, No. 1 (1993).

[23] S. Futatani, S. Benkadda, Y. Nakamura and K. Kondo. *Characterization of intermittency of impurity turbulent transport in tokamak edge plasmas*, Physics of Plasmas, 15, 072506, (2008).

[24] A. Kendl. *Two-dimensional turbulence in magnetized plasmas*, European Journal of Physics, 29, pp. 911-926, 2008.

[25] B.A. Carreras, B.Ph. van Milligen, M.A. Pedrosa, R. Balbin, C. Hidalgo et al.. *Self-similarity of the plasma edge fluctuations*, Physics of Plasmas, 5, 3632, 1998.

[26] B.A. Carreras, B.Ph. van Milligen, M.A. Pedrosa, R.Balbin, C.Hidalgo, D.E. Newman, E. Sanchez, R.Bravenec, G. McKee, I. Garcia-Cortes, J. Bleuel, M. Endler, C. Riccardi, S. Davies, G.F. Matthews, E. Martines and V. Antoni. *Experimental evidence of long-range correlations and self-similarity in plasma fluctuations*, Physics of Plasmas, Vol. 6 , No.5, 1999.

[27] T.S. Pedersen, P.K Michelsen and J.J. Rasmussen. *Resistive coupling in drift wave turbulence*, Plasma Physics and Controlled Fusion, 38, 1996.

[28] S.J. Camargo, M.K. Tippett and I.L. Caldas. *Nonmodal energetics of resistive drift waves*, Physical Review E, Vol 58, No. 3, 1998.


UNIVERSITY
OF TROMSØ